MASTER IN BIOCHEMISTRY AND MOLECULAR AND CELL BIOLOGY RESEARCH FOCUS

Characterization of Mesenchymal Stromal Cells Derived from Ovine Dental Pulp

Ems, Guillaume

Award date:
2022

Awarding institution:
University of Namur

Faculté des Sciences

Characterization of Mesenchymal Stromal Cells Derived from Ovine Dental Pulp

Mémoire présenté pour l'obtention

du grade académique de master 120 en biochimie et biologie moléculaire et cellulaire

Guillaume EMS

Janvier 2022

Faculté des Sciences

Characterization of Mesenchymal Stromal Cells Derived from Ovine Dental Pulp

Mémoire présenté pour l'obtention

du grade académique de master 120 en biochimie et biologie moléculaire et cellulaire

Guillaume EMS

Janvier 2022

~ Logic will get you from A to Z ...
Imagination will get you everywhere ~

- Albert Einstein

University of Namur
FACULTY OF SCIENCES
Biology Department Secretariat
Rue de Bruxelles 61 - 5000 NAMUR
Phone number: + 32(0)81.72.44.18 – Fax: + 32(0)81.72.44.20
E-mail: joelle.jonet@unamur.be - http://www.unamur.be

Characterization of Mesenchymal Stromal Cells Derived from Ovine Dental Pulp

Guillaume Ems

Abstract

Osteoarthritis (OA) is the most common degenerative disease of synovial joints. It is a global public health challenge, and its burden constantly increases with overall ageing of the population. The absence of therapeutics to efficiently prevent, reverse or cure OA is an opportunity to explore emerging therapeutic strategies. An encouraging approach in stem cell-based regenerative medicine is the administration of mesenchymal stromal cell (also known as mesenchymal stem cell or MSCs) that can be isolated from adult tissue such as dental pulp. To assess preclinically potential of such therapy, animal models of OA are required, a widely used model is the sheep. In order to exploit future stem cell therapy in OA ovine models, a thorough characterization of the dental pulp-isolated stem cells should be carried out, this includes several key questions as; Which incisors contain the largest amount of pulp and at what age the pulp volume is maximal? Once dental pulp is extracted; is it possible to enrich and expand those cells in culture? Do these cells show properties and biomarkers of human-equivalent MSCs?
Using CT scan imaging, we showed that sheep has the highest quantity of dental pulp in central incisors between 2- and 3-year-old. Pulp cells could be extracted from ovine dental pulp (hypothesized to be oDPSCs) and expanded in culture. As point of comparison, fibroblasts extracted from ovine dermis were in parallel cultured in standard medium (herein, referred as ovine Dermal Fibroblasts (oDFs)). Both cell types were characterized using the same pipeline of analysis, mostly based on ISCT (International Society for Cell Therapy) criteria for human MSCs and including gene expression profile, surface antigen expression, multipotency capacity, and specific methylation patterns. oDPSCs and oDFs did show some differences in mRNA profile where ITGA11 and MYH11 seemed to be good markers for positive selection of oDPSCs. However, most ISCT markers tested were similarly expressed between oDPSCs and oDFs (CD90, CD105, CD44). oDPSCs showed chondrogenic and adipogenic differentiation potential but no osteogenic potential, while oDFs showed slight chondrogenic and osteogenic differentiation but no adipogenic differentiation. Neither surface markers analysis (CD90, CD73 and CD45) or methylation pattern (CpG island of *oCIDEC*, *oASAM*, *oSERPINB5*) showed difference between oDPSCs and oDFs. In conclusion, this study showed slight differences between oDPSCs and oDFs, meaning that cell types as cultured in our experimental conditions were phenotypically close. ISCT markers did not allow discrimination between both cell types.

Master's Thesis for 120 ECTS Master's in Molecular and Cellular Biology-Biochemistry

January 2022

Promotors: J-M. Vandeweerd ; C. Nicaise ; F. Hontoir

Université de Namur
FACULTE DES SCIENCES
Secrétariat du Département de Biologie
Rue de Bruxelles 61 - 5000 NAMUR
Téléphone: + 32(0)81.72.44.18 - Téléfax: + 32(0)81.72.44.20
E-mail: joelle.jonet@unamur.be - http://www.unamur.be

Caractérisation de Cellule Stromale Mésenchymateuses Extraites de la Pulpe Dentaire Chez le Mouton

Guillaume Ems

Résumé

L'arthrose est la plus courante des maladies dégénérative des articulations synoviales. L'absence de thérapie permettant de prévenir, d'inverser ou de guérir efficacement l'arthrose constitue une opportunité d'explorer des stratégies thérapeutiques émergentes. Une approche encourageante en médecine régénérative est l'administration de cellules stromales mésenchymateuses (également appelées cellules souches mésenchymateuses ou MSCs), elles peuvent être isolées à partir de tissus adultes tels que la pulpe dentaire (appelée alors DPSCs). Pour évaluer pré cliniquement de tel thérapie potentielle, des modèles animaux d'arthrose sont nécessaires. Un modèle très utilisé est le mouton. Afin d'exploiter de future thérapie à base de DPSCs dans des modèles ovins d'arthrose, une caractérisation approfondie des DPSCs ovines doit être effectuée, ce qui inclut plusieurs questions clés telles que: Quelles incisives contiennent le plus de pulpe dentaire et à quel âge la quantité de pulpe est maximale? Une fois la pulpe extraite, est-il possible de sélectionner et faire proliférer des cellules en culture? Ces cellules présentent-elles les mêmes propriétés et biomarqueurs que ceux utilisés pour caractériser les MSCs humaines ? Par CT-scan, nous avons montré que la plus grande quantité de pulpe dentaire chez le mouton se trouve dans les incisives centrales à l'âge de 2-3 ans. Des cellules ont pu être extraites de la pulpe dentaire ovine (supposées être des oDPSCs) et cultivé *ex vivo*. À titre de comparaison, des fibroblastes ont été extraits du derme ovin et cultivés en parallèle dans un milieu de culture standard (appelés ici fibroblastes dermiques ovins (oDFs)). Les deux types de cellules ont été caractérisés à l'aide du même panel d'analyse, principalement basé sur les critères proposés par l'ISCT (Société international de Thérapie Cellulaire) pour les MSCs humaines. Ses analyses comprenaient: un profil d'expression génique, l'analyse d'antigènes de surface, la multipotence, et un profil de méthylation de l'ADN. Les oDPSCs et les oDFs ont montré quelques différences dans le profil d'ARNm où ITGA11 et MYH11 ont semblé être de bons marqueurs pour une sélection positive des oDPSCs. Cependant, la plupart des marqueurs ISCT étaient exprimés de manière similaire entre les oDPSCs et les oDFs (CD90,CD105, CD44). Les oDPSCs ont montré un potentiel de différenciation chondrogénique et adipogénique mais un léger potentiel ostéogénique, tandis que les oDFs ont montré un léger potentiel de différenciation chondrogénique et ostéogénique mais aucune différenciation adipogénique. Ni l'analyse des marqueurs de surface (CD90, CD73, CD45) ni le profil de méthylation (ilot CpG des gènes *oCIDEC*, *oASAM*, *oSERPINB5)* n'ont montré de différence entre les oDPSCs et les oDFs. En conclusion, cette étude a montré de légères différences entre les oDPSCs et les oDFs, mais les cellules étaient phénotypiquement proches. Les marqueurs proposés par l'ISCT n'ont pas permis de discriminer les deux types de cellules.

Mémoire de master 120 en biochimie et biologie moléculaire et cellulaire

Janvier 2022

Promoteurs : J-M. Vandeweerd ; C. Nicaise ; F. Hontoir

Acknowledgements

I would like to deeply acknowledge all my promotors: Jean-Michel Vandeweerd; Charles Nicaise and Fanny Hontoir for the supervising, advices, and helped during this master thesis.
J-F. Nisolle from the CHU Mont Godinne for his assistance for the CT analysis.
I would also acknowledge the technical staff of OASIS; Vincent Simon and Damien Houbotte and Urphym (LabCeTi and LNR); Kathleen De Swert, Valéry Bielarz and Valérie De Glas as well as URVI staff; Laeticia Wiggers, Benoît Muylkens and Damien Coupeau for the precious help in the methylation pattern part. Thank you all for having participated to the good progress of this master's thesis; by helping sometime for technical question, but also by being welcoming and kind, you positively impacted the course of our master's thesis.
Thanks to D. Le Tallec, B. Bihin and M. Regnier for the advice and the precious help in statistics and R programming.
I would also thank L. Severino who also worked on this project.
Finally, I would like to thank my lab/office/drinking mates Chloé, Margaux and Rémi, all my friend and classmates, my family, and in particular my wonderful boyfriend Thibaut, thank you all for supporting me, encouraging me and comforting me during my nervous breakdowns.

Abbreviations

ACL	Anterior cruciate ligament
ALM	Anterior lateral meniscus
AR	Alizarin red
B-cell	Lymphocyte B cell
BM-MSC	Bone marrow derived mesenchymal stem cell
CFU-f	Colony-forming unit-fibroblasts
CpG	CG dinucleotide site
CT	Computed tomography scanner
DNMT	DNA methyltransferase
DPSC	Dental pulp strem/stromal cell
ESC	Embryonic stem cell
FBS	Foetal bovine serum
HLA-G5	Human leukocyte antigen G5
I1 to 4	Incisors 1 to 4
ICM	Inner cell mass
IDO	Indoleamine 2,3-dioxygenase
IFN-γ	Interferon-γ
IL-12	Interleukin-12
iPSCs	Induced pluripotent stem cells
ISCT	International Society for Cellular Therapy
MSC	Mesenchymal stem cell
NK	Natural killer
NO	Nitric oxide
OA	Osteoarthritis
oDFs	Ovine dermal fibroblasts
oDPSCs	Ovine dental pulp stem cells
ORO	Oil red O
PCL	Posterior cruciate ligament
PGE2	Prostaglandin E2
PLM	Posterior lateral meniscus
PMM	Posterior medial meniscus
PSC	Pluripotent stem cell
RTqPCR	Reverse transcription quantitative polymerase chain reaction
SHED	Human exfoliated deciduous teeth
SJ	Synovial joints
T-cell	Lymphocyte T cell
TF	Transcription factor
TGF- β	Transforming growth factor-β

Table of content

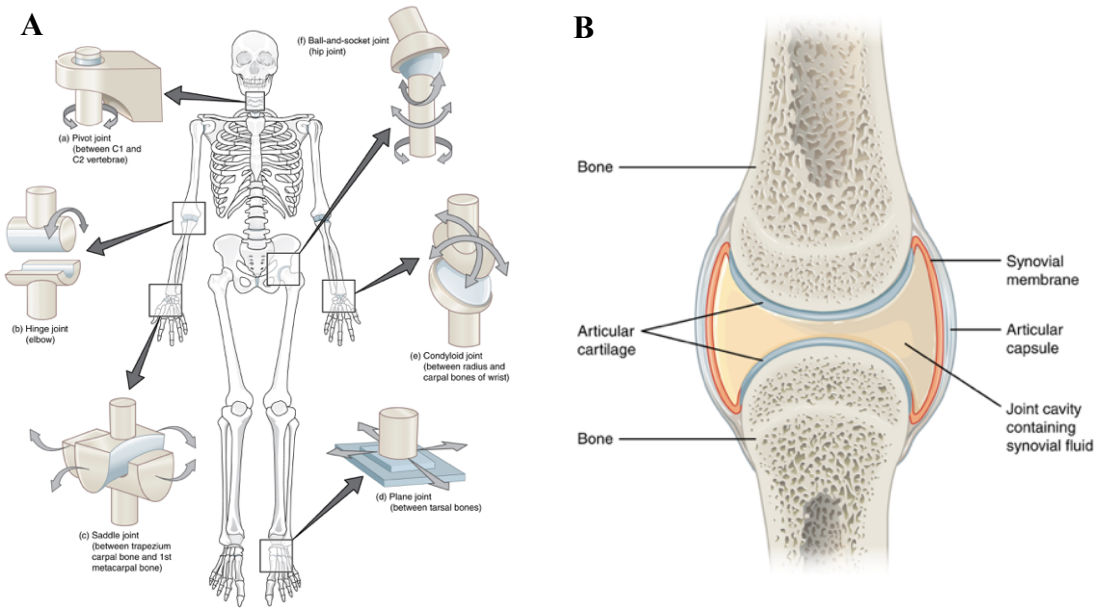

Figure 1- Synovial Joints A: *The six types of synovial joints allowing smooth movement in a variety of ways.* ***B:*** *A normal synovial joint is composed of a joint cavity defining an articular capsule filled with synovial fluid. The bones are recovered with a layer of articular cartilage*[1].

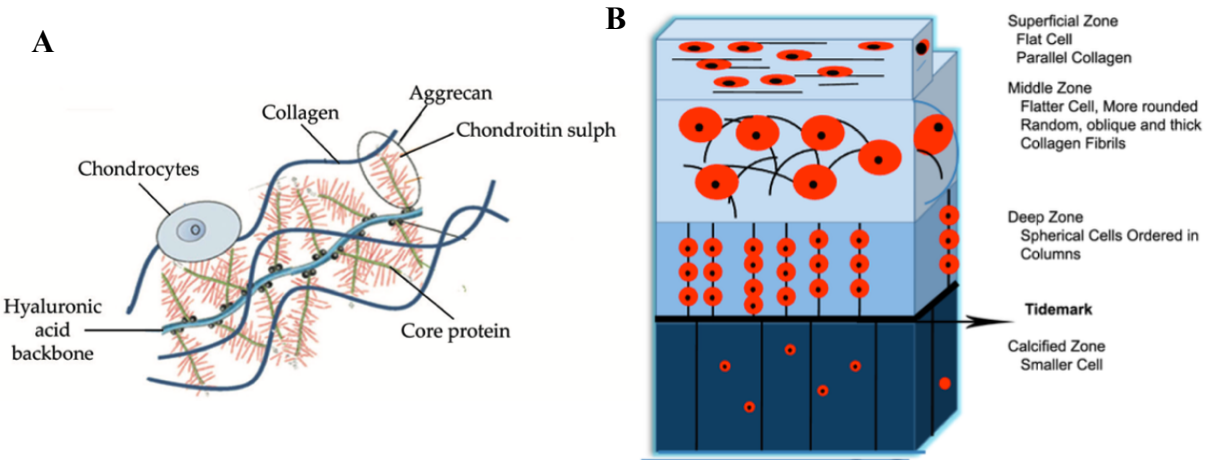

Figure 2 – Cartilage: A. *The extracellular matrix of cartilage is synthesized by chondrocytes, it is composed of different macromolecules that interact with each other; mostly collagen type II, proteoglycans monomers, and glycosaminoglycan (mostly chondroitin sulfate) link to hyaluronic acid*[7]. ***B.*** *Cartilage can be divided into four zone with different composition, architecture, and mechanical properties*[9].

Introduction

1) Synovial joint

Synovial joints (SJ) are the most common type of joint in the body allowing smooth movements between adjacent bones. There are several types of SJ: pivot, hinge, condyloid, saddle, plane, and ball/socket joints. Theses differ on the shape of the articular surfaces of the bones that form each joint[1] (figure 1 A). A healthy SJ is composed of a joint capsule that surrounds the joint. Its inner side is covered by the synovium (a membrane that produces the lubricating fluid of the joint, called the synovial fluid). The side of the bones facing the joint (subchondral bones) are covered by a thin layer of articular cartilage (figure 1 B). Several additional structures are located outside the joints; they stabilize the joints (ligament), and allow their movement (muscles)[1].

1.1) Articular cartilage

Articular cartilage is a flexible, porous, and highly hydrated connective tissue that covers the extremities of the articular bones[2]. This articular cartilage provides low friction and wear throughout life[3] and ensures smooth joint movement thanks to mechanical and viscoelastic properties: it responds to frictional, compressive, shear and tensile loading[4]. A vital characteristic of this tissue is the pressurization of its interstitial fluid upon loading[3].

Cartilage is synthesized by chondrocytes, it is devoid of blood vessels, nerves, or lymphatics. Cells nutrition occurs by diffusion of nutrients from the synovial fluid and from the subchondral bones[5]. Cells compose only 5% of the tissue volume. The extracellular matrix is mostly composed of water, collagen type II and proteoglycans[3], which represent about 90% of the dry weight of the tissue[6].

Water is the most abundant component of cartilage (up to 80% of the wet weight). This water is located: in the intracellular space, in the pore space of the matrix, and also associated with the components of the extracellular matrix[5,7].

Type-II collagen is a fibrillar protein, made of homotrimers of collagen type II alpha 1 chains[8]. This structure is essential to provide important shear and tensile properties to the cartilage[5].
Glycosaminoglycans are entrapped in collagen network. The predominant sulphated glycosaminoglycan is chondroitin sulfate, which links the core protein non-covalently to form aggrecan, the main proteoglycan of cartilage. These macromolecules have the capacity to strongly link the hyaluronan, an unsulfated glycosaminoglycan[6,7] (figure 2 A).
Other cartilage components are lipids, phospholipids, other types of collagen, non-collagenous proteins (such as fibronectin) and glycoproteins[5].

The cartilage tissue is organized in four zones[5,9]: the superficial zone, the middle zone, the deep zone, and the calcified zone (figure 2 B). Each of them has its own structure (orientation and diameter of collagen fibers as well as the shape, orientation, and size of the cells), composition (concentration of macromolecules, water, and cells), and mechanical properties.
The superficial layer contains a relatively high number of dense flattened chondrocytes and collagens fibers (highest level ~ 80%) packed tightly and aligned parallel to the tissue surface. The diameter of the fibers is relatively small[5,10].

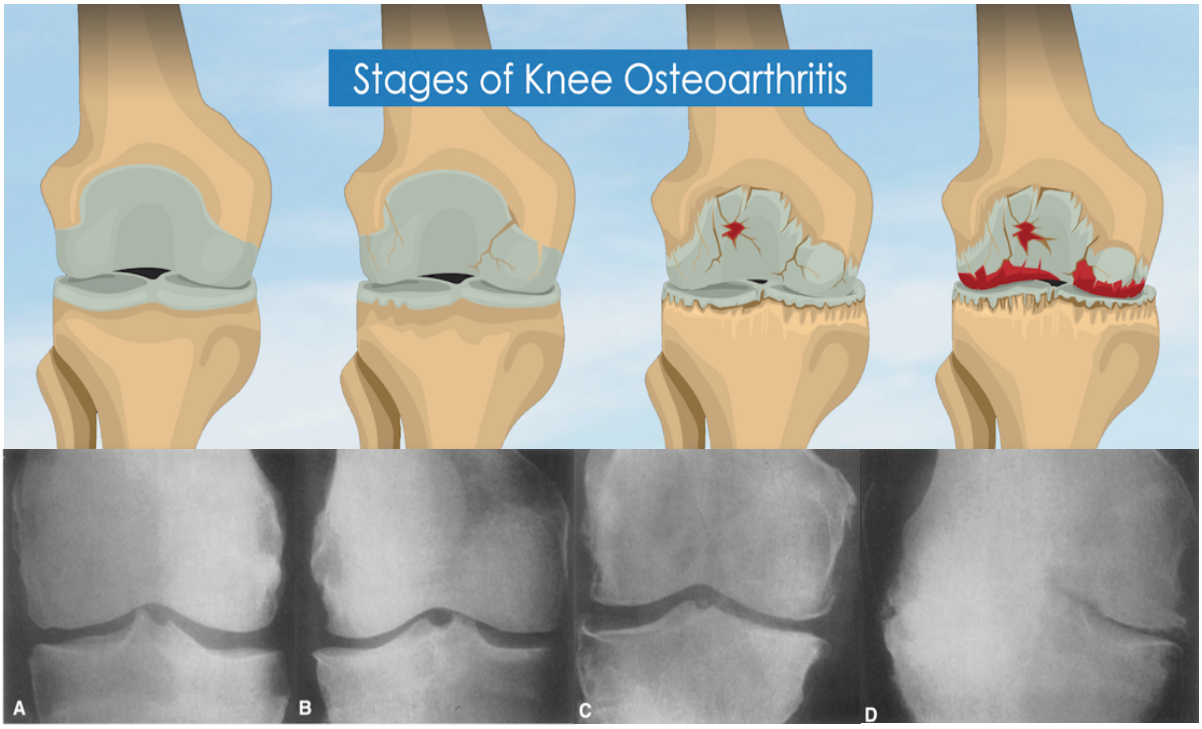

Figure 3 – Grade of osteoarthritis by Kallgren-Lawrence classification. *Osteoarthritis gravity is classified in four grades: (A) Grade 0 for absence of OA. Grade I is a minimal disruption (B) Grade II is the presence of superficial fissure and definite osteophyte formation (C) Grade III is a definite clear narrowing of the joint space, with deep fissure and moderate osteophyte formation (D) The grade IV, shows lack of cartilage and large osteophyte, severe narrowing of the joint space with marked sclerosis* [13,19].

The middle zone contains the highest number of proteoglycans and thicker collagen fibrils, which are more randomly aligned. Chondrocytes are spherical[5,10].
In the deep zone, the collagen fibers have the largest diameter and are arranged perpendicularly to the subchondral bone. Proteoglycan content is higher, and water content is lower than the superficial and transitional zone. Chondrocytes are arranged in column-wise orientation, parallel to the collagen fibers and perpendicular to the joint line[5,10].
The interface between the deep zone and the calcified cartilage is known as the tidemark. The collagen fibers of the deep zone are continuous with the collagen fibers of the calcified zone. This calcified zone contains sparse hypertrophic cells[5,10].
Given that cartilage is avascular, hypocellular, and that chondrocytes have limited potential for replication, its intrinsic healing and regeneration capacities are very limited[11].

1.2) Osteoarthritis:

1.2.1) Epidemiology

OA is characterized by wear and breakdown of the cartilage. Clinically, the predominant symptom of OA is severe articulation pain and loss of function/mobility. Stiffness, swelling or joint instability are also observed. The disease can affect any joint, so symptoms can appear in the hands, the neck, the lower back, and more frequently the knee and hip joints[12]. It is a degenerative disease, progressing from a low intensity (morning stiffness and pain after intense activity) to severe constant pain[13] (figure 3).

OA is the most common degenerative disease of synovial joint. Its burden constantly increases with life expectancy and the overall ageing of the population[14]. It will become one of the most prevalent diseases in the population from high-income countries in the coming decade[15]. For example, in Europe, OA is estimated to affect more than 40 million people[16]. In the US, it is also a major cause of disability with 22.7 million people having activity limitations due to OA[17]. The worldwide prevalence of hip and knee OA is approximately 303 million people, which makes OA a leading cause of disability in several countries[14].

OA clearly has a severe individual and socioeconomic impact, as individual impact are mostly the symptoms which markedly reduce the quality of life, socioeconomic impact refers to direct and indirect costs. Direct costs can be explained by all treatments (non-pharmacological and pharmacological), surgeries, adverse effects, long-term care and health care provision.
Obviously, direct costs cause "secondary costs" as absenteeism, reduction of employment, reduction of productivity, caregiver time, and premature mortality[18].
OA can be classified into different types depending on its origin. The primary OA is the most common diagnosed form, which is mainly due to the wear and tear of the articulation over time[12]. However, various risk factors can promote "secondary OA" to occur due to external conditions that induce a change in the cartilage[20]. Risk factors include: overweight[21], injury or surgery to a joint[22], overuse from repeated movements of the joint[12], joints dysplasia[23], and also genetic factors[23,12].

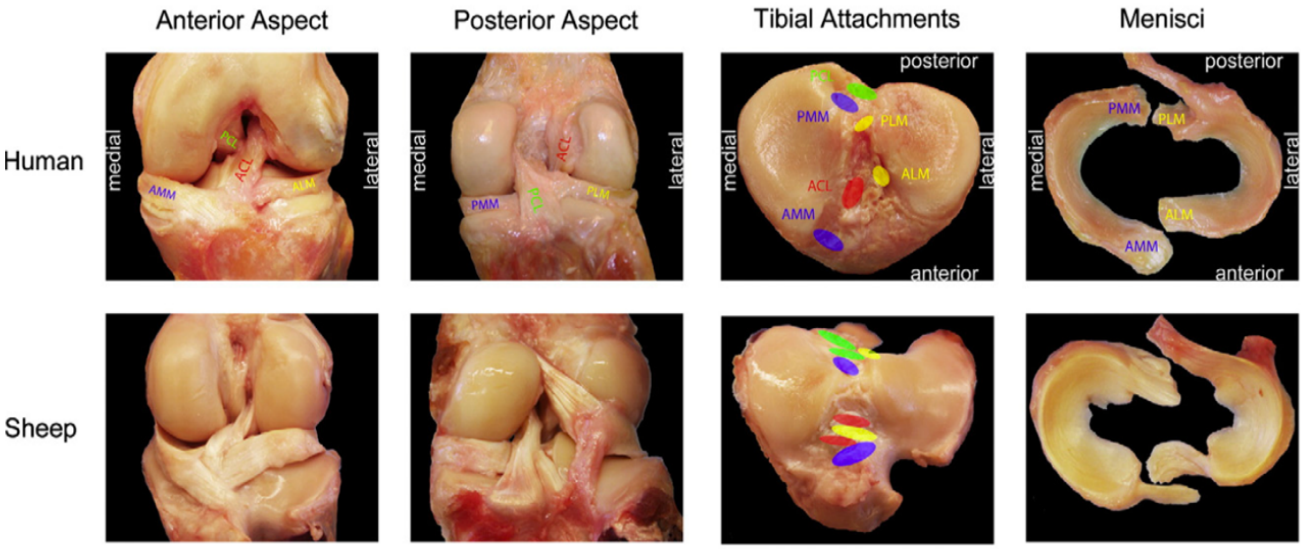

Figure 4 – Similarity of sheep and human knee: *Different view of human knee and sheep stifle. (ACL=anterior cruciate ligament; ALM=anterior lateral meniscus; AMM=anterior medial meniscus; PCL=posterior cruciate ligament; PLM=posterior lateral meniscus; PMM=posterior medial meniscus). The ACL size and proportion are similar between sheep and human, as well as the MM. The lateral and medial meniscus dimensions closely match the human meniscus. However, the splitting of the ACL insertion site differs from human*[42,43].

1.2.2) Sheep as a model of OA

1.2.2.1) Ovine joint

Various animal models (mice[24,25], rat[26], rabbit[27] and mini pig[28]) have been used to test drug for musculoskeletal diseases. Small animals are often used in research as they are easy to house, and available in a variety of genetically modified strains. However, it is difficult to have a surgical model for cartilage defects as they have very small joints and extremely thin cartilage (3-5 cells thick). It is difficult to produce a cartilage defect that is suitable for comparison to the human situation. Locomotion problem due to OA is primarily assess by observation of lameness and gait. These symptoms can be complicated to assess in small model as mice. Obtain larger or repeated samples for long-term assessment is also a problem.
Despite these issues, small animals can be useful for proof-of-principle study to assess the safety before moving on larger animals[29,30]. Large animal models, such as horse[31], mini pig[32] and sheep[33–37], should be used in preclinical studies for OA. They give several advantages as anatomic similarity to humans (comparable joint size and cartilage thickness), widespread occurrence of OA (naturally with ageing), the possibility to use diagnostic imaging, synovial fluid collection, arthroscopic intervention, and postoperative management[38]. The use of such models generates more clinically relevant data and are generally required for regulatory approval of drug development[38].

Sheep are commonly used as a model in OA studies. They are readily available, easy to handle and low cost relative to other large animal [29]. There is also a close similarity between the ovine stifle and the human knee, anatomy and biomechanics are relatively similar (figure 4)[29,39]. The cartilage thickness range from 0.4 to 1.7 mm (and up to 2 mm)[38] which is relatively close to human (2.4-2.6mm)[29]. This thickness allows either full- or partial- chondral lesion[38,40]. Sheep have also a similar body weight, bone composition, and comparative metabolic and bone remodelling rate[30]. The main disadvantages of such large model compared to small animals are primarily the cost of purchasing, greater difficulty of handling, housing, and experimentation[38,41].

1.2.3) Therapeutic strategies of OA

Current therapies for OA mostly rely upon:

- Activity modification: modifying lifestyle to include adequate exercises can reduce the symptoms occurrence or severity. Moreover, it has a major role in prevention strategy by reduction of risk factors (such as overweight)[44]. For example, physical activity can lead to weight loss. It is well established that weight loss reduces the risk of OA, and relieves pain and symptoms if OA is already present[45].

- Pharmaceutical treatments: although some drugs show promising results, most of the actual treatments remain mainly symptoms management with anti-inflammatory and analgesic drugs[46,47]. Pharmaceutical treatments target various aspects of OA; reducing cartilage breakdown, promoting cartilage repair, limiting inflammation, increasing joint lubrification, and reducing pain. Such treatments give several side effects as for example: an upset stomach, gastric ulcers, increased likelihood of cardiovascular event[48]. There is also some incompatibility and contraindication for patients with comorbidities (ex: corticosteroids are not recommended for diabetics because of the

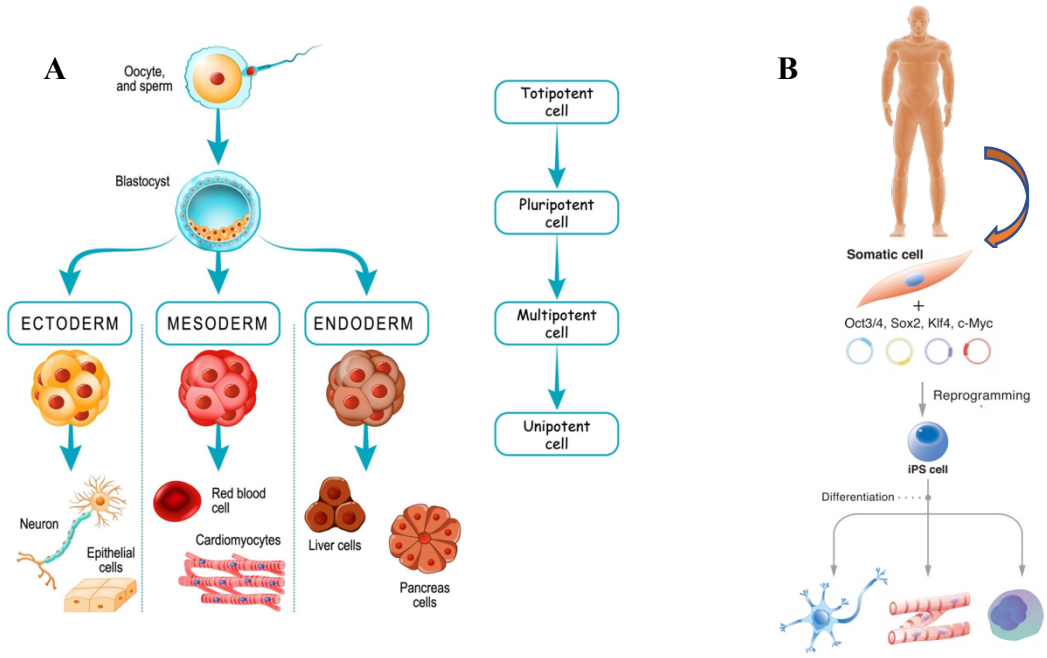

Figure 5 – Type of stem cells: A. *Hierarchy of stems; totipotent cells form embryonic and extra embryonic tissue. Pluripotent cells (embryonic stem cell) form the three germ layers. Multipotent cells can generate only one germ layer. Unipotent cell generate one cell type*[60,65] ***B.*** *Induced pluripotent stem cell are reprogrammed somatic cell, ectopic expression of four genes – Oct4, Sox2, Klf4, and c-Myc induced this pluripotency*[64].

effect on blood glucose level)[49] leading to the complexity of dealing with OA and other pathologies.

- Surgery: focal surgeries have been developed to treat articular cartilage lesions, such as a microfracture or an osteochondral graft to promote cartilage healing. Another surgery that has been studied in recent years is knee joint distraction[15]. During 6 to 8 weeks, external fixator led to joint distraction. This technique shows promising results: it induces cartilage regeneration and clinical improvement on short- and intermediate long term. Joints show decrease in inflammatory biomarkers which is associated to pain relieve and postponing more invasive surgeries. After 5 years, 75% of patients still have treatment effect results, and 50% of patients after 9 years still not undergo total articulation replacement[50].
  As a last resort, when the patient is severely affected, the joint can be replaced by a prothesis. Despite advances in these procedures and improvements of patient quality of life, these major surgeries are still associated with common risks, such as surgical site infections, venous thromboembolism, neurovascular injury, etc[15]. Moreover, as OA affects mostly elderly patients, complications due to age must be considered (anaesthesia risk, cardiovascular comorbidities, impaired/slow healing)[51].

The absence of therapeutics to efficiently prevent, reverse or cure OA is a challenge and an opportunity to explore new therapeutic strategies. For several years, stem cell therapy has been investigated in musculoskeletal diseases[52–54], such as osteonecrosis[55,56], meniscus tear[57] and OA[58]. An encouraging approach in regenerative medicine to treat OA is the use of mesenchymal stromal cell (also known as mesenchymal stem cell, MSC)[59].

2) Stem cell therapy

There are different types of stem cells. Basically, stem cell refers to a population of undifferentiated cells present during all the life stages: embryonic, fetal, and adult. The major characteristics of stem cells are their ability to self-renew and differentiate into different types of cells and tissues[60]. Depending on the type of stem cell, these properties can differ, giving characteristic of potency: from totipotent to unipotent cells (figure 5 A).

2.1) Type of stem cells

2.1.1) Totipotent stem cell

These stem cells, found in early development, are the most undifferentiated cells. Only the fertilized oocyte and the cells from the first two division are considered as totipotent[61]. Totipotent cells can form the embryo and the trophoblast (which later forms the placenta). These cells can give rise to an entire organism[60,62,63].

2.1.2) Pluripotent stem cell

During development, around four days after fertilization, the totipotent cells begin to specialize to form the blastocyte. This blastocyte is composed of cells cluster called the Inner Cell Mass (ICM), from which the embryo develops. The constituent cells of the ICM (often called Embryonic Stem Cell (ESC)) are pluripotent stem cells (see figure 5 A). They can differentiate

into almost all cells that arise from the three germ layers but not the embryo (they cannot form the placenta and supporting tissues)[60,62,63].

2.1.3) Multipotent stem cell

Multipotent stem cells can be found in almost all tissue and are able to differentiate into all cell types within one lineage. However, certain adult stem cell removed from their usual location can transdifferentiate into cells that arise from the three germ layers. The mesenchymal stromal cells are part of this class[60,63](see figure 5 A).

2.1.4) Unipotent stem cell

These cells can generate only their own cell type. Sometimes called "committed cells (progenitors)", they can self-renew which distinguishes them from non-stem cell, but this capacity is limited (e.g. muscle stem cell, in the epidermis, liver)[60,62,63] .

2.1.5) Induced pluripotent stem cell

Induced pluripotent stem cells (iPSCs) are a new type of cells that can be obtained in laboratory by reprogramming differentiated cells into pluripotent cells[64] (figure 5 B).

2.2) Pluripotent vs multipotent cells in cell therapy:

As pluripotent stem cells (PSCs) are able of unlimited proliferation and differentiation into all three germ layers, they are attractive sources for cell therapies for various diseases. The two sources of PSC (ESCs and iPSCs) come with several problems; for example the immunogenicity, the genetic stability and the epigenetic status of these cells limit the use in clinic[66]. There is also high challenges in term of processing, packaging, or quality control[67]. Above all, the safety of cellular therapy using PSC is a major limitation, injection of such type of cell can generate teratoma, a kind of tumor made up of elements of different germ layers[66]. For ESCs, another major limitation is the ethical concern for the use of cells coming from human embryo[68].

As mesenchymal stromal cells (MSCs) are adult multipotent stem cells that can be found in almost all postnatal organs and tissues, they can be isolated from various sources: adipose tissue, peripheral blood, synovium, endometrium, skin, muscle, and more commonly bone marrow[69]. MSCs are a good alternative to PSCs due to several advantages for clinical application including; easy isolation, high yield, high plasticity, ability to mediate inflammation, promote cell growth, and tissue repair, thanks to immunomodulation and immunosuppression capacities[52,70]. The immunomodulatory properties of MSCs make them useful for cellular therapy in inflammatory diseases such as OA. There are two major mechanisms involved in this immune privilege: (1) Paracrine production of several soluble factors (2) Cell-cell contact.

Soluble factors including nitric oxide (NO), prostaglandin E2 (PGE2), indoleamine 2,3-dioxygenase (IDO), transforming growth factor-β (TGF-β), and human leukocyte antigen G5 (HLA-G5) have several effects on immune cells. For example, PGE2 reprograms macrophages to increase the production of anti-inflammatory cytokines, and NO plays a role in suppression of T-cell proliferation by MSCs. These factors can also inhibit B-cell proliferation as well as cytokine production, cytotoxic activity, and proliferation of natural killer cells (NK). MSCs

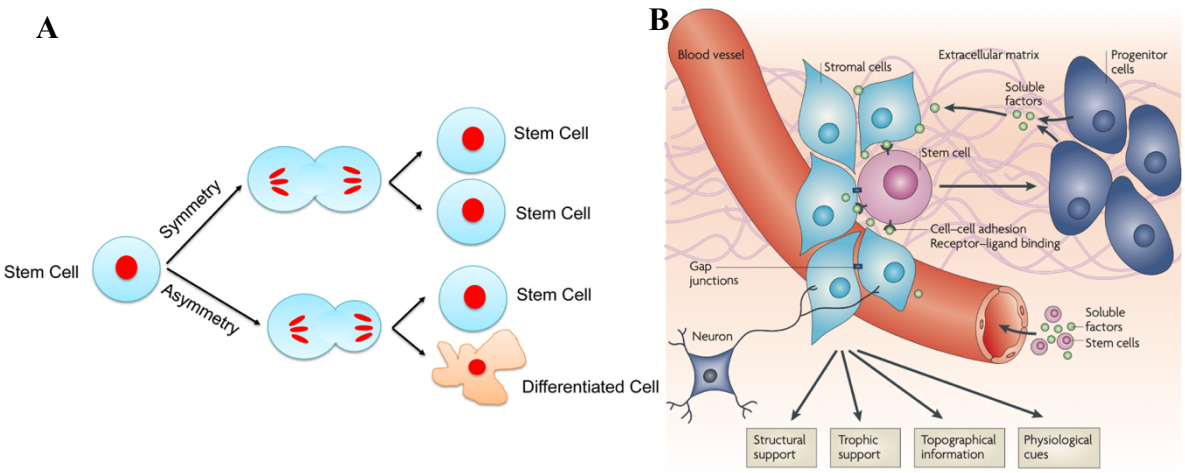

Figure 6 – Stem cell in vivo: A. *Symmetric division give rise to two undifferentiated cells while an asymmetric division produce a differentiated cell*[79]. ***B.*** *The stem cell niches are composed of stem cell, stromal cells, extracellular matrix, neural inputs and vascular network. Every niche does not necessarily include all of these components*[77].

also strongly inhibited the differentiation of alloantigen-induced monocytes to mature dendritic cells, and strongly hampered their ability to activate T cells. Effects can also be seen with decrease of pro-inflammatory cytokines such as TNF-α, IFN-γ,IL-12 and increase of anti-inflammatory cytokine as IL-10[71,72].

MSCs secretum and T-cell contact leads to T-cell apoptosis and inhibition of T-cell proliferation[72,73]. Importantly, this suppression has been observed with MSCs either autologous or allogeneic[71]. It has been reported that MSCs could promote regulatory T-cells (Tregs) proliferation, these cells displayed an immune regulatory phenotype by suppressing immune response (maintain homeostasis and self-tolerance)[74]. Direct cell-cell contact with macrophages has also been described to increase PGE2 secretion, which reprograms macrophages to produce anti-inflammatory cytokines[71].

Also, MSCs are ethically and socially acceptable as they are extracted from adult tissue[62,75]. Further all, MSCs do not form teratomas after transplantation, securing the transplantation[75]. They are considered the most clinically translatable cell type for regenerative medicine and they are widely studied in preclinical and clinical trials for several diseases touching different organs, for example: the heart, the liver, the eyes, and organs of the nervous system[75]. By June 2020, there were over 1, 138 registered MSC-clinical trials at *clinicaltrials.gov*[76].

2.3) Biology of MSCs

MSCs (found in almost all adult tissue) are adult stem cells. They maintain the homoeostasis and repair the tissue by generating differentiated cells that are needed in a tissue. One feature of these cells is their ability to either divide symmetrically or asymmetrically (depending on cell-cell contact and communication), in which there is production of one stem cell and one differentiated cell. This process allows to maintain a stem cell population without increasing it, so it is essential for the tissue homeostasis (figure 6A). MSCs reside in a specific area called "stem-cell niche" (figure 6B), which is described as the *in vivo* microenvironment where stem cells reside and receive stimuli determining their fate.
The conserved components of this niche are stromal support cells (these interact directly with the stem cells by cell surface receptor and secreted molecules), extracellular matrix (which acts as a cell anchor, it provides structure, organization, and mechanical signals), blood vessels (act as a nutritional support and give a systemic signaling), and neural inputs (might induce mobilization of stem cell by integrating signal from the environment). Not all niches are composed of all these elements[77–79]. There is not stem-cell niche within articular cartilage.

In the 1970s, Friedenstein's group demonstrated for the first time that cells residing in bone marrow could be isolated by their plastic adherence capacity. They formed "fibroblastic-like colonies" and possessed in vitro osteogenic differentiation abilities. These cells were called colony-forming unit-fibroblasts (CFU-f)[80].
Later on, other niches have been discovered in adult and fetal tissues including adipose tissue[81], placenta[82], umbilical cord[83], dental pulp[84], peripheral blood[85], and synovial membrane[86].
These cells are described to be mesenchymal stem/stromal cells. The precise definition of these cells remains in debate. In 2006, the International Society for Cellular Therapy (ISCT) set 3 criteria to standardize the characterization of MSCs in vitro [87]:

- MSCs should adhere to plastic culture dishes and have a fibroblast-like morphology. This property is a well described property of MSCs[88–90].

- MSCs must show a capacity for trilineage differentiation. Thus, cells must at least differentiate into adipogenic, chondrogenic, and osteogenic lineages using standard in vitro culture conditions. The differentiation of MSCs into lineage derived from other germ layer has also been reported, such as neurons (originated from ectoderm), and hepatocytes (derived from endoderm)[75].

- More than 95% of the cells must express surface markers such as CD73 (also known as ecto 5' nucleotidase), CD90 (also known as THY 1), and CD105 (or endoglin). The cells must lack hematopoietic markers (<2%) CD11b and CD14 (monocytes and macrophages marker), CD34 (primitive HSCs and endothelial cells marker), CD45 (pan-leukocytes marker), CD79α or CD19 (B cells marker), and HLA-DR (antigen presenting cells marker).

These markers are not specific to MSCs, they are also expressed in some immune cells and differentiated cells such as fibroblast. Additional markers are required. Difficulties to find unanimously accepted markers arise from the variability among studies, according to isolation techniques, culture time, species, and cells/site origin[62]. For now, no single marker or set of markers has been determined to unequivocally isolate and purify MSCs as they are largely non-specific.
Other surface markers described in the literature includes CD44, CD146, STRO-1, CD166, NANOG and OCT4[91]. Identification of MSCs should not only rely on surface markers but also on the multipotent capacities and plastic adherence.

Characterization of cells of interest can also include "OMICS" techniques, which aim to characterize different cellular aspect as metabolomics, proteomics, transcriptomics, and epigenomics[92]. Several studies have found specific gene expression profiles, proteomic profiles, and epigenetic profiles for MSCs [93–98]. However, like surface markers, OMICS profiles can vary from one study to another[99].

2.4) DPSCs; a kind of MSCs

2.4.1) Origin and capacities of DPSCs

Bone marrow (BM) is historically the main source of MSCs. However, this source requires an highly invasive and painful procedure which gives rise to potential adverse effects on the donor (pain, bleeding or infection)[69].
Interestingly, in 2000, *Gronthos et al.* first isolated MSCs from human dental pulp tissue and named the cells "dental pulp stem cells" (DPSCs)[84].

Unlike bone marrow derived MSC, harvesting DPSC's is safer, easily accessible, with a high initial yield of cells. For example, in Human the pulp coming from routinely extracted wisdom tooth or deciduous teeth can be easily biobanked for allogenic or autologous use[100]. Molar dental pulp would also be harvested without total tooth extraction, thanks to a root canal procedure[101]. This technique is commonly used in dentistry[101,102].
Stem cells from human exfoliated deciduous teeth (SHED) can also be isolated, but they exhibit distinct biological characteristics and gene expression profile[103]. Compared to SHED, DPSCs from permanent teeth show better osteogenic and odontogenic differentiation and seem more suitable as potential OA therapeutics[104].

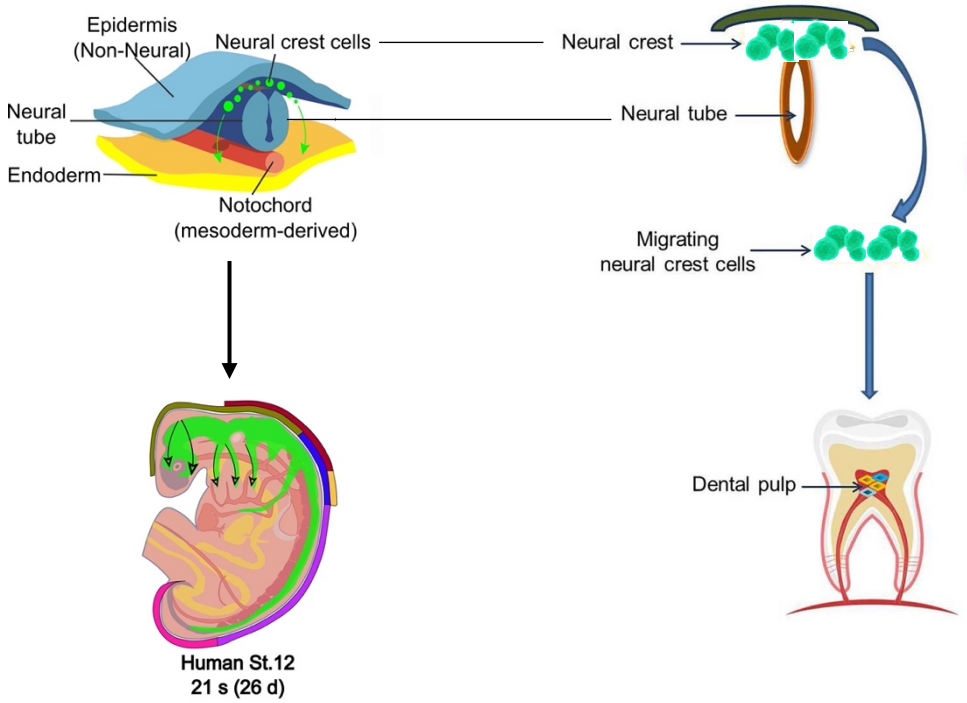

Figure 7: Origin of DPSCs*. Neural crest cells (NCCs) are represented in green. NCCs come from the neural ectoderm and migrate throughout the body to differentiate into several cell types as melanocytes, cranial cartilage, bone, and several other type. DPSCs originate from migrating neural crest cells*[108,109].

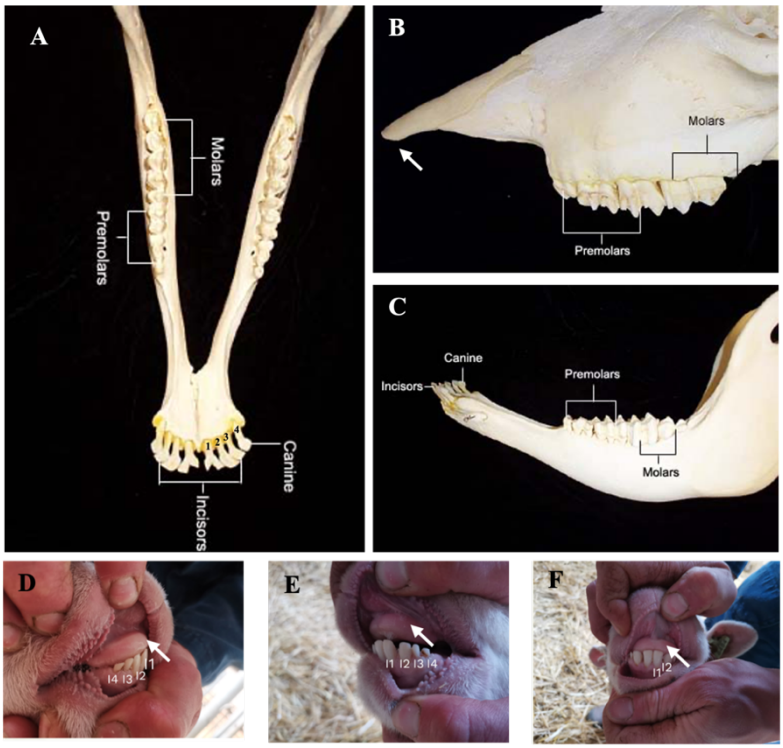

Figure 8 – Dental anatomy of sheep: A. *Mandibular arcade* ***B****. Maxillary arcade (lateral view)* ***C.*** *Mandibular arcade (lateral view)* ***D-E-F.*** *In vivo images of ovine incisors. Sheep lacks upper teeth at the maxillary arcade, replace by a dental mucosal pad instead (white arrows). They have eight incisors at the mandibular arcade, they are called I1 to I4, left and right (****A-D-E-F****). At the maxillary and mandibular arcades, there are three premolars and molars* ***(B-C)***[111].

DPSCs are ectodermal-derived stem cells originating during tooth development, cells migrate from the neural tube to the oral region and then differentiate into mesenchymal-like cells (figure 7)[105,106]. Though, DPSCs shows in vitro pluripotent capacity as they can differentiate into mesodermal cell lineages as adipocyte, chondrocyte and osteoblast, but also to ectodermal and endodermal cells including neurons, endothelial cells, hepatocyte, and cardiomyocytes[73,107].

Compared to BM-MSCs, DPSCs show higher immunomodulatory capacity and proliferative capacity in vitro in the first weeks of culture; and higher angiogenic, neurogenic, and regenerative potential[73,107]. The inhibition of stimulated T cell proliferation is stronger than BM-MSCs. They suppress the proliferation of peripheral blood mononuclear cells by TGF-β secretion and improve inflammation related to tissue injuries when they are injected[71].

To better study the potential of DPSCs in OA, it would be interesting to assess the possibility to extract them from ovine teeth.

2.4.2) Dental anatomy of sheep

The prominent feature of ruminant dental anatomy is the lack of upper teeth. Sheep have eight teeth at the rostral end of the mandibular arcade; eight incisors (some authors describe six incisors and two canines (figure 8). They have a dental mucosal pad at the rostral part of the maxillary arcade, facing the incisors of the mandibular arcade[110,111].
Caudally, both on the maxillary and mandibular arcades there are three premolars and three molars[110,111] (figure 8). The conformation of the mouth and the positions of molars and premolars make their surgical extraction difficult.
In addition, it could be detrimental for the health and normal alimentary behavior of such ruminant to remove premolar and/or molar teeth. Incisors seem therefore more suitable for extraction and pulp collection in order to isolate DPSCs.

3) Objectives of this master's Thesis

MSCs are really interesting to treat OA. In addition of having chondrogenic potential, they have a significant paracrine activity showing immunomodulatory properties by reducing inflammation, suppressing T cell proliferation and B cell antibody secretions. This reduces the risk of rejection for allogeneic use. Moreover, growth factor and cytokines secretion by MSCs improve cartilage healing capacities by cartilage nutrition (via angiogenesis) and direct chondrocyte proliferation[112,113].

Only few clinical trials have been published so far to assess the use of DPSCs for preclinical studies in OA. These studies are only based on small animal model as mice[25], rat[26,114], rabbit[27] and mini pig[28]. Studies with large animal model are required before further clinical use in Human. However, this requires an initial adequate characterization of the animal cell line before their use.
The main goal of this master's thesis was to characterize the ovine DPSCs in order to assess their efficacity in OA treatment. To accomplish this, this study aimed to answer two questions:

(1) Which incisors contain the largest amount of pulp and at what age the pulp volume is maximal?
(2) Is it possible to expand DPSCs from extracted ovine dental pulp? Are these cells MSCs?

To the best of our knowledge, such a study has not been conducted yet.

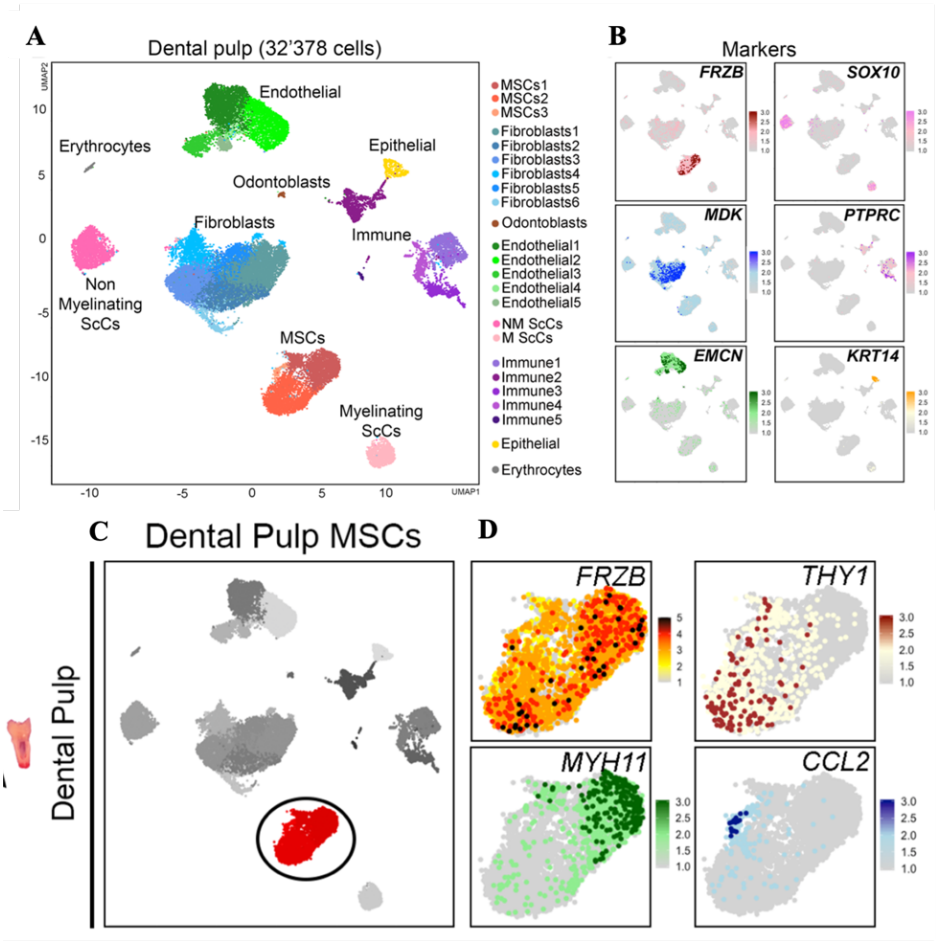

Figure 9 – Dental pulp MSCs population: ***A.*** *Color-coded clustering of dental pulp cell population* ***B.*** *Key genes used for the characterization of the cell clusters* ***C.*** *MSCs compartment* ***D.*** *Subclusters of MSCs withing the pulp characterized by different gene expression markers*[119].

3.1) Which incisors contain the largest amount of pulp and at what age the pulp volume is maximal?

To answer these questions, a morphometric study was conducted by computed tomography (CT) analysis and histology. CT aimed to illustrate general morphology of teeth and jaws, and to quantify the volume of dental pulp. Histology aimed to describe the microscopic features of the ovine incisors.

3.2) Is it possible to expand DPSCs from extracted ovine dental pulp? Are these cells MSCs?

Cells extracted from the ovine dental pulp (suggested to be DPSCs), were compared to extracted ovine dermal fibroblast (oDFs). Several aspects were investigated to determine the identity of the cells: gene expression profile, DNA methylation pattern, cell surface markers, multipotency capacities. A brief description of the current knowledge follows for each aspect.

3.2.1) Gene expression profile

Gene expression profiles allows us to investigate if genes are being expressed in cells at a specific time, under specific condition. This assessment can focus on global transcriptomic profile (regroup thousands of genes), or focus on specific transcript (thanks to RTqPCR) [14]. The current study aimed to find a specific transcript[115].

Global gene expression profiles have previously characterized human MSCs and highlighted up-regulated genes[94–97,116]. Using fibroblasts as a control, some up-regulated gene were described on various studies. For example, *Wagner et al.*[116] found a panel of up-regulated genes as HOXA5 and members of the CXCL family.

A comparison study suggested ITGA11, CD10, CD26, CD106, CD44, and CD146 as helpful gene marker for the discrimination between MSCs and dermal fibroblasts[117,118] and CD146, STRO-1, CD166, NANOG and OCT4 for stemness marker[109].

ISCT give several markers to identify MSCs: CD90 (THY1), CD73 (NT5E), and CD105 (ENG) as positive markers, and CD34, CD45 (PTPRC) for negative marker. The RNA expression can be measured for these markers.

In 2021, *Pagella et al.*[119] published a single cell atlas of Human teeth. They performed a single cell RNA profiling to elucidate the cellular composition of dental pulp. Their study identified the MSC population inside the dental pulp (figure 9 A-B). MSCs were characterized by a high expression of genes such as *FRZB*, *NOTCH3*, *THY1* (CD90), *MYH11*, *CCL2, CXCL14, KRT18.* Fibroblast were characterized by the expression of *MDK* (figure 9 C-D).

3.2.2) Cell surface markers

ISCT defined minimal surface marker to identify MSC as previously mentioned. At least 95% of the culture must be positive for CD73, CD90, and CD105 antigen marker. The cells must lack hematopoietic markers as CD11b, CD14, CD34, CD45 (pan-leukocytes), CD79α or CD19 (B cells), and HLA-DR. Commercially available kit should be tested for sheep cells. oDFs culture can be used as a control to see the potential enrichment of MSCs in the dental pulp derived cells.

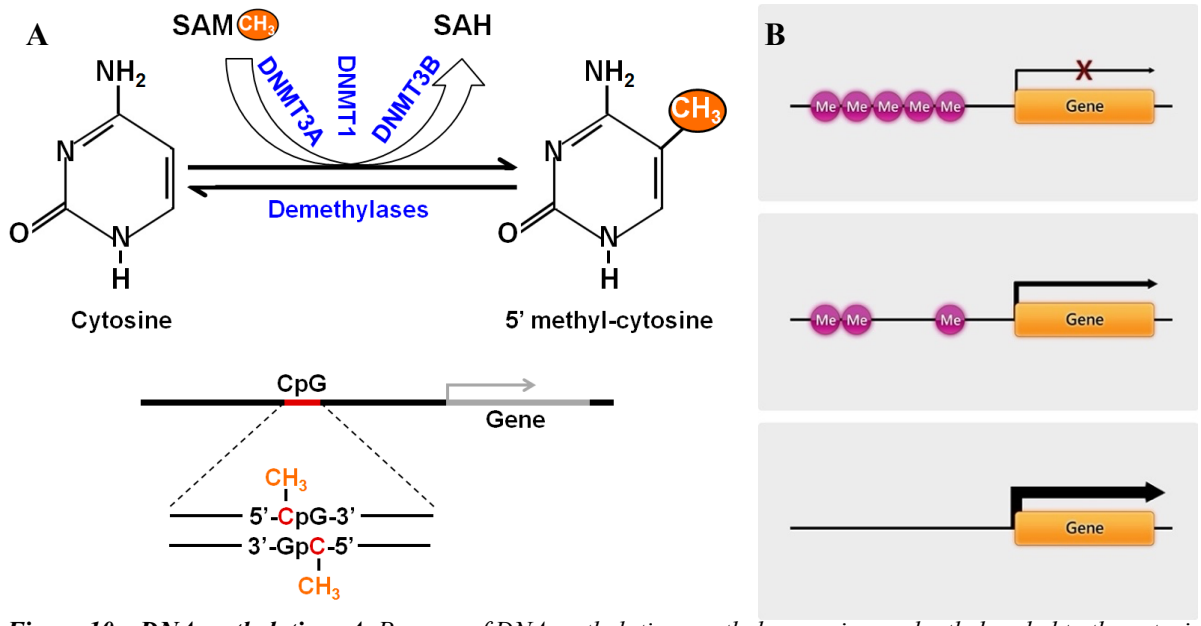

Figure 10 – DNA methylation: A. *Process of DNA methylation, methyl group is covalently bonded to the cytosine to form 5-methylcytosine. The reaction is catalyzed by enzymes called DNA methyltransferase (DNMTs)*[123]. ***B.*** *Methylation of CpG site induces gene expression suppression.*

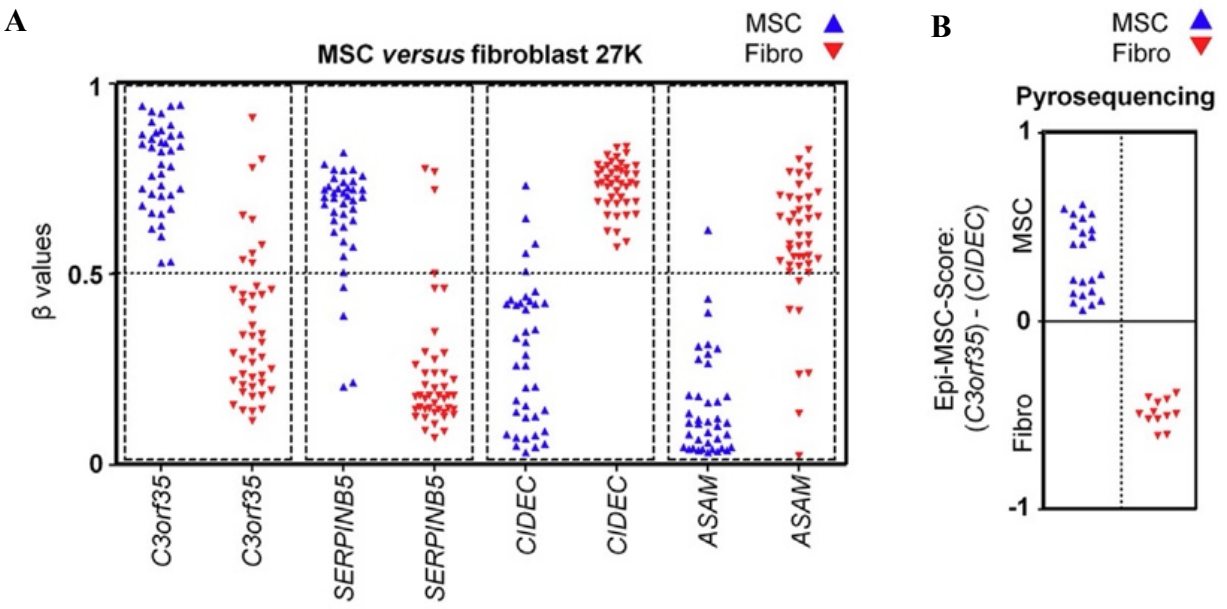

Figure 11 – Epigenetic classification of MSCs and Fibroblasts: A. *Result of a 27K BeadChips to find CpG site that could be used as a marker to discriminate MSCs and Fibroblasts. Four CpG sites situated in C3orf35, SERPINB5, CIDEC, and ASAM genes were found to be differentially methylated between MSCs and Fibroblast.* ***B.*** *Pyrosequencing validation of C3orf35 and CIDEC's CpG sites that can completely discriminate MSCs and fibroblasts*[98].

3.2.3) Multipotency

As a part of minimal ISCT criteria to identify MSCs, hypothesized oDPSCs isolated from sheep must be able to differentiate into three lineages: adipogenic, osteogenic, and chondrogenic. This is achieved by cell culture with differentiation medium. As a control, oDFs can also be submitted to the same media to show absence of differentiation in oDFs culture compared to oDPSCs.

3.2.4) DNA methylation pattern

Epigenetics refers to the study of changes in gene expression that does not produce a change in DNA sequence[120]. Among DNA modification (acetylation, phosphorylation etc), DNA methylation is one of the major DNA modifications[121]. Methylation occurs on a specific CpG dinucleotide (CpG site) often located on a cluster (CpG islands) in the promotor region. It is characterized by the covalent addition of a methyl group at the 5-carbon of the cytosine ring, resulting in 5-methylcytosine[120,121] (figure 10 A).This methylation modification at specific CpG site is a regulatory mechanism by which expression of gene is suppressed[122] (figure 10 B)

As a specific CpG site can be methylated differently depending on the type of cell, epigenetic patterns have been suggested as a way to discriminate cell types. For example, epigenetic signature of B-cell was found to identify subgroup of leukemia[124]. Another study also distinguished pluripotent and non-pluripotent cell by such methylation pattern biomarkers[125]. Such biomarker of MSCs (methylation pattern) could be an interesting tool when specific surface markers are complicated to highlight.

De Almeida et al. discriminated human MSCs from fibroblasts[98] thanks to methylation patterns assessment. Four CpG sites were found to be differentially methylated (figure 11 A) in four genes; *C3orf35, SERPINB5, CIDEC*, and *ASAM*. A ratio between *C3orf35* and *CIDEC* differentiated at 100% MSC and fibroblast (figure 11 B).

Thanks to genome search (ENSEMBL), we found that all these genes are present in the Sheep genome except *C3orf35*. As the conservation of these three genes structures and sequences (*SERPINB5, CIDEC*, and *ASAM)* between human and sheep is not high enough, CpG sites identified in the cited study cannot be target specifically (except for *CIDEC*).
In order to identify hypo- or hyper- methylated CpG sites allowing discrimination between ovine DPSCs (oDPSCs) and ovine Dermal-fibroblasts (oDFs), each methylation pattern of CpG islands can be characterized.

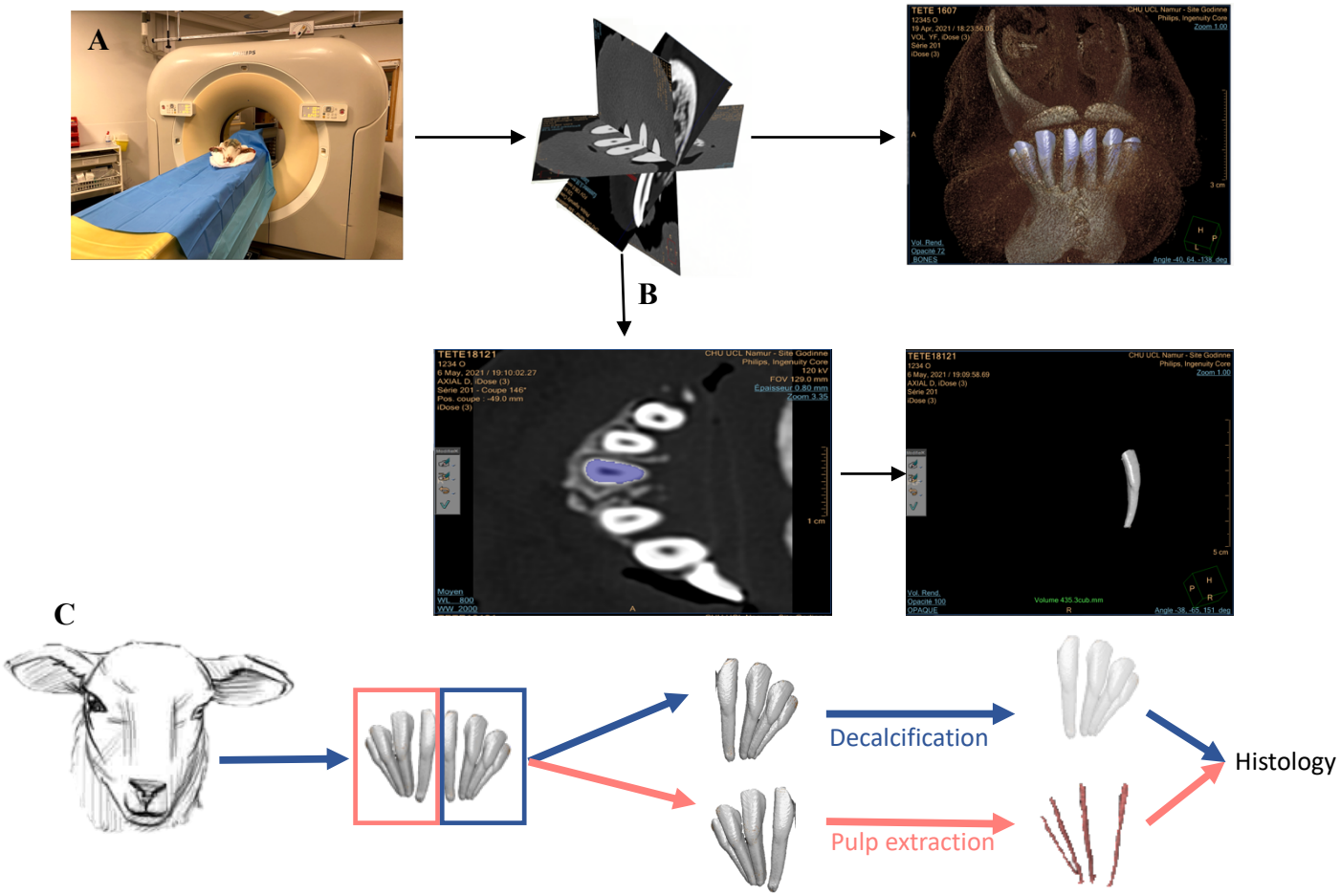

Figure 12: A. *The sheep's head went into the CT scanner to produce image slices used for 3D reconstruction* ***B.*** *Teeth and pulp cavity can be delineated by Philips Intellispace Interface software to generate 3D images and give a volume.* ***C:*** *Preparation of the teeth used for the histological analysis*

Materials and methods

1) Morphometric study of the dental pulp of incisors in sheep

1.1) Animals

Ile-de-France ewes (50 to 75 kg) euthanized for reasons not related to our study (teaching of anatomy, external project) were used. They were healthy and had no mouth pathology. These animals came from the pedigree flock of the breeding farm of the University of Namur. When ewes are no longer suitable for breeding due to loss of fertility or mastitis, they are retired and used for research or teaching. The experimental protocol (10/150/VA) was approved by the local ethical committee for animal welfare.

1.2) CT analysis

For imaging, the number of animals in each category of age depended on availability, i.e: 2-2.5 years (n=3), 3-3.5 years (n=9), 4-4,5 years (n=3) and 6-7 years (n=5) were used, and one additional animal per age (2/4/6 years) was dedicated to histological descriptive study (n=3).
After euthanasia, heads were detached at the atlanto-occipital joint. They were frozen and kept at 4°C before imaging. Images were acquired with a Philips ingenuity Core BZC33 CT unit. Acquisition protocol was 120 kV, 269 mAs with slices of 0,67 mm. After acquisition, the images were assessed using a medical digital imaging system (Philips Intellispace Interface software, CHU Mont Godinne, Belgium).
Volume rendered images of teeth and dental pulp were generated to document the 3D anatomy of the teeth and measure the volume of the dental pulp. Briefly, the outline of the teeth and the pulp cavity was drawn on the Philips Intellispace Interface software (Figure 12 A-B). Once all the outlines were acquired, the software stacked all the slices to calculate volumes and generate 3D images.

1.3) Histology of dental pulp

For the three animals dedicated to histology, left I1 I2, I3, and I4 (figure 12 C) were extracted and crushed with a vice. The dental pulp was harvested and transferred in an Eppendorf containing 10% buffered formalin for 24-h fixation. The specimens were then processed for histology. Briefly, “inclusion” step in paraffin was performed with a HistoCore PEARL (samples were dehydrated through a series of methanol and toluol baths followed directly by 4 paraffin baths). The pulps were embedded in paraffin block using an THERMO SCIENTIFIC Histostar Embedding Center. Blocks were trimmed. After soaking in Mollifex for 2 hours followed by 10 min in ice/water, 6 µm sections were obtained with a microtome. They were transferred on Superfrost Slides and dried overnight at room temperature followed by one-hour oven drying at 40°C. The samples were stained with Hematoxylin-Eosin-Safran (HES) using an automated Tissue Stainer COT 20 by Medite. Sections were observed with an Olympus BX63 microscope (Olympus, Tokyo, Japan) equipped with Hamamatsu Orca-ER camera and images were acquired with the Cell Sens software.

1.4) Histology of teeth

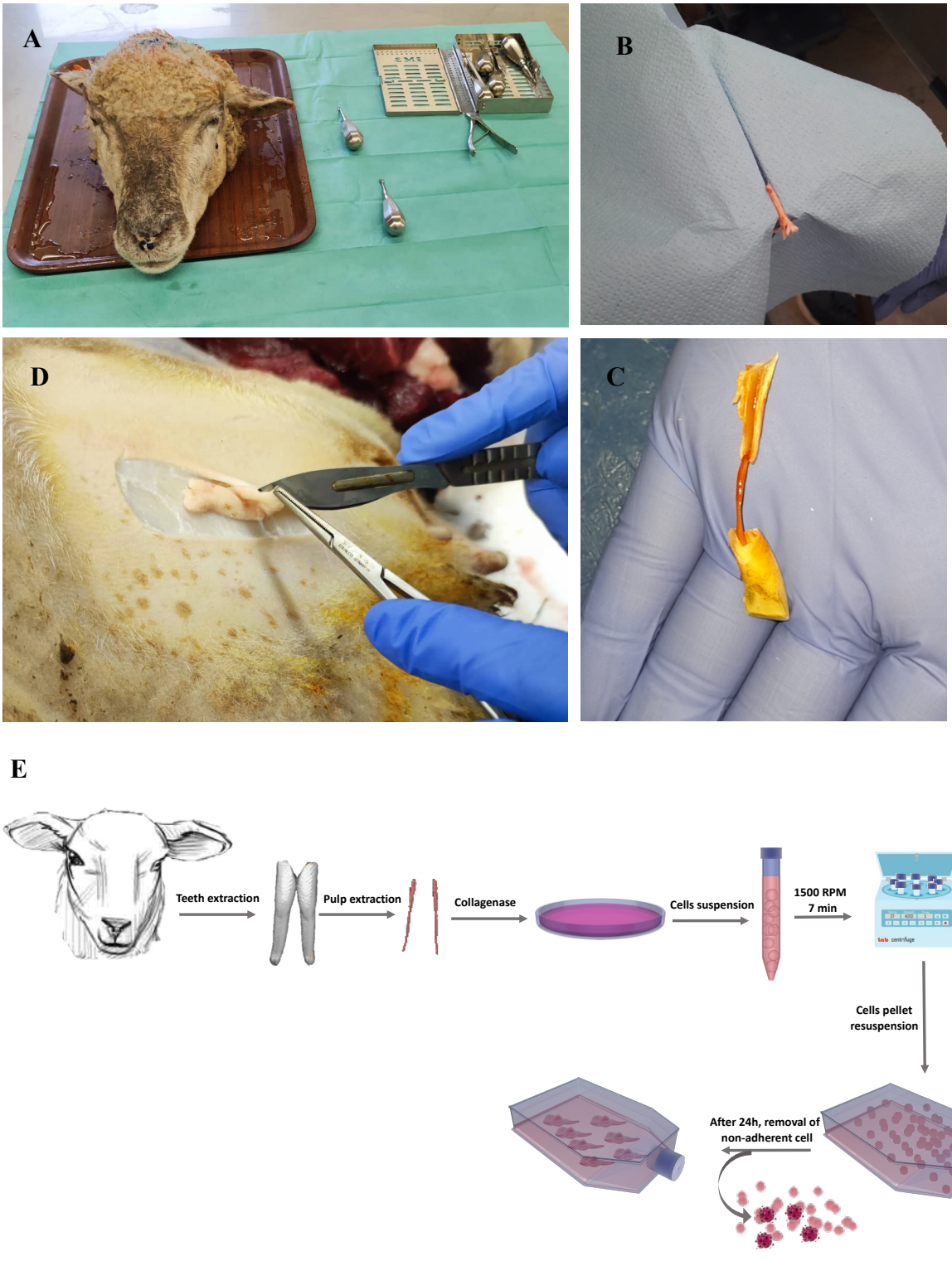

Figure 13 - A. *Sheep head prepared on sterile area, there was sterile instruments to extract incisors* ***B-C.*** *Incisors were crushed with a bench vise clamp to access the dental pulp* ***D.*** *Biopsy of dermal* ***E.*** *oDPSCs isolation; dental pulp was extracted from teeth and incubated with collagenase. Cell suspension was centrifuged, and pellet resuspended into medium. The cell suspension was incubated for 24h hours in culture flask and then non adherent cells were removedl from the culture.*

Right incisors I1 I2, I3, and I4 (figure 12 C) were extracted and immersed in 10% buffered formalin for 48 h. After fixation, decalcification was performed with 10% formic acid in 4% formalin solution in a 1L beaker for 10 days under magnetic-bar agitation (Choube et al. 2018). All specimens were checked every two days for decalcification status and the decalcification solution was renewed. Complete decalcification was determined by chemical methods (Culling 1974, Drury and Wallington 1980). Briefly, 10mL of 5% ammonium hydroxide-5% ammonium oxalate solution (V/V) was added to 5 mL of the decalcification solution containing the teeth. Absence of calcium oxalate precipitate after 30 minutes was an indicator of advanced decalcification. When the chemical methods indicated that advanced decalcification had been reached, the physical method was used as a control. It consisted of inserting a small needle in the sample. If it went through the sample easily, it indicated that decalcification was achieved. After PBS wash, teeth were cut in the sagittal plane and placed in ethanol 70% for 24 hours before inclusion. The paraffine inclusion and embedding were performed as previously described (1.3), with an overnight Mollifex incubation. Section, staining, and analysis steps were also similar as those used for dental pulp.

1.5) Statistical analysis

In R studio, a mixed linear model was produced. The departure modalities were three factors; age (four modalities: 2-, 3-, 4-, 6- years old), teeth (4 modalities: for I1-I2- I3-I4) and animal. Statistical analysis (paired t-test, Friedman test) was performed.

2) Characterization of oDPSCs

2.1) Dental pulp stem cell's isolation

Freshly euthanized sheep were used. Jaws and teeth were scrubbed with betadine soap three times followed by ethanol. Both I_1 were extracted with sterile dentistry equipment (figure 13A) and crushed sterilely with a bench vise clamp to harvest the pulp (figure 13 B-C). Pulps were then maintained in a Complete Medium overnight at 4°C, or directly processed for DPSCs isolation. Complete medium was alpha-MEM (Lonza BioWhittaker BE1-2-169F), with 10% decomplemented FBS (Gibco, 10091-148), 0.5% Penicillin/streptomycin 10.000mg/mL (Gibco, 15070-063), 0.5% of fungin (*InVivo* gen, ant-fn-1) and 1% Glutamax (Gibco 35050-061).
Pulps were cut into 1-2mm^3 pieces and rinsed with PBS, then incubated for an hour at 37°C with 2 ml of sterilized collagenase solution (3mg/mL in pure alpha-MEM (Sigma-Aldrich C9891)). Collagenase was then deactivated by adding 13 mL of complete medium. The solution was homogenized to totally disrupt the tissue, which was then passed through a 70-μm filter.
Cell suspensions were then centrifuged at 1 200 RPM for 7 min. Cell pellets were resuspended into 7mL of complete medium and transferred in a T-25 flask and incubated at 37°C, 5% CO_2. After 24h, non-adherent cells were removed by removal of the medium (figure 13 E). The medium was replaced every 2/3 days.
At confluence (around 21 days), cells were rinsed with PBS and detached by trypsinization (TRYPSIN, 0,05%-EDTA, Lonza, BE17-161E) at 37°C for 1-5 minutes. Cell suspensions were centrifuged for 7 min at 1200 RPM, rinsed, and resuspended (=one passage).

Table 1. Primer sequences for transcriptome profile by qRT-PCR

Gene	Sequence
oCD90	Sense 5'-GAATACAGCTCCCGAACCAA-3' Antisense 5'- GAGAGGCGGAGTTCACATGT-3'
oCD45	Sense 5'- AAATGCTTCACGGACGAAAG-3' Antisense 5'-CCGAGGTAGTTCCAATTCTCA-3'
oCD105	Sense 5'- GATAGGATCAACCCTGGCTTC-3' Antisense 5'- GAGCTCCACGAAGGATGCTA -3'
oCD73	Sense 5'-CACTGGGAAATCACGAATTTG-3' Antisense 5'-CCCTTGGCTTTAATGTTTGC-3'
oCD34	Sense 5'-AGCAGCCACCAGAGCTATTC-3' Antisense 5'- GCGGTTCATCAGGAAATAGC-3'
oITGA11	Sense 5'-ATGGATGAGAGGCGGTACAC-3' Antisense 5'- GTGGAAGTTGATCCGCTCAC-3'
oHOXA5	Sense 5'-CCCGGACTACCAGTTGCATA-3' Antisense 5'-TTGTAGCCGTAGCCGTACCT-3'
oCXCL12	Sense 5'-CAACGTCAAGCACCTCAAGA-3' Antisense 5'-GCTTCGGGTCAATGCATACT-3'
oCD44	Sense 5'-ATGGTCGCTACAGCATCTCC-3' Antisense 5'- GCAGGTCTCAAACCCTATGC-3'
oCD10	Sense 5'-ACTGATCCAGAACATGGATGC-3' Antisense 5'- GCTGGTCTCAGGAATGACGT-3'
oMYH11	Sense 5'-GAGCGAAAACTCCTTGAAGAGA-3' Antisense 5'-TCGTGCTTATTTTTCAATTTGG-3'
oMDK	Sense 5'-CCGACTGCAAGTACAAGTTTGA-3' Antisense 5'- GTCACTCGGATGGTCTCCTG-3'
oGAPDH	Sense 5'-GGCGTGAACCACGAGAAGTATAA-3' Antisense 5'-CCCTCCACGATGCCAAAGT-3'
oβ-actin	Sense 5'-CTGGCACCACACCTTCTACAAC-3' Antisense 5'- GAGGCGTACAGGGACAGCAC-3'
oNANOG	Sense 5'- GAGTGTGGACCCAGCTTGTC-3' Antisense 5'- ATTTGCAAGGACGCGTAACT-3'
oOCT3/4	Sense 5'-ACACCTCGCTTCTGACTTCG-3' Antisense 5'-ATCCCTCCGCACAAGTCATA-3'
oSOX2	Sense 5'-AACGGCAGCTACAGCATGAT-3' Antisense 5'- GCCCTGCTGAGAATAGGACA-3'
oCD271	Sense 5'- CCCTGGACGTTGGATTACAC-3' Antisense 5'-CTCTTGAAGGCGATGTAGGC-3'
oNOTCH1	Sense 5'- CTCCCAGCACAGCTACTCGT-3' Antisense 5'- GAGATGCCCTCAGACCAATC-3'
oKRT18	Sense 5'-TCCACCTTCTCCAACTACCG-3' Antisense 5'-CTTGCATGGTCTCCTTCTCG-3'

2.2) Fibroblast's isolation

Fibroblasts were isolated to compare the characterization profile of oDPSCs with totally differentiated cells.Fibroblast were isolated from freshly euthanized sheep's dermis. Briefly, skin was shaved and disinfected, then the epidermis was scratched to reach the dermis. A biopsy was then collected and transferred into fibroblast complete medium (DMEM (Lonza BioWhittaker cat: 12-604F lot: 0000718561) with 10% decomplemented FBS (Gibco, 10091-148), 0.5% penicillin/streptomycin 10.000mg/mL (Gibco, 15070-063), 0,5% of fungin (*InVivo* gen, ant-fn-1), and 1% Glutamax (Gibco 35050-061). The biopsies were cut in 1mm^3 fragments and transferred into a 12-well culture plate. Fragments were maintained on the bottom of the well by coverslips. After 7 to 10 days, fibroblasts adhered to the well and coverslip. Cells were harvested by trypsinization and transfered into a T25 flask. Fibroblasts were also isolated with collagenase treatment as described for DPSCs.

2.3) Transcriptome profile

2.3.1) Real-Time quantitative Reverse Transcription - Polymerase Chain Reaction (RTq-PCR)

In order to better characterize oDPSCs, RTqPCR for several genes were performed. It was also done on oDFs to assess an enrichment of DPSCs in our pulp's extract, but also to compare DPSCs with differentiated cells. Cells were rinsed with PBS and detached with trypsin, cells were then centrifuged, rinsed and counted. One million cells were resuspended into Trizol Reagent for RNA extraction (Life Technologies, Bleiswijk, NL). RNA extraction was conducted according to the manufacturer's instructions with a purification step using High Pure RNA Tissue Kit (Roche Diagnostics, catalogue #2033674). Briefly, after 5 min of incubation at RT, the cell lysate was centrifuged for 5min at 12.000g. Supernatant was transferred in an Eppendorf and chloroform (1/5 volume of Trizol) was added. Tubes were then strongly stirred with a vortex, incubated for 3min and centrifuged 15min at 12 000g. The upper phase was then transferred into a clean Eppendorf and 70% ethanol was added. Next, the solution was transferred into a purification column (High Pure RNA Isolation KIT ROCHE cat.11828665001) and processed with DNAse following three washes and harvested with manufacturer's buffers. RNA concentration was measured using a Nanodrop 1000 (Thermo Scientific). RNA was reverse transcribed using the High-Capacity cDNA reverse transcription Kit according to the manufacturer's instructions (Applied Biosystems, Thermo Fisher Scientific). Subsequently, cDNA was amplified using specific primers targeting selected genes (see table 1 for primer sequences and 2.3.1 for design method) with the Takyon SYBR green according to the manufacturer's instructions (Eurogentec, Liège, BE) in a Light Cycler 96 system (Roche Diagnostics, Mannheim, DE). Relative gene expression was calculated by the 2^-ΔΔCT method with GAPDH as housekeeping gene, fibroblast ΔCT mean was used as reference for the 2^-ΔΔCT.

2.3.2) Primer design

The sheep's genome from Ensembl was used as a template to design primers for mRNA target (Sheep. Oar_rambouillet_v1.0).
Exons sequences were used as a target to design primers with Primer3 (v.0.4.0). Once primers were proposed, the specificity was tested *in silico* on the sheep's genome with Primer Blast. Only primers with 100% specificity for the target mRNA were selected.

2.3.3) *Statistical analysis*

On Graphpad Prism software, Mann-Whitney test (non-parametric equivalent to independent samples t-test) was used on ΔCT and ΔΔCT to assess a statistically significance difference.

2.4) Differentiation into multiple lineages

One major characteristic of MSCs is the *in vitro* multipotency. This can be assessed by inducing differentiation with specific media. oDPSCs and oDFs were subjected to three differentiation media:

2.4.1) *Adipogenic differentiation*

Adipogenic differentiation was performed according to the manufacturer's guidelines (STEMCELL TECHNOLOGIES, catalog #05412). oDPSCs were seeded in 6 wells-plates at a density of 20 X 10^3 cells/well. Control oDPSCs and oDFs (cultured with complete medium without differentiation supplement) were fixed when confluence was reached. Other oDPSCs and oDFs were incubated with adipogenic differentiation medium 24h post-seeding. This differentiation medium was changed every 2-3 days. After eleven days of differentiation, cells were tested to assess the differentiation:

- Colorimetry: cells were rinsed with PBS and fixed with a 4% formalin solution for 30 minutes at RT. The cells were then rinsed and incubated with 0.1% Oil Red O (ORO) staining under soft agitation for 30 min to color oil droplet. To quantify the ORO, the wells were washed four times with distilled water following a wash with 50% ethanol. Afterward, ORO was extracted with 500μL of 100% isopropanol and absorbance was measured at 415 nm. The amount of ORO was quantified using a standard curve produced with a serial dilution of ORO in isopropanol (from 2 to 0,015 mg/mL).

- RTq-PCR: RNA extraction and RTq-PCR were conducted as previsouly described. Specific primers targeting adipogenic specific genes o*C/EBP-alpha* and o*ADIPOQ* were used (primer sequences are described in Table 2). Relative gene expression was calculated by the 2-ΔΔCq method with GAPDH as a housekeeping gene.

2.4.2) *Chondrogenic differentiation*

Chondrogenic differentiation was performed according to the manufacturer's guidelines (STEMCELL TECHNOLOGIES, catalog #05455). Once cells were harvested and counted, pellets containing 2.5 x 10^5 oDPSCs were formed into 15 mL-falcon by centrifugation at 300g for 7min. The pellets were subjected to chondrogenic differentiation medium with medium change every 2-3 days. Control cells were cultured with complete medium without chondrogenic differentiation supplement. After three weeks of differentiation, cells were tested to assess the differentiation:

- Colorimetry: pellets were rinsed with PBS and fixed with 4% formalin at RT for 30min. Pellets were then covered by agarose gel (agarose was added to the tube and the pellets bring up with a tips) to be processed for histology as previously described. Once the slides were ready, Alcian blue coloration was performed.

Table 2. Primer sequences of differentiation assessment.

Gene	Sequence
oC/EBP-alpha	Sense 5'-TGGACAAGAACAGCAACGAA -3' Antisense 5'-CGGTCATTGTCACTGGTCAG-3'
oADIPOQ	Sense 5'-GCTGGGAGCTCTTCTACTGC-3' Antisense 5'-TCCTTTCTCACCCTTCTCACC-3'
oACAN	Sense 5'-AGTGTCAGCATCCCTGAACC-3' Antisense 5'-GATATGCGGCTCCACTTGAT-3'
oRUNX2	Sense 5'-TTTGTTCTCTGATCGCCTCA-3' Antisense 5'-AGGACTTGGTGCAGAGTTCAG-3'

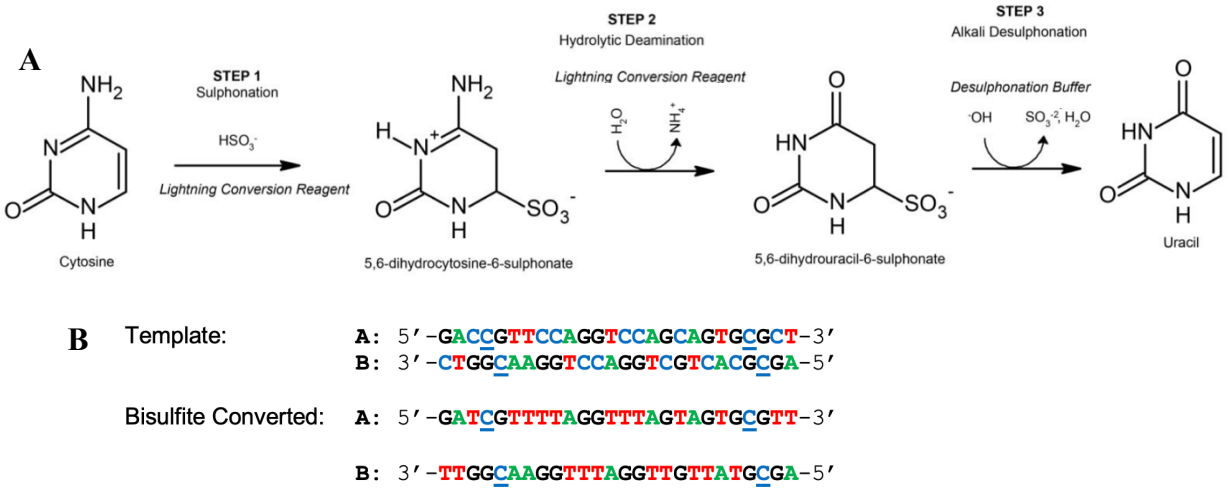

Figure 14 – Bisulfitation treatment of DNA: A. *Reaction of bisulfite conversion. Steps 1 and 2 occur during bisulfite conversion with buffers, while step 3 is performed when DNA is bound to a column matrix.* ***B.*** *Illustration of a bisulfited sequence. Methylated "C" are underlined. Following bisulfitation, all Cytosine molecules are converted to Uracil except methylated C, after PCR "U" are deducted to be T (Data sheet of EZ DNA Methylation-LightningTM Kit by Zymo Research).*

- RTqPCR: RNA extraction and qRT-PCR on the pellet were performed as previously described. Specific primers targeting chondrogenic specific gene *oACAN* were used (sequences on table 2).

2.4.3) Osteogenic differentiation

Osteogenic differentiation was performed by complementing culture medium with 0.1µM dexamethasone, 10mM β-glycerophosphate disodium salt hydrate, and 50µM ascorbic acid. oDPSCs were seeded in a 12 well-plate at a density of $1x10^5$cells/well. Control cells were cultured with complete medium without osteogenic differentiation supplement and fixed at confluence. Twenty-four hours post-seeding, cells were incubated with osteogenic differentiation medium. The differentiation medium was changed every 2-3 days. Control cells were cultured with complete medium without osteogenic differentiation supplement. After three weeks of differentiation, cells were tested to assess the differentiation:

- Colorimetry: cells were rinsed with PBS and fixed with 4% formalin for 30 minutes at 37°C. The cells were then rinsed with distilled water and allowed to air dry. The cells were then incubated with 500μL of 0,1% Alzarin Red (AR) solution under agitation for 15 min. Next, three washes with water were performed. To quantify the AR, 500μL of 5% formic acid was added to the wells to extract the dye. Absorbance was then measured at 450 nm. The amount of AR was quantified using a standard curve produced with a serial dilution of AR in 5% formic acid (from 2 to 0,015 mg/mL).

- RTqPCR: Cells were processed as previously described (see 2.3.1) for assessment of expression of osteogenic specific gene *oRUNX2* (sequences on table 2)

2.5) Methylation pattern

2.5.1) Genomic DNA extraction

Genomic DNA was extracted on 10^6 cells pellet of oDermal Fibroblast and oDPSCs according to the manufacturer instructions (DNeasy® Blood & Tissue Handbook, Qiagen). Briefly, cells were incubated with proteinase k and lysing buffer. Afterward, DNA was precipitated with an ethanol-based solution and purified using DNeasy Mini spin column (DNeasy® Blood & Tissue Handbook, Qiagen). After several washing, DNA was eluted and then quantified using a Nanodrop 1000 (Thermo Scientist).

2.5.2) DNA bisulfitation

Bisulfite treatment (figure 14) was performed with the EZ DNA Methylation-Lightning™ Kit (Zymo Research cat. D5030T, D5030, D5031) according to the manufacturer's recommendations: 500ng of genomic DNA was added to the first conversion reagent and placed in a thermocycler to complete following steps: 98°C for 8 minutes, 54°C for 60 minutes. The next steps were accomplished on the zymo-spin IC column where the last conversion buffer was added, followed by repeated washing and elution of bisulfited DNA.

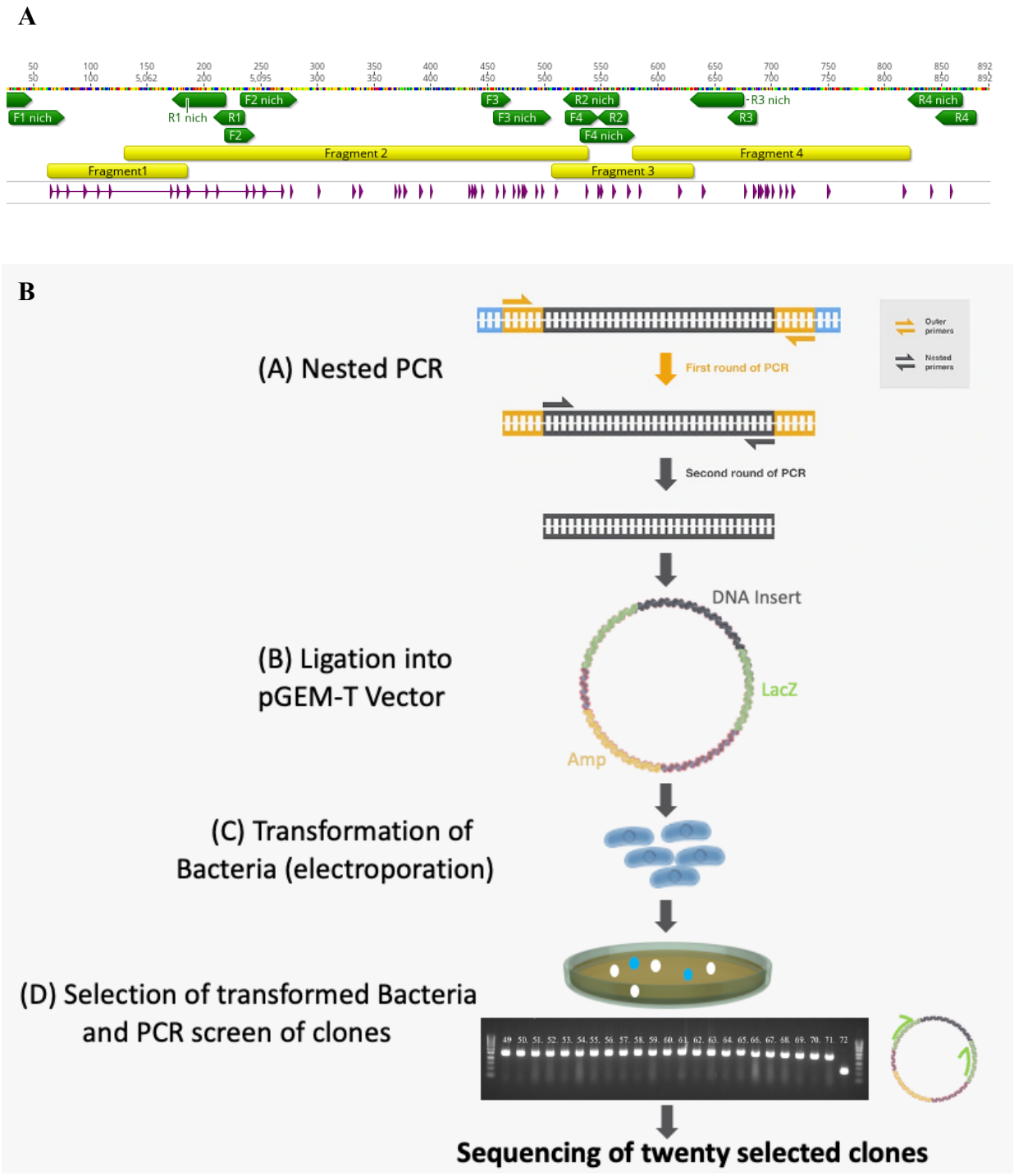

Figure 16 – Method used to determine methylation pattern of CpG island: A. *Primer were design to cut the CpG island into fragment of 250-300pb. Primers are in green, fragment in yellow, and CpG site represented by purple triangle* ***B.*** *Genomic DNA is bisulfited as described in 2.5.2. Once treatment accomplished, nester PCR was used to amplified target region of CpG island. Once amplified, the PCR product was inserted into a pGEM-T vector and transformed into bacteria by electroporation. Twenty-four transformed bacteria (clone) were selected by blue-white screen and presence of targeted insert was confirmed by PCR screen.*

2.5.3) Polymerase Chain Reaction (PCR)

Nested PCR of bisulfited DNA was performed using primers for *oASAM*, *oSERPINB5*, *oCIDEC* targeting specific CpG islands detected in promotor region with Geneious software (see Table 3 for primers sequence and 2.5.5 for primer design). If the CpG island exceeded 300-350 nt, the sequence was fractioned with multiple primer coupling. Amplicons were named according to the fragment number, for instance "CIDEC-1" for the first fragment," CIDEC-2" for the second fragment etc. (figure 16A).
PCR was performed with the Epimark HotStart Taq DNA polymerase (New England BioLabs) or according to the manufacturer's instructions. Thermocycling condition were: (1) 95°C for 30 seconds (2) 35 cycles of 95°C for 30 seconds, 50°C for 30 seconds, 60°C for 1 minutes (3) 68°C for 7 minutes. .
After control of amplicons on an agarose gel, produced amplicons were cloned into the pGEM-T Easy Vector system (Promega) followed by transformation of bacteria (*E.coli*) by electroporation. Transformed bacteria were selected by using white-blue screening. Following this, PCR screening of 24 colonies was performed and maximum 20 clones with the expected insert length were send to sequencing (EUROFINS GENOMICS), see figure 16B.

2.5.4) Data analysis

Following sequencing, DNA sequences were "cleaned" by removing vector DNA from the sequence. Cleaned sequences were then aligned in Geneious software with in-silico bisulfited sequence to assess the number of clones methylated in CpG site. After bisulfitation treatment, if dinucleotide CG were seen to be TG, the cytosine was not methylated. If the CG was still there, cytosine was methylated. The percentage of methylation was then calculated based on the number of clones (figure 17).

2.5.5) Primer's design

Primers were manually designed on Geneious prime software with *in silico* bisulfited sequence as a template. Primers were between 20 and 35 nt long and should target a region without CG dinucleotide (only one CG maximum, if no other options). All primers were tested *in silico* for self-interaction and couple primers interaction.

2.6) Surface antigen analysis

ISCT proposed a cell surface marker panel for minimal identification of MSCs. The cells must be positive for CD73, CD90, and CD105 whilst negative for CD34, CD45, CD11b or CD14, CD19 or CD79α, and HLA-DR. oDPSCs and oDFs were characterized for these markers with the Human MSC analysis Kit (BD Stemflow ™). Cells were harvested using accutase (StemPro® Accutase® Cell Dissociation Reagent, Gibco), pelleted by centrifugation, rinsed and fixed 15 min with 4% formalin, and washed. Cells were then resuspended in PBS and the antibody cocktails were added. The positive cocktail contained antibodies against CD90, CD105 and CD73 antibodies. The negative cocktail contained antibodies against CD34, CD11b, CD19, CD45 and HLA-DR.
Three other antibodies described in the literature for ovine cells were tested[126]; CD73 (PE rat anti-mouse CD73 cat: 550741, clone TY/23 BD Pharmingen), CD90 (APC mouse anti-human CD90 cat: 559869, clone 5E10) and CD45 (mouse anti sheep CD45:FITC, Bio-Rad catalogue MCA2220F, clone 1.11.32).

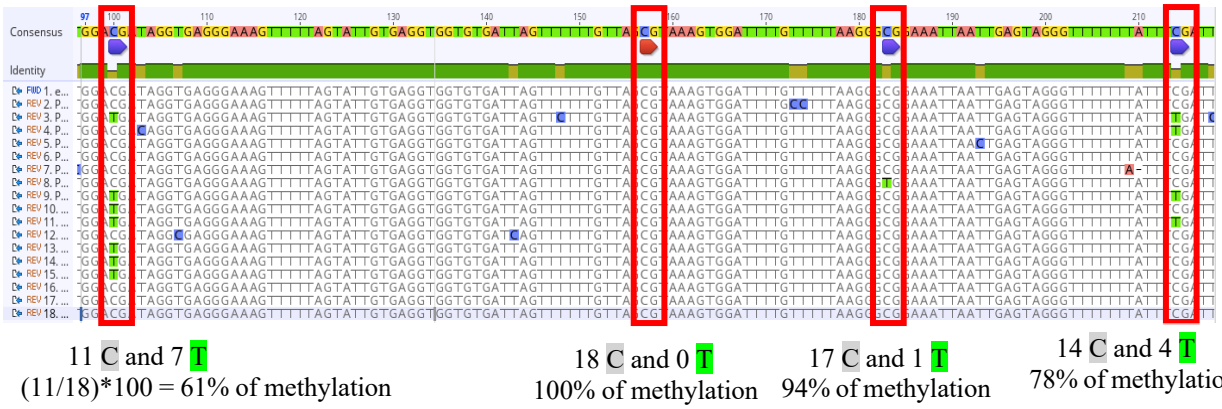

Figure 17 – Data analyzing for methylation pattern: *Sequences were aligned with in-silico bisulfited sequence. Dinucleotide CG was considered as methylated if CG was conserved after bisulfitation treatment. If not, the CG is represented as TG dinucleotide. A percentage can then be calculated with methylated sequences in ratio with all sequences.*

Table 3. Primer sequences for nested PCR of bisulfited DNA.

Gene	Sequence
oCIDEC (1)	Outer primers: Sense 5'-TAAAAAGGTAGTTTAAAATGAGGTTTAA -3' Antisense 5'-ACACCTCCCAAATCCCCTC -3' Nested primers: Sense 5'-AAAATGAGGTTTAATTAGGAGTTAGG -3' Antisense 5'- -3'
oCIDEC (2)	Outer primers: Sense 5'- TGTTAGGTGGAGGGGATTTG-3' Antisense5'-AAACTATTAACTTAACTAAACTAAAACAATAC-3' Nested primers: Sense 5'-GAGGGGATTTGGGAGGTG-3' Antisense 5'-ACTTAAAAAACTCCAAAAATCTAAAC-3'
oCIDEC (3)	Outer primers: Sense 5'-TTTTTTTYGTTTAGATTTTTGGAG-3' Antisense 5'-ATTCTAAAAAATCAACTTCAACCC-3' Nested primers: Sense 5'- GTTTAGATTTTTGGAGTTTTTTAAGT-3' Antisense 5'-CTTAACAAAACCCCCAAACAC-3'
oCIDEC (CpG site)	Outer primers: Sense 5'- GGAAAGAGTAGTTTTAGTTTATGGG-3' Antisense 5'-TAACCCCTAATTCCAATCACAC-3' Nested primers: Sense 5'- TTATGGGGTGTTTGGTTTGG-3' Antisense 5'-CCAATCACACTAATAAAAAATCCC-3'
oSERPINB5 (1)	Outer primers: Sense 5'- GAGGTTTTTAGAAGTTGTGTAGATAATAG-3' Antisense 5'-AAACAAAAACACCACCAAACC-3' Nested primers: Sense 5'-AAGTTGTGTAGATAATAGTAATTTTAGTTTG-3' Antisense 5'- AACACCACCAAACCCTACTACC-3'
oSERPINB5 (2)	Outer primers: Sense 5'-TTTTGAGATGATTTGTAATGGTGTA-3' Antisense 5'-CCTCAAAACAATCTAAACTCCAA-3' Nested primers: Sense 5'-TGTAATGGTGTAGAGGGGGTAG-3' Antisense 5'-AACAATCTAAACTCCAAAACAAAAC-3'
oSERPINB5 (3)	Outer primers: Sense 5'-TTAGTTTTGTTTTGGAGTTTAGATTG -3' Antisense 5'-TCCCTAAAAAAAAAACTAAAAACC-3' Nested primers: Sense 5'-GTTTTGGAGTTTAGATTGTTTTGAG-3' Antisense 5'-AAAAAAACTAAAAACCAACCTATTC-3'
oASAM (1)	Outer primers: Sense 5'-GAGAATTGGTTGAAAGTGTGATG-3' Antisense 5'-CCAAATACCTAAAACTCTACCCAC-3' Nested primers: Sense 5'-AGTAGTTTGTTAGGTTTAGGGATGA-3' Antisense 5'-CTAAAACTCTACCCACCAAAACC-3'
oASAM (2)	Outer primers: Sense 5'-GGGGTTTTGGTGGGTAGAG-3' Antisense 5'-ACTTCCCRGTCTTCCCTTC-3' Nested primers: Sense 5'-GTGGGTAGAGTTTTAGGTATTTGG-3' Antisense 5'-ATCCTRGCTCTTTCCCTCTC-3'
oASAM (3)	Outer primers: Sense 5'ATTTTAGGGTGGGTTGTTGG-3' Antisense 5'-CTTCCATCTCTCTCCATTTCTCT-3' Nested primers: Sense 5'-GGGTGGGTTGTTGGGATTAT-3' Antisense 5'-CTTTTACATTCTCCTTACCTCTCC-3'
oASAM (4)	Outer primers: Sense 5'-AGGAGGTGGGAGAGGTAAGG-3' Antisense 5'-AAACRGAAAACACTTAAACCAC -3' Nested primers: Sense 5'-GTGGGAGAGGTAAGGAGAATGTA-3' Antisense 5'-AARGAAAATAAAACCTTATCAATCT-3'
oASAM (5)	Outer primers: Sense 5'-GYGAAGTGGAGAGATGAGGA-3' Antisense 5'-AAAAAAAAAATAAACTAAAACCACAT-3'

	Nested primers: Sense 5’-AGAGATGAGGAYGAAGTGAGGA-3’ Antisense 5’-AACCACATAATTACCTCCCACC-3’
oASAM (6)	Outer primers: Sense 5’-TTTTTTTTTAAATAGGGAAAAGTGT-3’ Antisense 5’-AACTCCCCAAACACTCACCTA-3’ Nested primers: Sense 5’-AATAGGGAAAAGTGTTTTAYGAAG-3’ Antisense 5’-CAACAAAACAAAAAAAATCATCC-3’
oASAM (7)	Outer primers: Sense 5’-TTTTGTTGGGGTTAGGTGAGT-3’ Antisense 5’-CCCTAATTCTCCACTTTCCCTA-3’ Nested primers: Sense 5’-GTTAGGTGAGTGTTTGGGGAGT-3’ Antisense 5’-TCCACTTTCCCTAAATACCCTT-3’

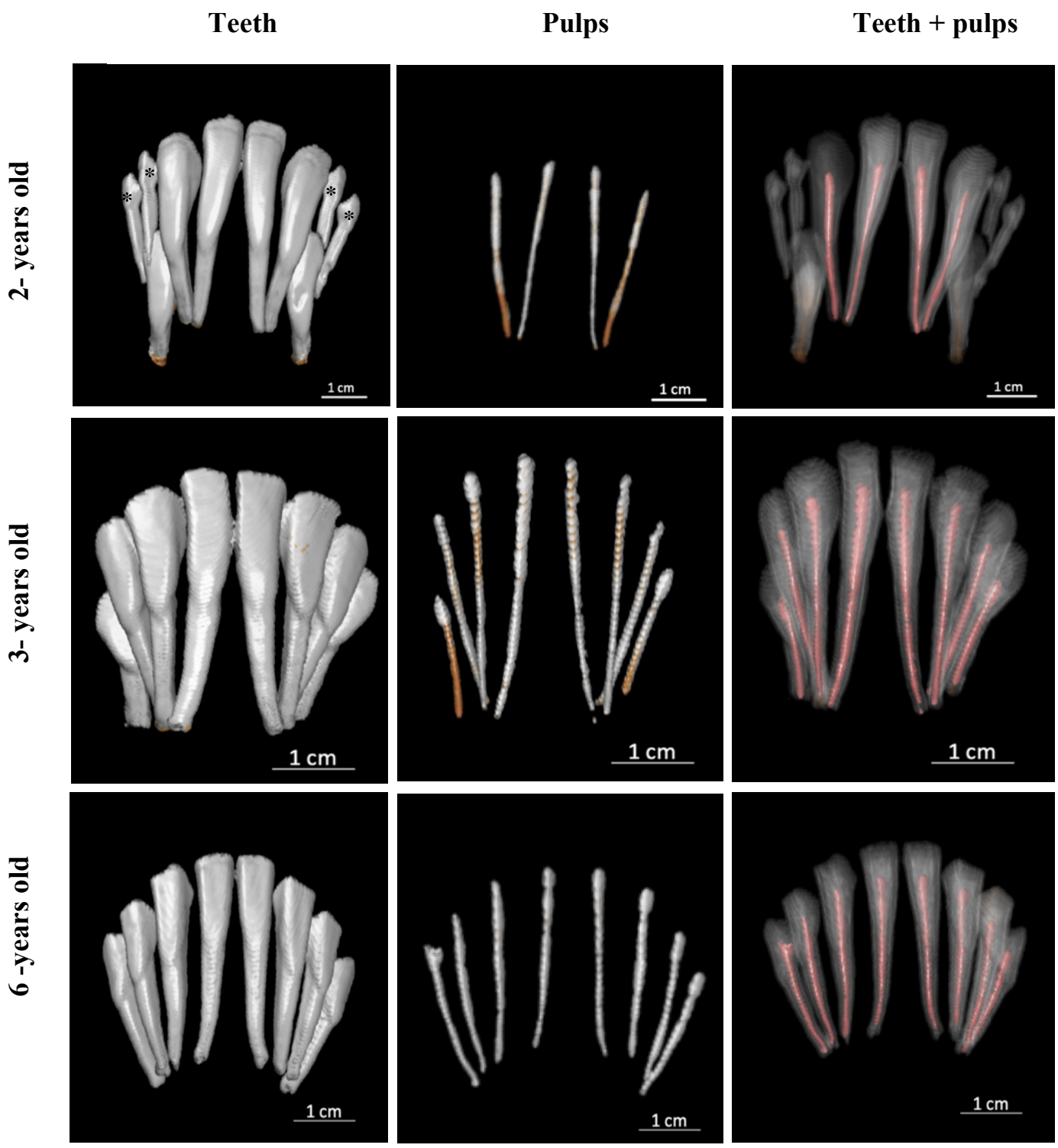

Figure 18: 3D reconstruction of teeth and dental pulp of sheep. *Images show 3D reconstructed teeth and dental pulp of a 2-, 3-, and 6- years old sheep. Decidual teeth are shown with *.*

Results

1) Morphometric study of the dental pulp of incisors in sheep

1.1) Computed tomography

1.1.1) Images

CT enabled to produces 3D images of all incisors, as well as to recognize permanent from decidual teeth (figure 18). Decidual teeth were identified only in I3 and I4 in the youngest animals. All teeth in all other animals were adult (permanent teeth). An illustration of reconstructed dental pulp is shown in figure 18.

The dental pulp volumes of erupted adult teeth were quantified. All the values are shown in a descriptive graph (figure 19 A) and means with confidence interval (CI) are represented on figure 19 B and table 4 for quantified values.

A mixed linear model was created, it takes in account three variable: the teeth, the animal, and the age. As the number of 3-year-old sheep was the highest, the volume results were used as a baseline to compare with other ages (figure 19 C, left part). The predicted volumes (from the mixed linear model) can be seen on table 5. To compare the volume of pulp in function of the position of the teeth, I1 was used as the baseline (figure 19C, right part). The data was analyzed by handling missing values by two ways: removing the empty columns (red color), or replacing the dental pulp volume by 0 mm^3 (blue color).

The model estimated the mean volume of dental pulp at 3-year-old as 33.69mm^3 (std. error 1.88, p.val< $1.09.10^{-12}$). At 4-year-old, there is a decrease of pulp volume, with a loss estimated at 9.39 mm^3(std. error 3.59, p.val<0,019). The greatest decrease was observed at 6-year-old, were the model estimate the lost at 11,48 mm^3 (std. error 3.01 mm^3, p.val<0.00176). The results are substantially the same if missing values were replaced by 0. However, at 2-year-old, depending on replacing or removing the missing value, the result is different. If missing values are removed, the total volume is higher than at 3-year-old; +5.45 mm^3 (std. error 4.30, p.val>0,05), if they are replaced by 0, a decrease of 5.49 mm^3 (std. error 3.63, p.val>0.05) is observed.

The model showed a decrease of dental pulp volume with the position of the teeth. The highest volume is found in I1, decreasing progressively with I2 (-3,99 mm^3), I3 (-8,54 mm^3) and I4 (-12,80 mm^3). Some differences in the result are observed if missing values are replaced by 0 in I3 and I4; respectively -10,51 mm^3 and -16,19 mm^3.

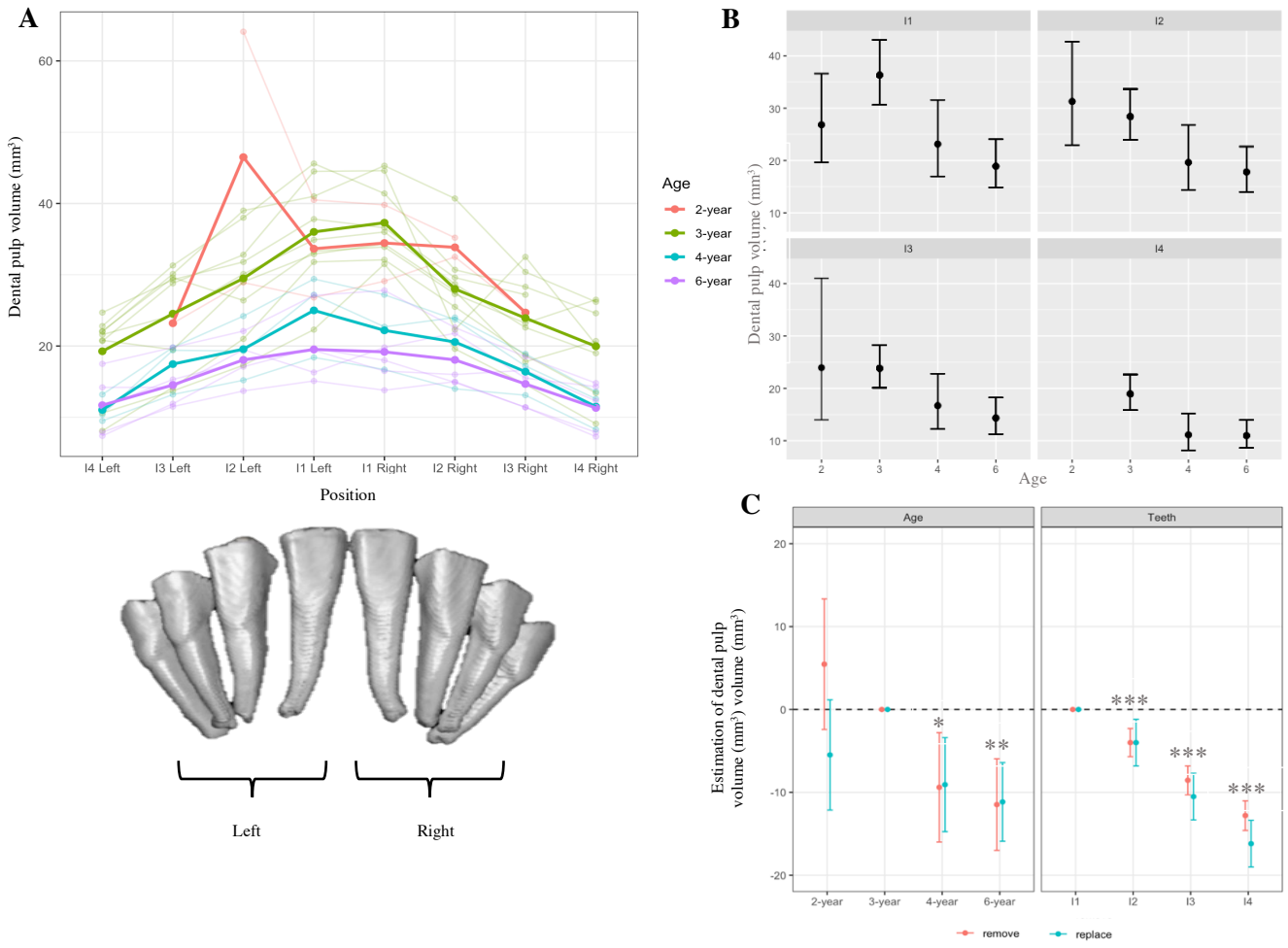

Figure 19: Dental pulp volume quantification and linear mixed model. A. *Descriptive graph showing all the value of dental pulp volume for each age and which teeth (means are overlined)* ***B****. dental pulp volume's means are shown with confidence interval (CI)* ***C. Age:*** *linear mixed model estimated total dental pulp volume at each age. Three-year-old group were the most numerous, so it was used as the baseline to compare each age. Two ways were used to handle missing value; removing the column or replacing by 0. It is possible to see a statistically significant decreasing of dental pulp volume with age.* ***Teeth:*** *I1 was used as a baseline to compare other teeth position. It is possible to see a statistically significant decreasing of dental pulp volume with teeth position.*

Table 4: Measured values of dental pulp volume by CT scan (with CI).

Teeth / Age	I1	I2	I3	I4
2-year-old	34,05 +- 7,11	40,18 +- 16,15	-	-
3-year-old	36,65 +- 6,14	28,75 +- 6,42	24,22 +- 6,39	19,59 +- 5,78
4-year-old	23.6 +- 5,19	20,07 +- 4,62	16,93 +- 3,06	11,26 +- 2,17
6-year-old	19,35 +- 4,71	18,06 +- 3,28	14,61 +- 3,07	11,51 +- 3,69

Table 5: Prediction of total dental pulp volume giving by the linear mixed model (mm^3 with SE).

Teeth / Age	Total volume of pulp ($mm^{3)}$ if missing values are removed	Difference compared to 3-year-old (mm^3)	Total volume of pulp ($mm^{3)}$ if missing values are replaced by 0	Difference compared to 3-year-old(mm^3)
2-year-old	39.15 +- 4,29	+5.46	29.22 +- 3.627	-5.49
3-year-old	33.69 +- 1.87 (***)		34.71 +- 1.78 (**)	
4-year-old	24.35 +- 3.59 (*)	-9.39	25.642 +- 3.09 (*)	-9.07
6-year-old	22.22 +- 3.01 (**)	-11.47	23.55 +- 2.59 (**)	-11.5

Table 6: Prediction of dental pulp volume difference with teeth position (I1 as the baseline) (mm^3, with SE).

Volume of pulp if missing values are removed			
I1	**I2**	**I3**	**I4**
0	-3.99 +- 0.87	-8.54 +- 0.89	-12.81 +- 0.92
Volume of teeth if missing values are replaced by 0			
I1	**I2**	**I3**	**I4**
0	-3,99 +- 1,44	-10,51 +- 1,44	-16,19 +- 1,44

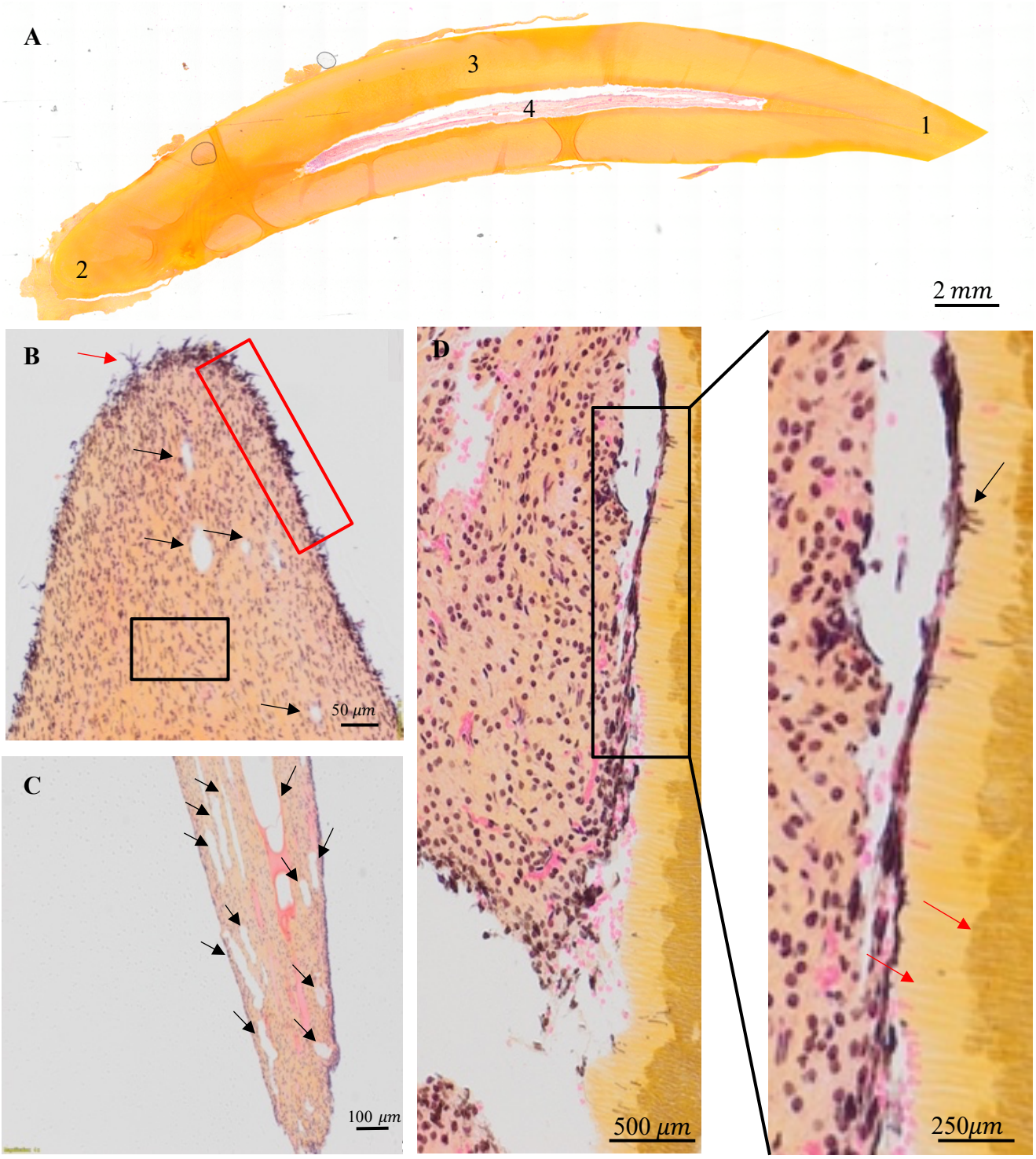

Figure 20: Histology of Ovine dental pulp. A: *Scan view of tooth coming from a 4- years old sheep. 1: Coronal part, 2: Apex, 3: Dentine, 4: Dental pulp. The apex is the deepest part in dental anatomy.* ***B:*** *HES of an apical part of ovine dental pulp, black arrows show blood vessels and the red arrow show cell extensions (suspected from odontoblasts). Black frame shows central pulp composed of conjunctive tissue enriched in fibroblast. The red frame shows the odontoblastic-enriched area at the periphery of the pulp.* ***C:*** *HES of a basal part of the ovine dental pulp, black arrows show all the blood vessels* ***D:*** *HES of ovine dental pulp, red arrows show pre-dentine (clear yellow) and dentine (dark yellow). The black arrow shows odontoblast which still have extensions in the dentine.*

1.2) Histology

The histology analysis showed a typical tooth structure: a coronal part, an apex, the dentine (mineralized tissue), and the dental pulp. The dental pulp is at the center of the tooth in the pulp cavity. There is a space between the pulp and the dentine which is a separation artifact due to the technique[127] (figure 20A). The histology of extracted pulps revealed an abondance of blood vessels at the apex compared to the coronal part (figure 20 B-C). The pulp is centrally composed of conjunctive tissue which is rich of fibroblast. There is a rich odontoblast area at the periphery of the pulp (figure 20 B). Some pieces of dentine are still attached to the extracted pulps. When it is the case, it is possible to see cells at the periphery of the pulp (odontoblast) lining the pre-dentine at the periphery of the pulp; (1) either as a cuboidal epithelium detached from the dentine (figure 21 A) (2) or as cells being pulled between the dental pulp and the dentine (figure 21 B) (3) or at the periphery of the pulp and link by a unique cellular prolongment to the dentine (figure 21 C) (4) making the link between the dental pulp and the dentine and being a cuboidal epithelium (figure 21 D). At the periphery of the dentine, it is possible to see when the dentinal tubules disappear at the enamel-dentine interface (Figure 21 E).

2) Characterisation of oDPSCs

2.1) Cell culture

Adherent cells were isolated from the dental pulp according to the protocol with alpha-MEM. After 7 to 10 days, the cells had a spindle-shape morphology, described as “fibroblastic-like” morphology, they were believe to be oDPSCs (figure 22A). Cells were also isolated from the derm, they had also spindle-shape morphology, speculated to be oDFs (figure 22B)

2.2) Transcriptome profile

ISCT Marker CD90 and CD105 were equally express between oDFs and oDPSCs (figure 23 B-C). However, CD73 and CD34 were differentially expressed (figure 23 A and D), CD73 was more detected in oDPSCs (mean fold change 6,45 +- 3,42 compared to fibroblast), and CD34 was not expressed in oDPSCs (CT > 33). CD10 and CD44 were not differentially expressed (figure 23 E-F), even if CD10 tended to be more express in oDPSCs, the variability was high, making the difference not statistically significant (mean fold change 7,02+-7,61). For oDPSCs, the expression of CXCL12 was much lower than oDFs (figure 23 G), and HOXA5 was unexpressed (CT>33) (figure 23H). MDK, MYH11 and ITGA11 were more expressed in oDPSCs (figure 23 I-K), mean fold change respectively: 3,25; 35,96 and 21,8. Notch1 expression was not strongly different between both cell type, with a fold change at 3,03 +- 1,98. The markers CD271, KRT18 were not expressed in both cell line as well as embryonic stem cell marker NANOG, SOX2 and OCT3/4 (CT>33).

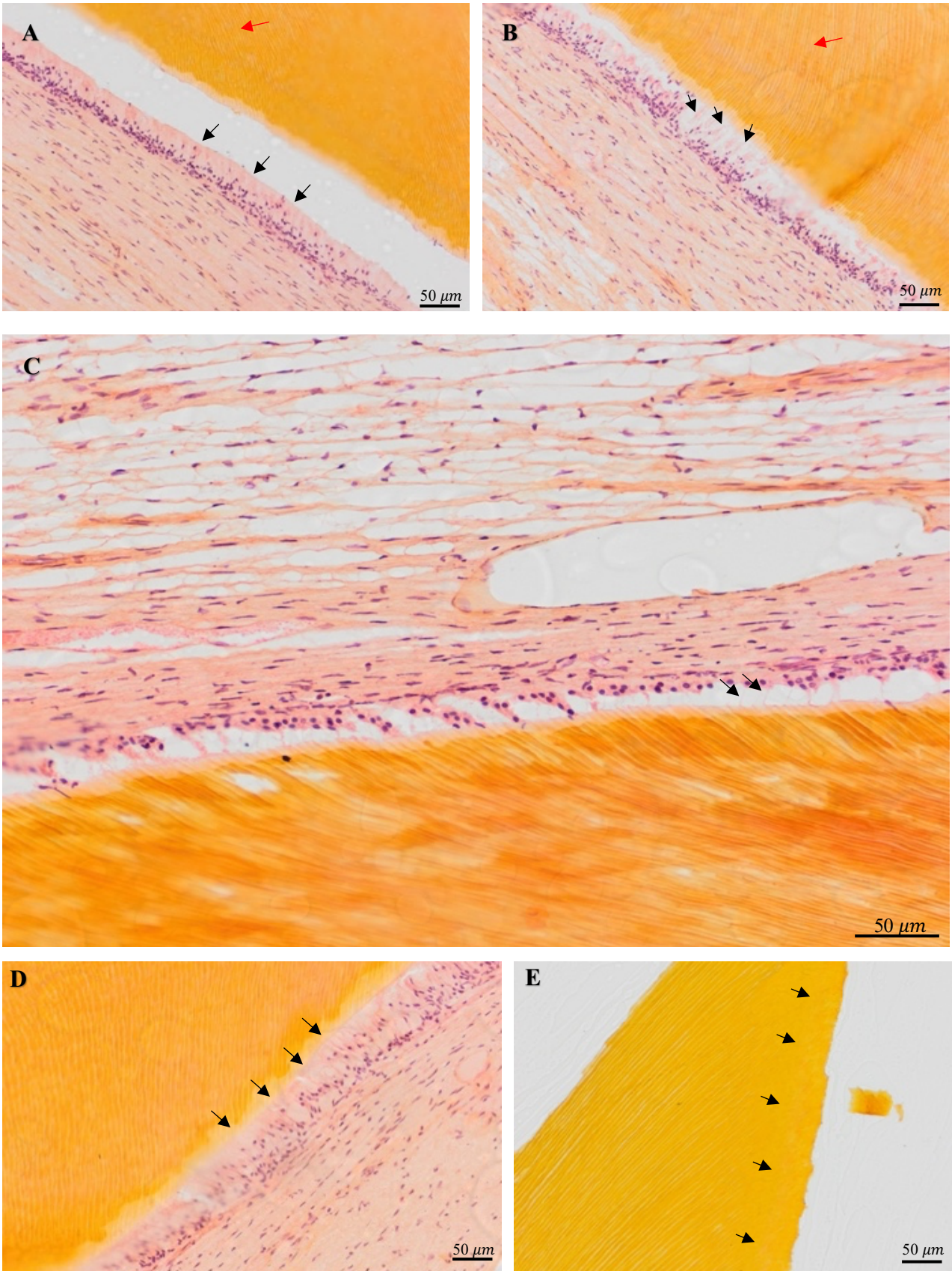

Figure 21: Histology of Ovine Incisives. A: HES of ovine incisive*. Black arrows show a simple prismatic epithelium at the pulp periphery; it is a zone of odontoblast. The red arrows show dentinal tubules.* ***B-C:*** *Black arrows show cellular extension attached to the dentine; corresponding to Tomes fibers.* ***D:*** *Black arrows show a simple cuboidal epithelium (at the pulp periphery) attached to the dentine.* ***E:*** *Blacks arrows show the loss of dentinal tubules corresponding to the junction where the dentine layer stops and the enamel start.*

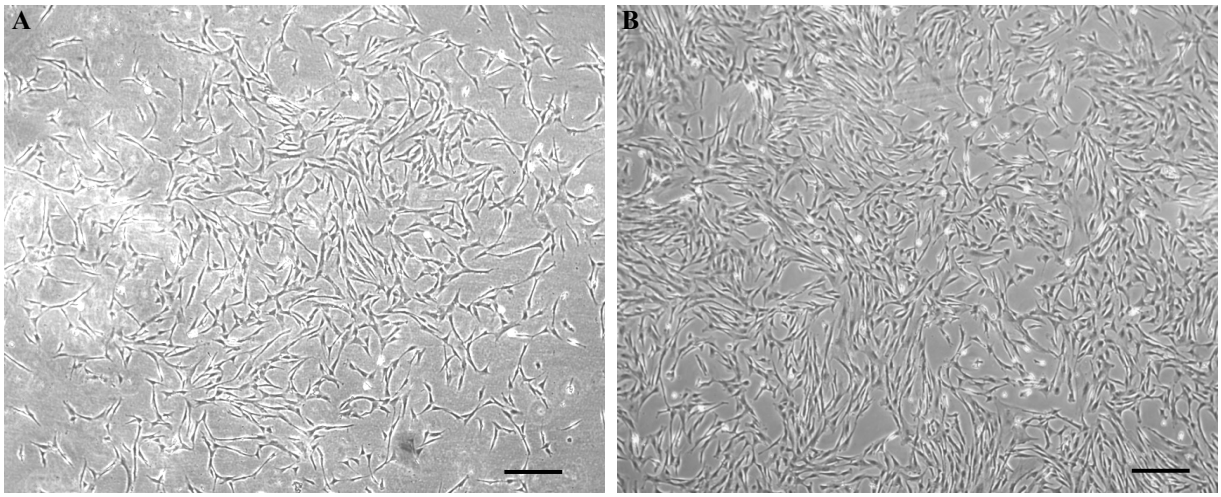

Figure 22: Cell culture of oDPSCs and oDFs. A. *Plastic-adherent cells isolated from ovine dental pulp; they have a spindle- shape morphology.* ***B.*** *Cells isolated from ovine dermis, they also have a spindle-shape morphology, characteristic of fibroblast. Scale bar 50 µm*

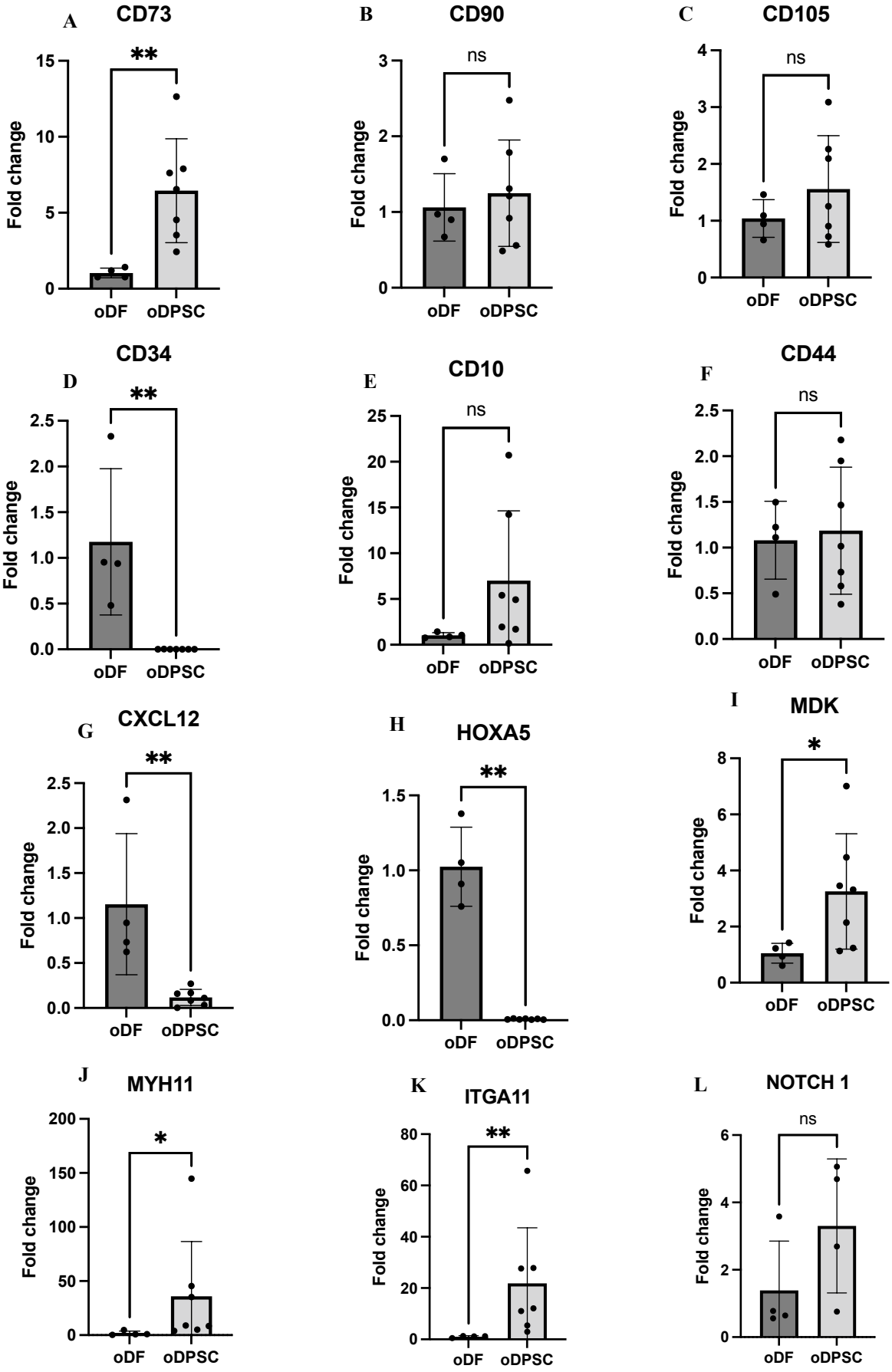

Figure 23: Transcription profile of oDPSCs and oDFs. *Markers such as CD90, CD105, CD10 and CD44 were equally expressed between oDFs and oDPSCs. oDPSCss had higher expression of CD73, MDK, MYH11 and ITGA11. However, oDFs highly expressed CD34, CXCL12 and HOXA5 compared to oDPSCs. CT > than 33 were considered as non-expression.*

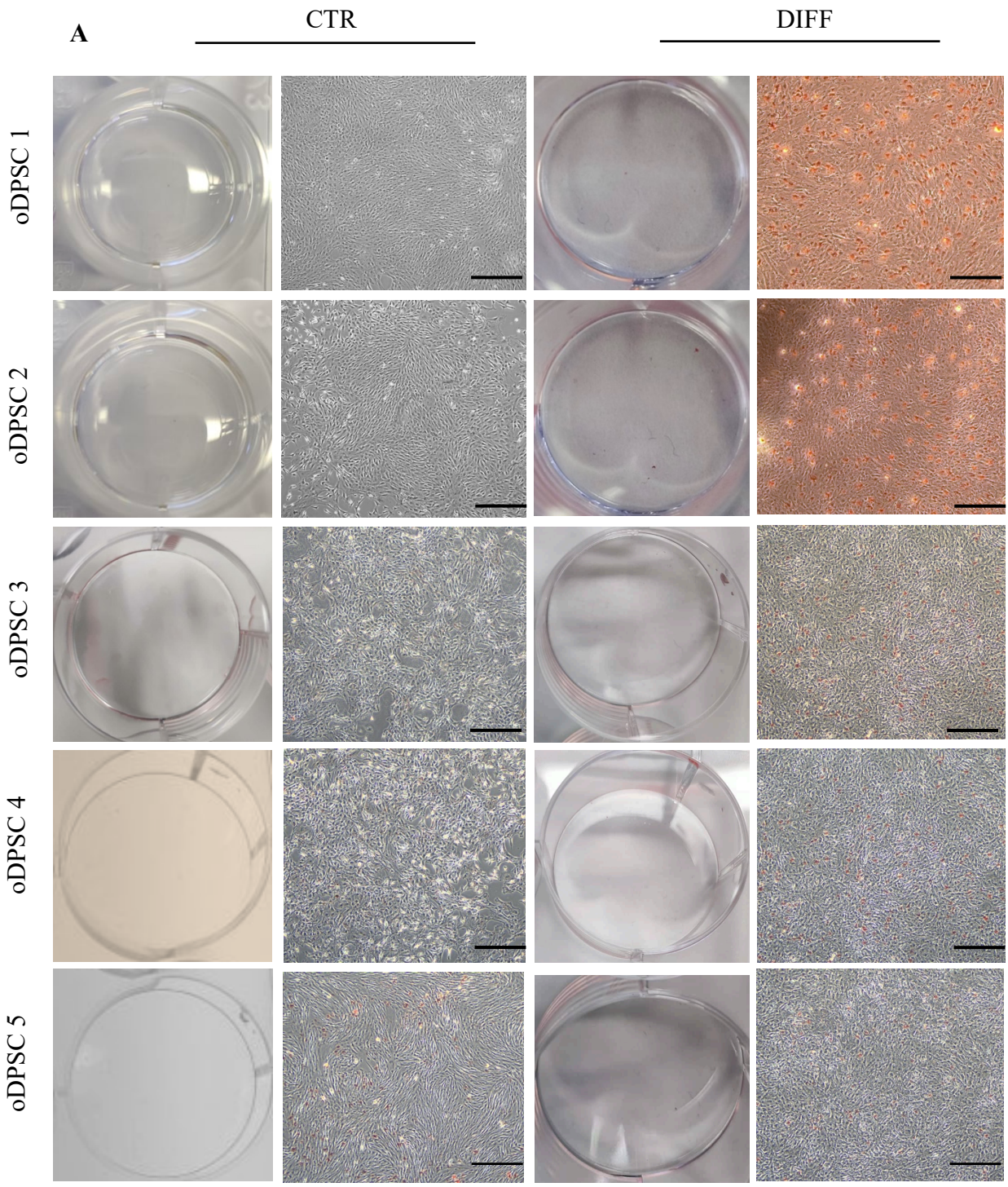

Figure 24: Adipogenic differentiation of oDPSCs and oDFs A-B. *Cells were differentiated using adipogenic differentiation medium for 11 days. Cells were stained with Oil Red Oil (ORO) to highlight intracellular lipid droplets.* ***C.*** *ORO was extracted and quantified by spectrophotometry.* ***D.*** *C/EBP-α gene expression was quantified to see the differentiation state after culture in differentiation medium of oDFs and oDPSCs. The gene expression was quantified in differentiated and undifferentiated cells to calculate 2^ - ΔΔCT. Scale bar 100 µm*

2.3) Differentiation

2.3.1) Adipogenic differentiation

Lipid droplets could be observed in oDPSCs when adipogenic differentiation was induced (figure 24 A). This was not observed in oDFs under the same differentiation medium (figure 24 B). ORO was extracted from the wells and quantify by spectrophotometry. After normalization with ORO extracted from the controls, the ORO quantity was higher in oDPSCs extract compared to oDFs (statistically significant), meaning a greater amount of lipid in oDPSCs (figure 24C). Transcription of the marker gene of adipogenic differentiation C/EBP-α was measured in control and differentiated cells, no expression of this gene was observed (figure 24D).

2.3.2) Osteogenic differentiation

Production of unmineralized matrix by both cell types was assessed upon exposure to osteogenic differentiation was induced (figure 25 A-B). Unexpectedly, this matrix induced the detachment of the cells, leading to the formation of a matrix-cell spheroid (DPSC 1, 2 and oDFs 1). If such spheroid was formed, it was processed by histology. The cells detachment was at different stage depending on the cell batches (oDFs 3 did undergo detachment, at the same time oDFs 2 was still correctly attached, while oDPSCs 1 already formed a spheroid). The AR staining did not show extra-cellular calcium deposits at microscope examination. AR was extracted from the wells if it was possible (cells still attached) and quantified by a standard curve in spectrophotometry. No AR was extracted either from differentiated oDPSCs wells or oDFs (figure 25C). Transcription of the marker gene of osteogenic differentiation RUNX2 was measured, expression of this gene was detected in oDFs but not in oDPSCs (figure 25D).

2.3.3) Chondrogenic differentiation

Chondrogenic differentiation of oDPSCs (figure 26A) gave spheroid showing cartilage matrix staining. For oDPSCs 1 and 2, it was clearly possible to see cartilage morphology with chondroplast containing chondrocytes (black arrows). Other oDPSCs also showed Alcian blue staining but less clear chondroplast formation. Controls were lacking due to the difficulties to harvest and process the pellets that never formed a solid tissue. Indeed, these control pellets felt apart, making difficult their processing. Chondrogenic differentiation of oDFs did not show such chondroplast/cartilage deposit formation. The staining of differentiated pellets showed similar colour compared to the control (absence of cartilage matrix), but a solid spheroid formation could be observed. oDFs 2 showed soft cartilage formation.

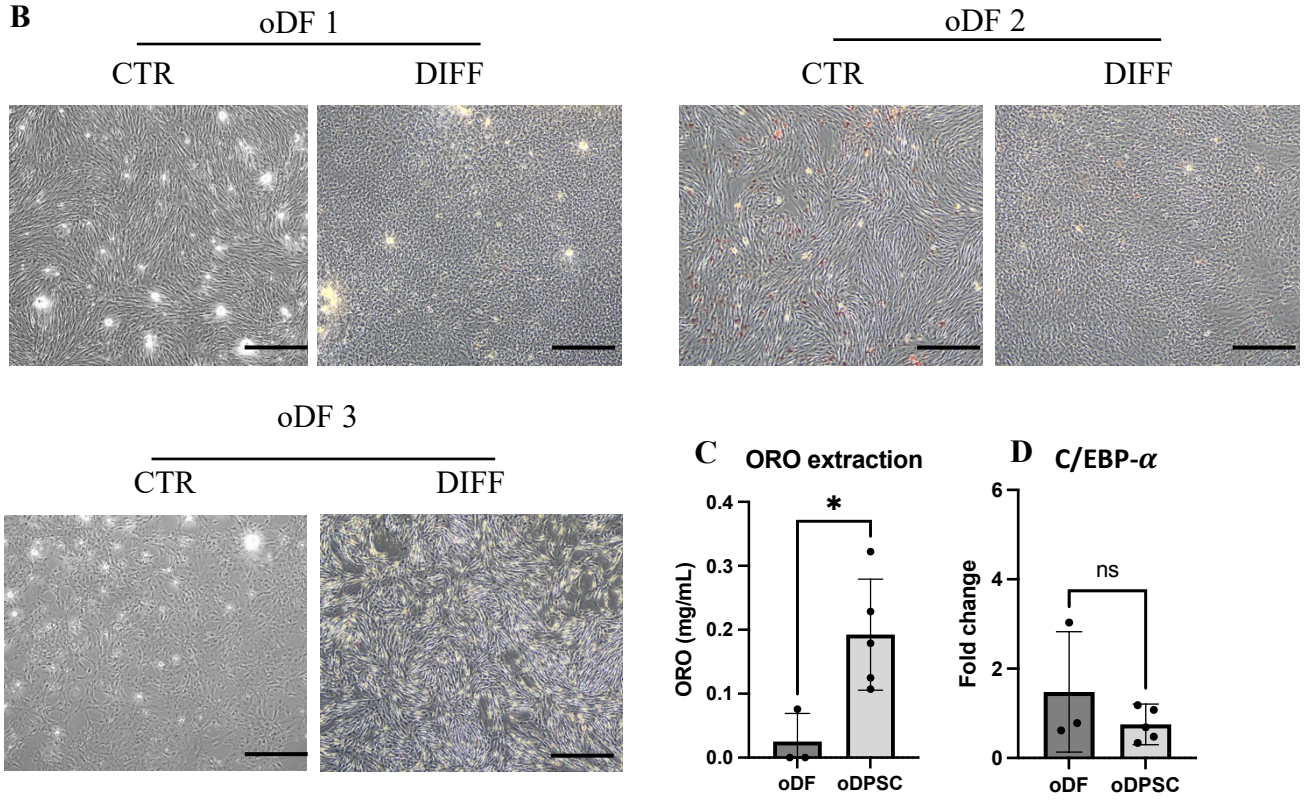

Figure 24: Adipogenic differentiation of oDPSCs and oDFs A-B. *Cells were differentiated using adipogenic differentiation medium for 11 days. Cells were stained with Oil Red Oil (ORO) to highlight intracellular lipid droplets.* ***C.*** *ORO was extracted and quantified by spectrophotometry.* ***D.*** *C/EBP-α gene expression was quantified to see the differentiation state after culture in differentiation medium of oDFs and oDPSCs. The gene expression was quantified in differentiated and undifferentiated cells to calculate 2^ -ΔΔCT. Scale bar 100 µm*

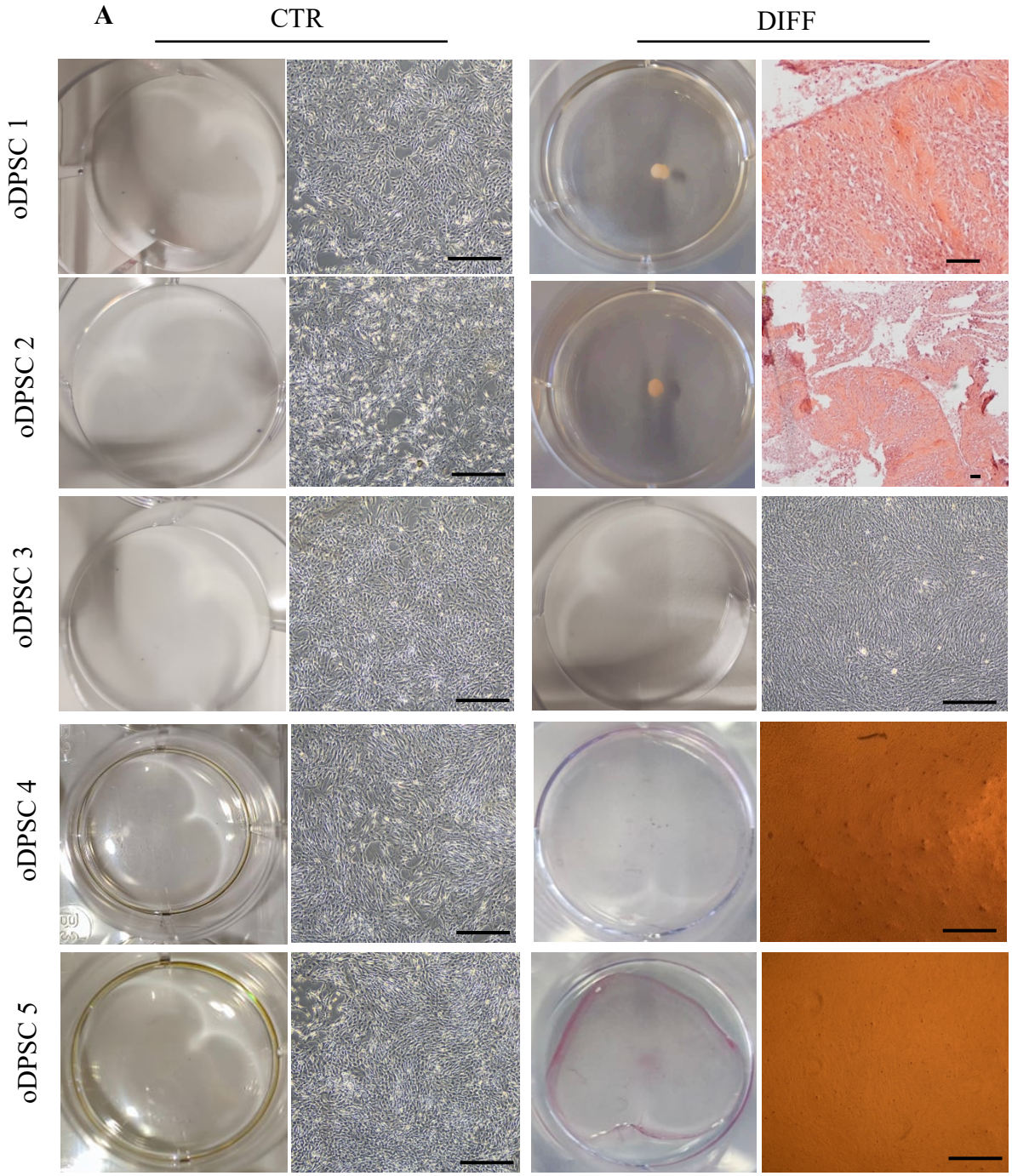

Figure 25: Osteogenic differentiation of oDPSCs and oDFs A-B. *Cells were differentiated using osteogenic differentiation medium for 11 days (oDPSC 3 and 4), or 14 days (oDPSC 1-2-3). They were then stained with Alizarin Red (AR) to highlight extra-cellular calcic deposits or processed by histology following AR staining* ***C.*** *AR was extracted and quantified by spectrophotometry.* ***D.*** *RUNX2 gene expression was quantified and detected only in oDFs. The gene expression was quantified in differentiated and undifferentiated cells to calculate 2^ -ΔΔCT. Scale bar 100 µm*

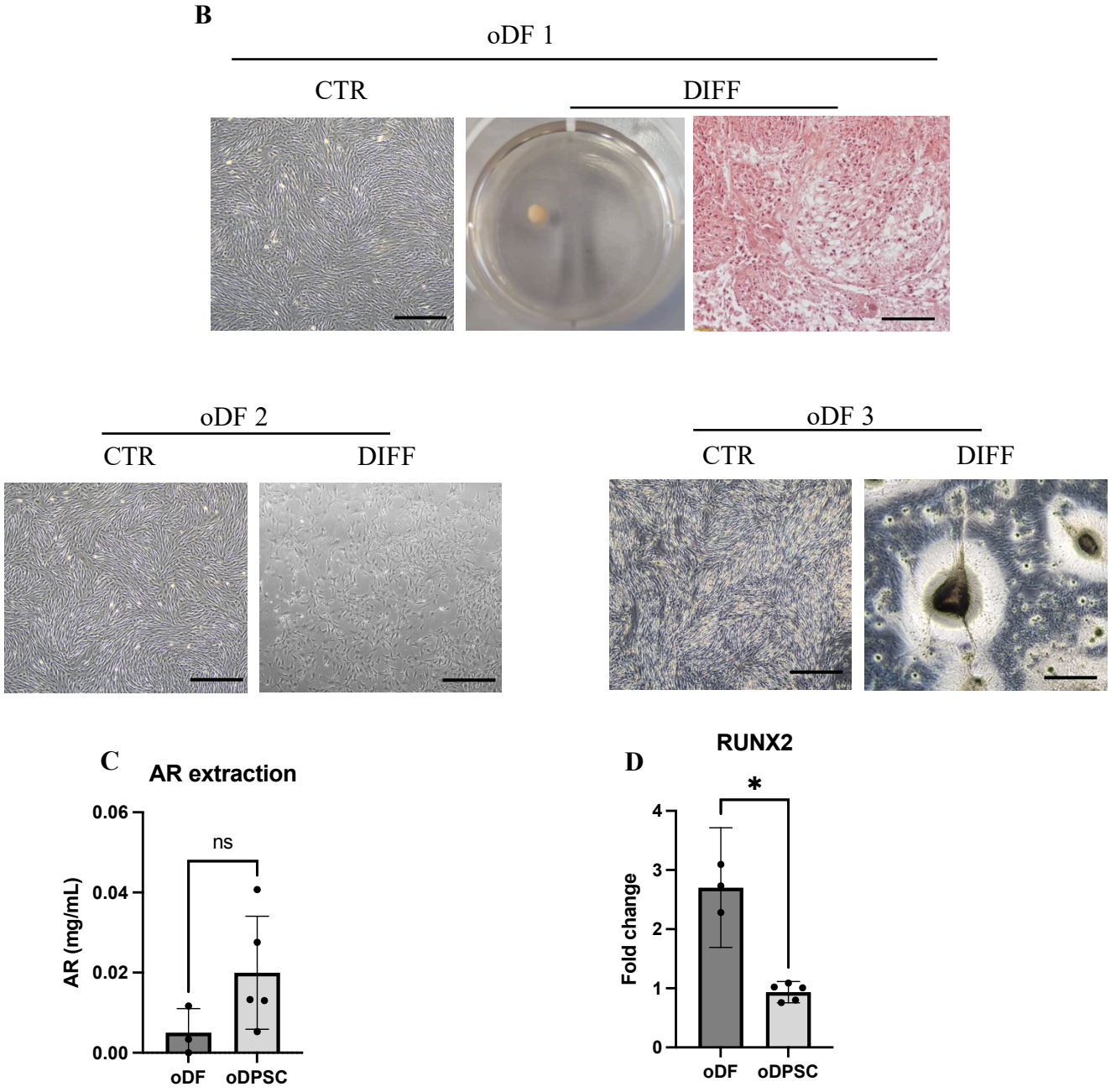

Figure 25: Osteogenic differentiation of oDPSCs and oDFs A-B. *Cells were differentiated using osteogenic differentiation medium for 11 days (oDPSC 3 and 4), or 14 days (oDPSC 1-2-3). They were then stained with Alizarin Red (AR) to highlight extra-cellular calcic deposits or processed by histology following AR staining* ***C.*** *AR was extracted and quantified by spectrophotometry.* ***D.*** *RUNX2 gene expression was quantified and detected only in oDFs. The gene expression was quantified in differentiated and undifferentiated cells to calculate 2^ -ΔΔCT. Scale bar 100 µm*

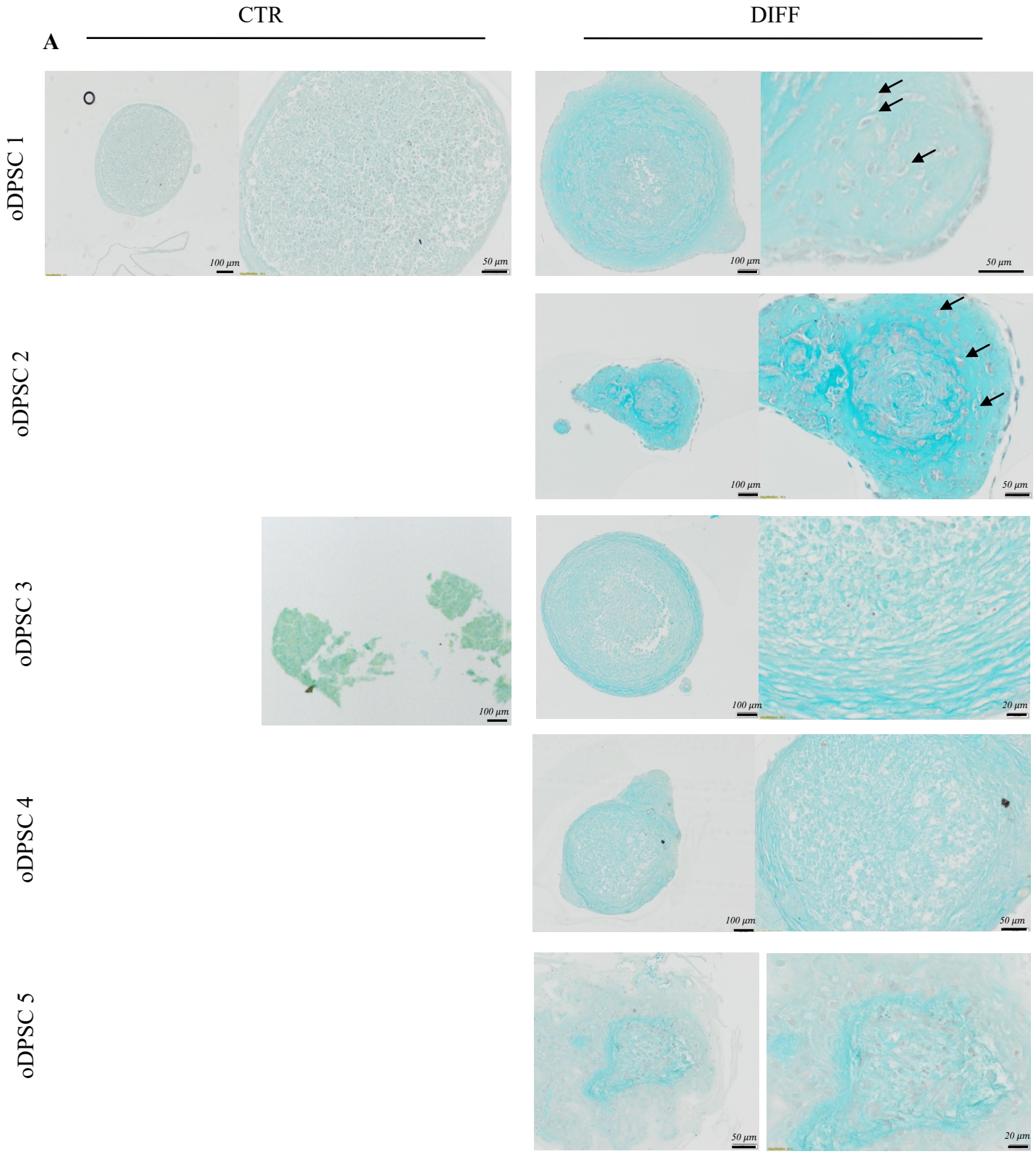

Figure 26: Chondrogenic differentiation of oDPSCs and oDFs. *Chondrogenic differentiation was induced on oDPSCs* ***(A)*** *and oDFs* ***(B)*** *using differentiation medium on cells pellet. After 21 days, pellets were process for histology and stained with Alcian Blue to highlight cartilage matrix deposit and neutral red to show cell nucleus. Black arrows showed chondrocyte.*

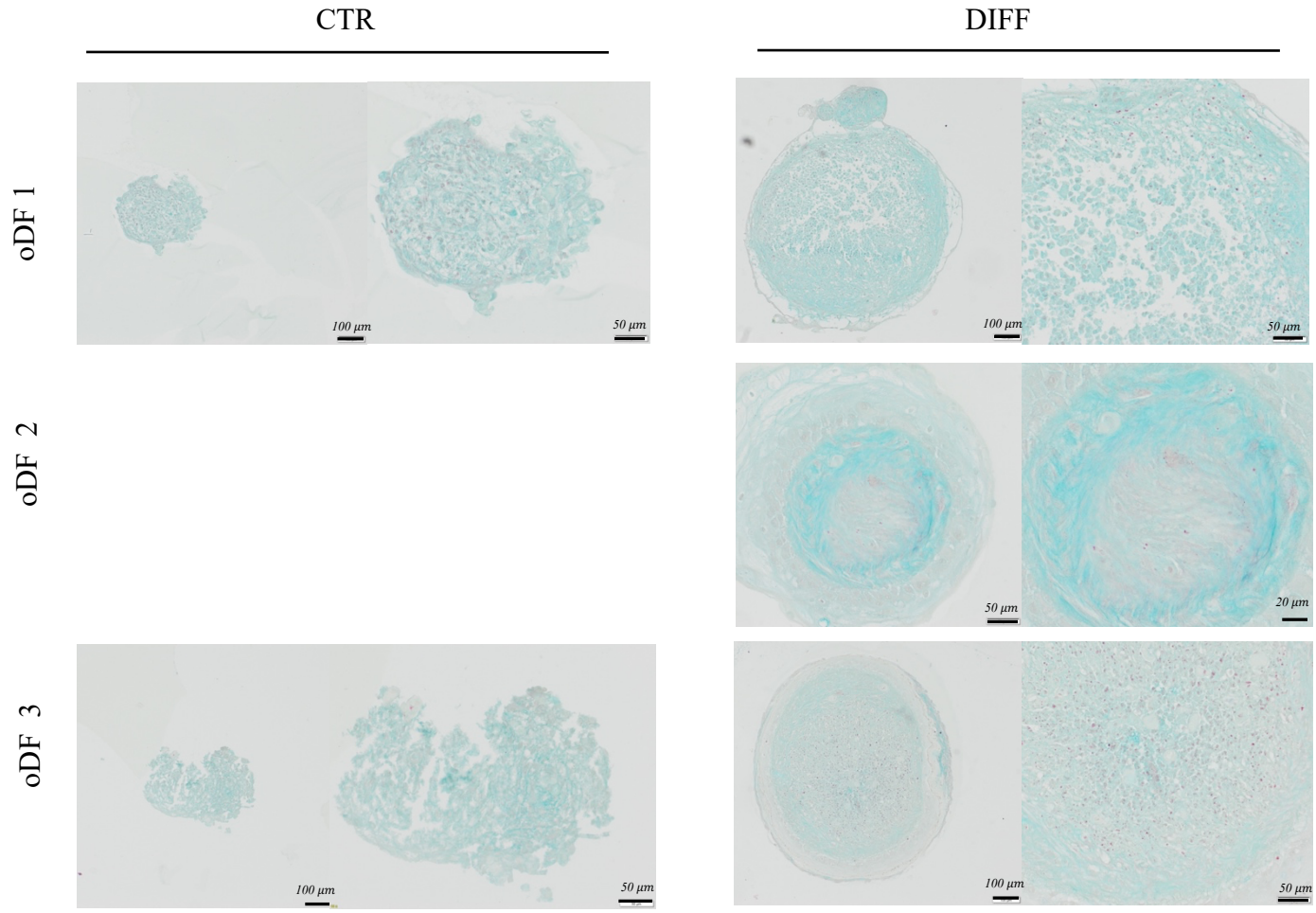

Figure 26: Chondrogenic differentiation of oDPSCs and oDFs. *Chondrogenic differentiation was induced on oDPSCs* ***(A)*** *and oDFs (****B****) using differentiation medium on cells pellet. After 21 days, pellets were process for histology and stained with Alcian Blue to highlight cartilage matrix deposit and neutral red to show cell nucleus. Black arrows showed chondrocyte.*

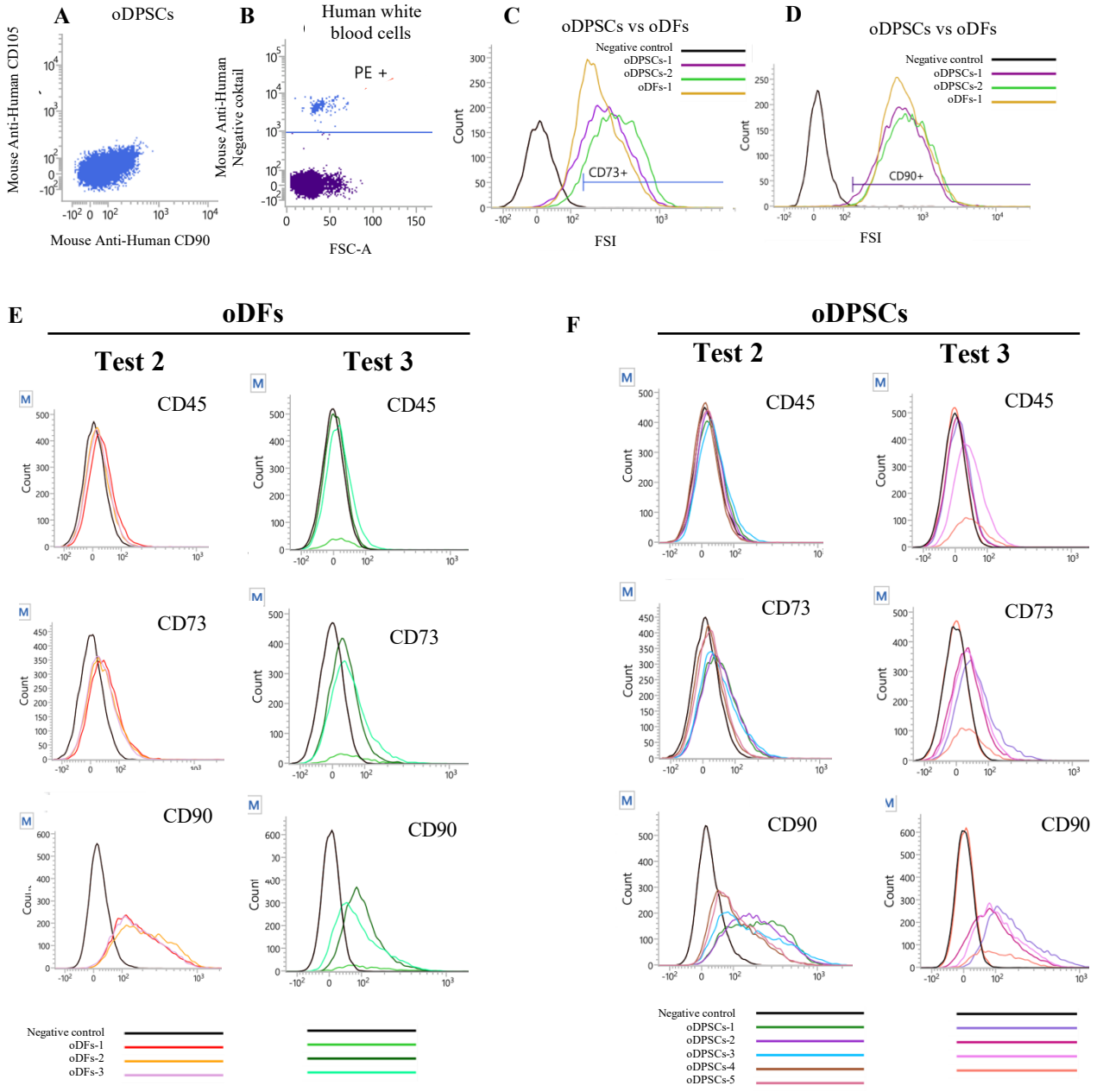

Figure 27: Surface antigens analysis of oDPSCs and oDFs A. *FACS analysis of oDPSCs with human MSC identification kit. The kit did not work on ovine cells* ***B.*** *Human white blood cells were tested to assess the functioning of the kit (cocktail contained antibodies against white blood cells markers).* ***C-D****: FACS analysis of oDPSCs and oDFs using antibody described in the literature as working on ovine cells (CD73 and CD90)* ***E-F.*** *The manipulation was reproduced 2 times (test 2 and test 3), and it was not possible to reach the signal observed in the first test. The signal was less intense. However similar expression profile was observed between oDPSCs and oDFs*

2.4) Surface Antigens

oDPSCs were analysed by FACS with a commercially available kit containing antibodies targeting ISCT recommended human surface antigens; CD105, CD90, CD73, and a negative cocktail containing anti- CD34, CD11b PE, CD19, CD45, HLA-DR PE. The kit did not work on ovine cells (figure 27 A). Human peripheral white blood cells were tested with the negative cocktail (containing antibodies against white blood cell marker) in order to assess the proper Ab recognition towards human antigens (figure 27B).
Following this, three antibodies described in the literature as working on ovine cells were tested: anti-CD90, CD73 and CD45. oDPSCs and oDFs were similarly positive for CD73 and CD90 (figure 27C and D, respectively). It was not possible to reproduce this preliminary result. Indeed, the results showed again a similar positive profile between oDPSCs and oDFs, but with a lack of signal (figure 27 E and F).

2.5) Methylation patterns

Depending on the study, expression profile, surface markers and differentiation potential can be very similar between MSC and fibroblast. One promising alternative to better discriminate these cells is the characterization of their methylation pattern.

2.5.1) Nested PCR

CpG sites were previously described to be differentially methylated between human MSC and fibroblast. After genomic DNA bisulfitation, nested PCR allowed the amplification of these specific CpG island zones (figure 28). Each CpG island was fragmented to amplified fragment no longer than 250-350nt; CIDEC region was fragmented in 3 fragments, ASAM in 7 and SERPINB5 in 3 fragments. For each fragment, it is possible to see an amplification band at expected size for oDPSCs and oDFs. The third fragment of ASAM had a contamination, as suspected by an amplification band in the control (which does not contain DNA).

2.5.2) Screen

After amplifications, PCR products were inserted into a plasmid vector which was used to transform bacteria. Clones were selected after a PCR screen confirming the length of the insert. Here an example of a PCR screen of 24 clones that integrated a vector containing the first fragment of CIDEC CpG island (coming from oDPSCs bisulfited genome DNA) (figure 29). Two clones were carried another fragment of unwanted size (clone 17 and 19). For all fragments, either for oDFs and oDPSCs, maximum 20 clones were selected after screening.

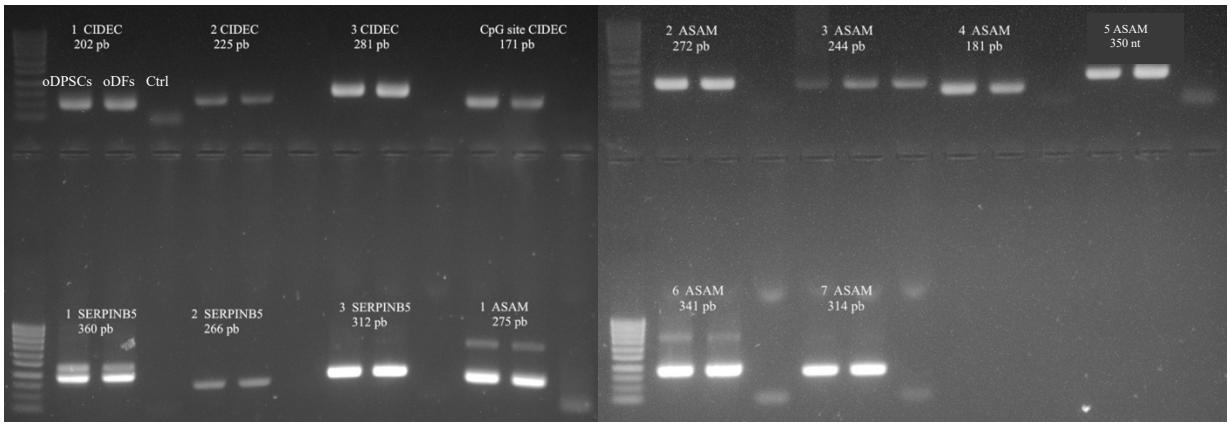

Figure 28: Agarose gel highlighting nested PCR amplicons. *After bisulfitation, DNA was used as a template for nested PCR. A primary PCR was done using 14 couples of primary primers, following nested PCR with 14 couples of nested primers (these targeted a zone inside the first amplicon).*

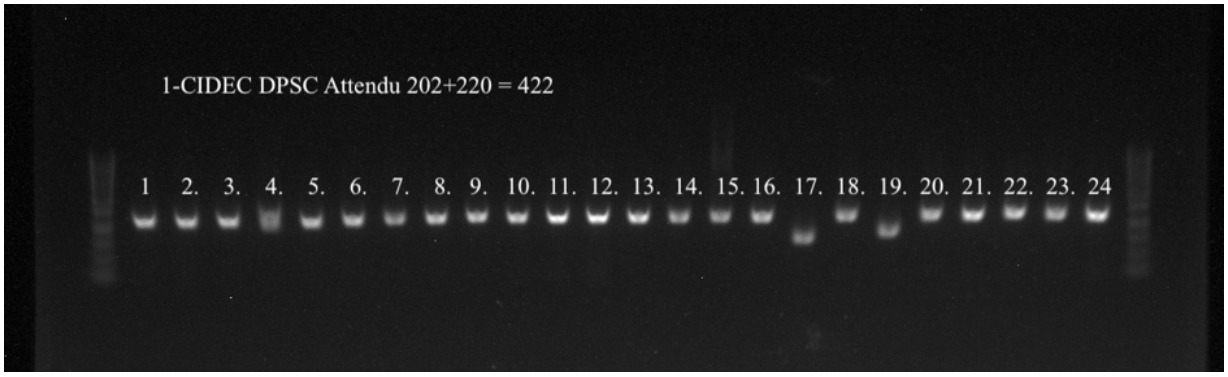

Figure 29: Example of screen allowing discrimination between clone having the good amplicons or another one. *Here, the length of the targeted zone was 202 nt, adding 220 nt due to the vector, clones at 422 pb were carrying the targeted insert (clones 17 and 19 were discarded).*

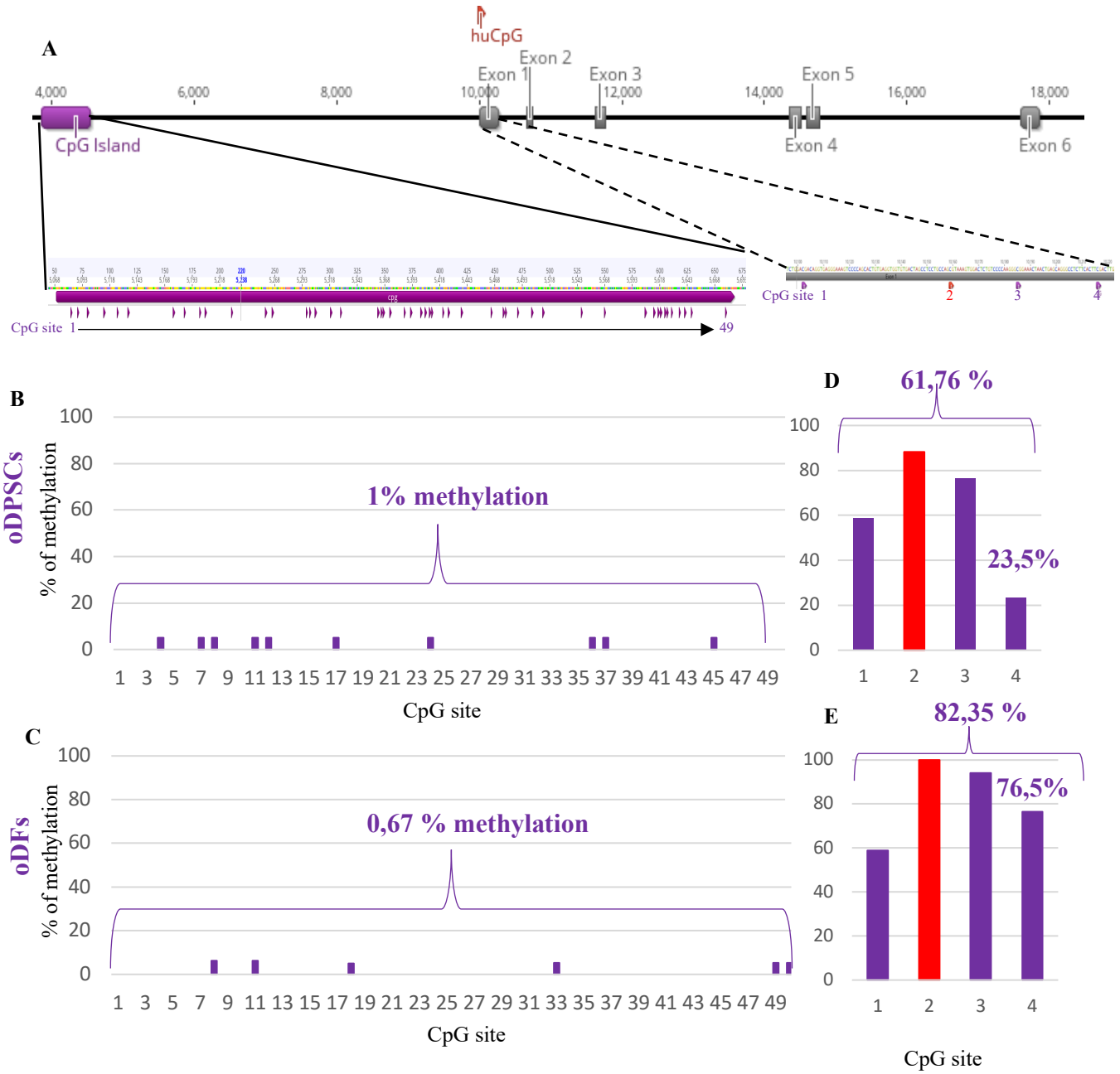

Figure 30: Methylation pattern of oCIDEC CpG island A. *oCIDEC gene organization, CpG island is in purple with CpG site represented as purple triangle. huCpG represent the CpG site conserved with human CIDEC gene that was identified in the study where human fibroblasts could be discriminate from MSCs thanks to their methylation pattern.* ***B-C.*** *Percentage of methylation of the oCIDEC CpG island for oDPSCs (**B**) and oDFs (**C**). The percentage of methylation was obtained by analyzing maximum 20 clones, a ratio between methylated and non-methylated site was calculated.* ***D-E****. Percentage of methylation of huCpG site (red in the graph). Three others CpG sites were analyzed as they were on the sequence.*

2.5.3) Methylation rate

2.5.3.1) oCIDEC

The CpG island analyzed for o*CIDEC* gene contains 49 CpG site. The huCpG site contains 4 CpG sites (figure 30 A). For oDPSCs, total methylation reached 1% (figure 30B). For oDFs, it reached 0,67% (figure 30C). The huCpG area methylation reached 61,76% in oDPSCs and 82,35% in oDFs (respectively figure D and E). For the only CpG site conserved between human and sheep (huCpG site) situated in exon 1 of *oCIDEC*, 88% of clones showed a methylation in oDPSCs, against 100% in oDFs. In the same area, an interesting CpG site is the fourth, where 23,5% methylation was observed in oDPSCs compared to 76,5% in oDFs, giving a difference of 63%. All other CpG site showed a similar methylation pattern for *oCIDEC*.

2.5.3.2) oSERPINB5

The CpG islands analysed for o*SERPINB5* gene contains 61 CpG site (figure 31A). For oDPSCs, total methylation reached 15,69% (figure 31B). For oDFs, it reached 17,37% (figure 31C). Some CpG site showed a slight difference between 5% and 34%. All other CpG site showed a similar methylation pattern for *oSERPINB5.*

2.5.3.3) oASAM

The CpG islands analysed for o*ASAM* gene contains 165 CpG sites (figure 32A). For oDPSCs, total methylation reached 1,79% (figure 32B). For oDFs, it reached 1,89% (figure 32C). Some CpG site showed a slight difference between 5% and 29%. All other CpG site showed a similar methylation pattern for *oASAM.* Red crosses at CpG site 37 to 52 mean absences of data, the amplicons were not used because of DNA contamination (described in 2.5.1). The red cross at CpG site 141 to 166 means absences of data due to a technical issue.

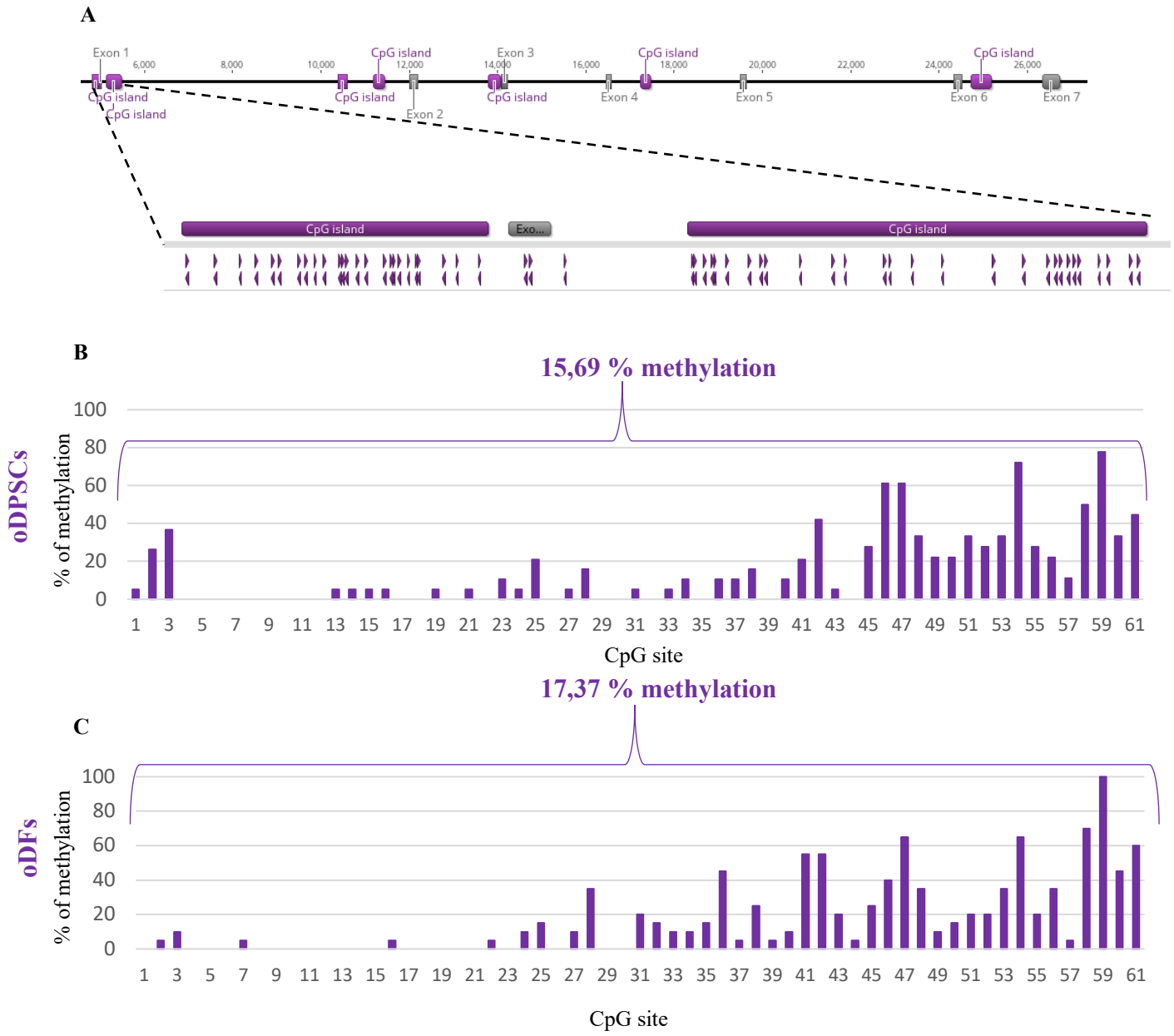

Figure 31: Methylation pattern of oSERPINB5 CpG island A. o*SERPINB5 gene organization, CpG islands are in purple with CpG site represented as purple triangle.* ***B-C.*** *Percentage of Methylation of the selected oSERPINB5 CpG islands for oDPSCss (**B**) and oDFs (**C**). The percentage of methylation is obtained by analyzing 20 clones, a ratio between methylated and non-methylated site is calculated.*

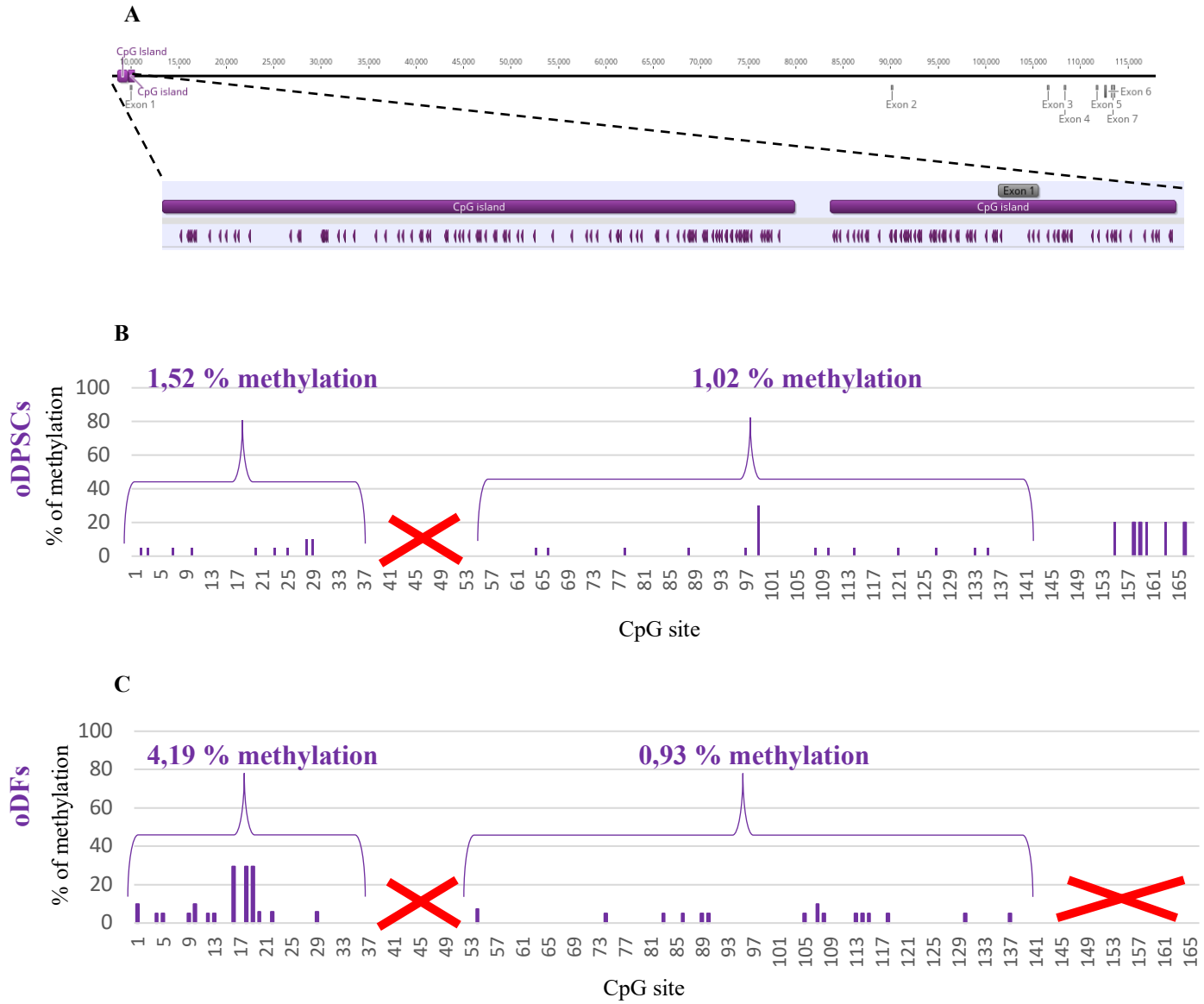

Figure 32: Methylation pattern of oASAM CpG island A. o*ASAM gene organization, CpG islands are in purple with CpG site represented as purple triangle.* ***B-C.*** *Percentage of Methylation of oASAM CpG islands for oDPSCs (**B**) and oDFs (**C**). Red crossed shows regions not analyzed.*

Discussion

1) Morphometric study of the dental pulp of incisors in sheep

As previously described[128,110,111], our sample population had a typical ovine dental anatomy; eight incisive at the rostral end of the mandibular arcade. The timing of eruption of the permanent teeth is subject to wide individual and breed variations[129]. In sheep, the central incisors (I1) were described by various authors to erupt within a period of age ranging from 10 to 24 months after birth. The permanent middle teeth (I2) over a period of 15 to 30 months and the lateral incisors (I3) erupted over period up of 24 to 42 months. Finally, the permanent corner teeth (I4) is described to erupt over a period of 32 to 54 month[129]. Permanent tooth shedding was described around 7 years old[129]. In the current study, we observed that teeth were erupted in those described periods. All 2-year-old specimens analyzed in this study had permanent I1, but I2 eruption was variable. From 3 years-old, all incisors were erupted. The teeth in this study had similar histological features in comparison to human teeth[127]. Teeth were composed of dentine and pre-dentine with a dental pulp cavity at the center. The pulp contained cells, conjunctive tissue and blood vessels. The layer of cuboidal odontoblastic cell was also observed with heterogenous morphology due to the histological procedures and artifacts.

Our study showed that the dental pulp volume of incisors decreased with age in sheep. It has already been related in man that the age could be correlated with a reduction of the size of the molar pulp chamber[130]. Age estimation using canine pulp volumes in human was also reported and showed a decrease of volume with age[131,132]. Our study also showed the decrease of dental pulp volume with the position of the teeth, I1 having the highest volume and I4 the lowest.

A weakness of the study is the low number of 2-year-old specimen. Indeed, this give a significant uncertainty about what was happening at this age. Based on literature and our data, we can easily speculate that pulp volume at this age should at least be similar to the value observed at 3-year-old, or greater. This should be confirmed experimentally by analyzing higher number of 2-year-old specimens. Based on our result and a sample size calculation, four animals should be added to the study to more precisely characterized the difference at 2-year-old

However, at this stage, if dental pulp of incisors should be collected in sheep for dental pulp stem cell isolation, we can strongly support that I1 of animal aged between 2- and 3-year-old should be selected in order to maximize the tissue volume and the downstream number of isolated cells. For *in vivo* study, where a single incisor should be removed to extract oDPSCs and keep sheep alive, animals of 3-year-old should be given preference as all adult incisors are erupted, giving more comfort for alimentary behavior.

2) Ovine dental pulp stem cell characterization:

2.1) Cell morphology

Both oDFs and oDPSCs shared a spindle-shape morphology. It is thus impossible to discriminate them in cell culture based on this unique criteria. For MSCs isolated from fibroblast-rich tissue such as dental pulp, it is essential to discriminate these cells as fibroblast contamination could easily occur.

2.2) Transcription profile

The mRNA expression of four markers being part of minimal criteria defining MSC by the ISCT were assessed: $CD90^+$, $CD73^+$, $CD105^+$ and $CD34^-$. This analysis was achieved either on oDPSCs culture and oDFs to observe an enrichment of oDPSCs. Both **CD90** and **CD105** markers were similarly expressed, they did not allow discrimination between both cell types. Antigen surface analysis should be performed to support this transcriptional observation. Such results have already been related in the literature, where ISCT markers such as CD90 and CD105 have been equally observed in either MSC or fibroblast[133–136]. However, CD34 and CD73 were differentially expressed.

CD34, predominantly used as a marker of hematopoietic stem cells, is not expressed in our oDPSCs. Even if there are studies supporting the fact that CD34 is expressed in other progenitor cells[137], and that its negative status in MSCs is an artifact of cell culture[138(p34),139(p45),140] , in our study it allows a discrimination with oDFs, making potentially possible to see a contamination of fibroblasts in the culture.

CD73 (or NT5E) is an ectonucleotidase which converts AMP to adenosine. In this study, mRNA expression was supporting a difference in the expression between our cell types. However, after antigen analysis by FACS, CD73 was present similarly in oDPSCs and oDFs. This could be explained by post-traductional regulation, leading to contradictory result between mRNA expression and protein. mRNA analysis is a first approach to identify promising markers.

CD44 is a hyaluronan receptor, it has been shown that this receptor facilitate MSCs migration[141].
It was described to be a MSC marker[142], but some studies related its presence in fibroblast[136,117].
In our study, expression of mRNA was similar. Surface proteins analysis should correlate this observation.

CD10, a metalloendopeptidase, have been described to be strongly expressed on human dermal fibroblasts compared to bone-marrow derived MSCs[133]. Our mRNA analysis suggested the opposite, as CD10 seems to be more strongly express in oDPSCs. However, this expression seemed very heterogeneous (fold change from 1 to 20 compared to oDFs). It should be confirmed by FACS analysis.

HOXA5 is a transcription factor (TF) involved in proliferation and stem cell fate[143]. Indeed, studies have indicated that HOXA5 acts downstream of the Wnt signaling pathway[144]. It has been related that Wnt and HOXA5 exert mutual antagonism to control stem cell fate; the expression of HOXA5 induces differentiation and inhibits Wnt pathway[145]. In an other hand, gene expression profiles between dental-derived stem cells and non-dental-derived stem cells showed HOXA5 downregulation in dental-derived stem cells[143]. These information's about HOXA5 are encouraging regarding our data. As HOXA5 seems to be a marker of differentiation/loss of stemness, its absence in our oDPSCs might be interpreted as a stemness phenotype.

CXCL12 is a chemokine (C-X-C motif) protein, with important roles in embryogenesis, hematopoiesis, angiogenesis and inflammation. Indeed, upon binding to its receptor Cxcr4, it induces migration of hematopoietic progenitors and stem cells, endothelial cells and leukocytes[146]. In MSC context, CXCL12 has been shown to promote DPSC differentiation into odontoblasts. DPSCs expressing Cxcr4 could migrate to a decay area, where they engrafted and differentiated into new odontoblasts[147]. They could also demonstrate that non-endothelial CXCL12-expressing cells were mostly concentrated in the core of the dental pulp and did not express either DPSC markers, neuronal cells, or immune cells markers, supporting these to be fibroblasts[147]. Based on this, our data is again pointing in the good direction, as CXCL12 mRNA was mostly detected in oDFs and not in oDPSCs.
Even if HOXA5 and CXCL12 are not expressed in our culture of oDPSCs, such markers cannot be used for positive selection. They could be suggested markers to discriminate oDPSCs from fibroblasts.

ITGA11, an integrin first identified in cultured skeletal muscle cells, later on in mesenchymal tissues. It was associated with cell migration control as it forms a collagen receptor that interacts with fibrous collagen[148]. *Halfon et al.* identified ITGA11 as a MSC marker[135], in their study, they demonstrated a fold change mean around 20 between MSCs and fibroblasts, which was similar to our result. Even if we have non-negligeable variability (2 to 65), this marker seems really promising and should be investigated by flow cytometry.

MYH11 and **MDK** are two markers identified in a recent single cell atlas analysis of human dental pulp[119]. MYH11 (myosin heavy chain family) is known as a major smooth muscle contractile protein, using chemical energy to produce mechanical energy through the hydrolysis of ATP[149]. In our experimental condition, oDPSCs expressed more strongly MYH11 than oDFs. Even if the variability was again non-negligeable (fold change from 3 to 144), the difference is promising for discrimination of both cell types. Analysis by FACS should be again assessed. MDK is coding for the Midkine protein which is part of a small family of secreted growth factors. This protein has been described to promote cell growth, migration and angiogenesis[150]. This protein was firstly shown to be expressed in dental pulp fibroblasts[119], but it was also expressed in MSC coming from the periodontium. In our study, MDK was slightly up regulated in oDPSCs, with some variability (fold change 1 to 7).

KRT18 expression was also investigated in the single-cell atlas study where it was reported as strongly expressed in human dental pulp MSCs. The authors were surprised as this gene was reported to be exclusively expressed in cells of single-layered and pseudo-stratified epithelia. However, none of oDFs and oDPSCs expressed this marker in this study.

NOTCH1 is a member of NOTCH family proteins. These proteins play a role in a variety of development process by controlling cell fate decision, including proliferation, lineage commitment and terminal differentiation in many adult stem cells. The intracellular signal pathway is regulated by physically adjacent cells[151,152]. Recently it has been described that NOTCH1 inhibition reduces the proliferation and promote the differentiation on human MSC[153]. The expression of this protein was barely observed in our oDFs and oDPSCs culture. The level of mRNA was similar between both cell types, discarding this marker as it does not discriminate our cell types.

Pluripotent stem cell markers such as **NANOG, SOX2 and OCT3/4** have been also investigated to characterize the stemness of DPSC[154–157]. In this study, neither oDPSCs or oDFs did show such expression (CT>33). This result should be repeated, and lack of expression should be confirmed by protein analysis using western blotting.

2.3) Surface Antigens

As specific antibodies targeting ovine antigens were quite difficult to find, we tested on this study a commercially available kit against human mesenchymal stem cells in order to characterize the immunophenotype of our oDFs and oDPSCs based on ISCT markers. Although, the kit gave satisfactory results on human MSCs (tested by Leandra Severino, data not shown here), or on human white blood cells, antibodies present in the cocktails never react with neither ovine DPSCs or fibroblasts. There were two hypotheses for these results: there was no cross-reactivity of Ab from the cocktails, or there was no MSCs in our culture.
We decided to test antibodies against CD73, CD90 and CD45 previously described as working on ovine MSCs[126]. These Ab gave better results; CD90 and CD70 were detected at the cells surface of oDPSCs. Unfortunately, oDFs had the same immunophenotype. The protein presence was not in accordance with mRNA expression. However, this difference could be explained partly by the fact that mRNA analysis was done on a different moment. The passage number were not the same, while it has been shown that immunophenotype changed with passages[158] and more precisely, discriminant marker between MSCs and fibroblasts could change with passaging[135]. It could partially explain this change. In another hand, numerous studies related the similar expression of CD90 and CD73 between MSCs and fibroblasts[99]. A weakness of the result is that the experiment could not be reproduced.

2.4) Multilineage differentiation

Efficiency of **adipogenic differention** was variable from batch-to-batch. Lipid droplets highlighted by Oil Red O staining were clearly observed in oDPSCs compared to control. The differentiation was undertaken in two steps: DPSC1 and 2, and DPSC3-4-5 afterward. The first picture did not have white balance while other did have such treatment. It means that technical parameters were not the same when the picture were taken, giving this variability in the picture. However, variability was observed during microscopic observation, and it was also reflected in ORO extraction values. Two adipogenic gene markers were used to confirm the differentiation; C/EBP-α (early adipogenic differentiation) and ADIPOQ (coding for adiponectin, a marker of mature adipocyte)[159]. While the primer for ADIPOQ were not properly designed, C/EBP-α was expressed in both cell type but not differentially express between control and differentiated conditions. C/EBP-α was also not differentially expressed between differentiated oDFs and oDPSCs. It could be really interesting to design other primers for ADIPOQ because the analysis used differentiated cells after 11 days of differentiation, C/EBP-α is a marker of early differentiation so the expression might be missed at 11 days. Extending the differentiation time could also be tested because variability in culture time needed for inducing adipogenic differentiation depending of MSCs sources was reported[160].

The **osteogenic differentiation** showed surprising results: from the detachment of cells from plastic to the formation of gelatinous spheroids in the well. Alizarin Red staining did not allow to observe extra-cellular calcium deposit.
According to *Hanna et al,* in vitro osteoblastic differentiation of MSCs should generate different cell layers with distinct properties, but these layers were shown to be strongly attach to the well[161]. We tried to coat the well with fibronectin, but this had no effect on the cell detachment. However, the fact that calcification was not observed can be explained by the time we had to stop the differentiation. Indeed, as layers were detaching to form large clumps of cells in the well after 11-14 days of differentiation, we decided to stop the differentiation. It is described in the literature that during MSC differentiation, calcification of the matrix occurs between the 14 and 21 days of differentiation[161,162]. The RTqPCR analysis of the differentiation marker RUNX2 did not help to understand the phenomena. Indeed, no difference of transcription was observed for oDPSCs in differentiation medium compared to the control (oDPSCs in classic medium, giving fold changes around 1). However, oDFs showed higher RUNX2 expression in differentiation condition, where a fold of 2,7 +-0,4 is observed.
However, even if more RUNX2 is detected on differentiated oDFs, calcification deposit was not observed, and cell detachment was also occurring.

The **chondrogenic differentiation** of oDPSCs gave convincing results. Indeed, compared to control, oDPSCs could produce matrix and form a cartilage-like tissue with chondrocytes into chondroplasts. Even if all the cell batches did not show chondrocyte formation, they have all shown cartilage matrix deposit under Alcian blue staining. It strongly supports the chondrogenic potential of oDPSCs. It was not the case for oDFs, as only a single batch seemed to show soft cartilage matrix deposits. mRNA quantification of ACAN, a marker of

chondrogenic differentiation was planned, but the RNA extraction of these spheroid was unsuccessful.

One of the major disappointing outcomes of multilineage differentiation and transcriptional marker analysis is the wide variability within the batches. Our major hypothesis to explain that is the number of passage and the maturity of the cells. For example, DPSC1 and 2 were freshly extracted while other DPSCs were cryopreserved during few months before undergoing the differentiation and RTqPCR analysis. DPSC1 and 2 were also at an early passage, while others were at least from passage 3 to 4. In another hand, the extraction protocol and the medium used was maybe not appropriate to properly enrich our culture with MSC.

In our experience, we clearly observed a difference in the differentiation potential and in the mRNA expression of some genes between freshly extracted/low passaged oDPSCs and others. There is a lot of report in the literature that support the fact that during *in vitro* culture, passaging impact the stemness and the differentiation potential of MSCs[163–167] as well as cryo-preservation[168].

2.5) Methylation patterns

oCIDEC, oSERPINB5 and *oASAM* CpG islands methylation patterns were not different between oDFs and oDPSCs. Even if some CpG site had slight difference in the methylation, these differences were not enough strong to be considered. Only a difference of 50% was considered as having a potential for discriminate the cells.

However, one CpG site, situated in the first exon, seems to be promising to discriminate oDPSCs from oDFs. This CpG site (with three other) were the only ones to be localized outside the CpG islands. They were investigated for one reason: it was the single region conserved between sheep and human genome that have been described to have difference in methylation pattern[98]. However, the cited CpG site did not show difference in the methylation pattern, but it was the CpG site situated few nucleotides after that showed such difference (mostly 63% of difference between both cell types). Even if it is promising, the study here is based on only one oDFs and one oDPSCs batch, so the analysis has to be replicated.

General Conclusion and perspectives

In this study, cells were extracted from ovine dental pulp using plastic-adherence properties in presence of low-glucose and low amino acid medium (alpha-MEM). If we only take into account ISCT recommendations, our cells pointed to match the criteria to be considered as MSCs (so oDPSCs). Indeed, our cells were plastic adherent and demonstrated fibroblast-like morphology. The expression of central markers such as CD73, CD90 and CD105 was detected and CD34 was not express. FACS analysis showed presence of CD73 and CD90 at cell surface, as well as absence of CD45.

Our oDPSCs showed strong chondrogenic differentiation capacity, a start to adipogenic differentiation, and high matrix production during osteogenic differentiation (even if the matrix was not calcified yet, probably due to premature differentiation cessation). Therefore, we can assume that oDPSCs have shown a potential capacity for tri-lineage differentiation. Other

markers described in the literature to be MSC markers and absence of specific protein related to be differentiation marker, support a kind of stemness phenotype of our oDPSCs.

However, oDFs shared most of these markers. Indeed, ISCT marker CD90 and CD105 were expressed, and even if CD73 mRNA analysis did show lower expression compared to oDPSCs, antigen surface analysis detected the proteins in the same way as oDPSCs. Markers described in the literature as specific to fibroblast were not really specific to our oDFs. However, oDFs were negative for expression of other MSC related-markers (other than ISCT's).
oDFs were also plastic adherent, however the protocol used was not identical between the two-cell type. The medium was also richer in nutrient to promote fibroblast extraction. oDFs did not really show a potential for adipogenic differentiation, however, induction of osteogenic differentiation showed similar phenotype as oDPSCs; pointing a potential osteogenic differentiation capacity. Cells showed a tightly chondrogenic differentiation potential. The methylation pattern of both cell type for 3 CpG island were similar, only one CpG site showed difference of >50% of methylation.

In conclusions, our results pointed out that there is a real difference between oDPSCs and oDFs in our experimental conditions, but similarities could be observed. Tested ISCT markers seemed to weakly discriminate the two cell types, however all markers were not tested and mRNA analysis results have to be confirmed by antigen surface analysis. Based on our mRNA analysis, MYH11 and ITGA11 are promising markers that would discriminate the two cell types.

In future perspectives, markers should all be investigated by protein analysis. However, it is well known that antibodies against ovine antigen are challenging to find.
In this study, we compared oDFs with oDPSCs, it could be interesting to try to extract ovine dental pulp fibroblast (with oDFs extraction protocol) and compare them to oDPSCs. Indeed, maybe all our culture were fibroblasts, and the difference observed in this study is due to cells are extracted from different tissues. If we extract cells from the dental pulp using the protocol that should select fibroblasts and compare them to cells isolated with MSCs isolation protocol, we should confirm a difference between both cell types. We should also have included human DPSC as positive control to compare with our oDPSCs.

Few studies only used fibroblast as an independent control of differentiated cells when MSCs are characterized, and when it was done, only slight difference could be observed; the majority of ISCT criteria (multipotency, surface marker and plastic adherence) could not discriminate the cells. Fibroblasts and MSCs are often phenotypically indistinguishable using only ISCT criteria[169–175].

Bibliography

1. Biga L, Dawson S, Harwell A, Hopkins R, Kaufmann J, Le Master M, Matern P, Morrison-Graham K, Quick D, Runyeon J. Synovial joints. https://open.oregonstate.education/aandp/chapter/9-4-synovial-joints/

2. Knapp S. Cartilage. Published October 27, 2020. https://biologydictionary.net/cartilage/

3. Ateshian GA, Hung CT. The natural synovial joint: Properties of cartilage. *Proceedings of the Institution of Mechanical Engineers, Part J: Journal of Engineering Tribology*. 2006;220(8):657-670. doi:10.1243/13506501JET86

4. Hayes WC, Mockros LF. Viscoelastic properties of human articular cartilage. *Journal of Applied Physiology*. 1971;31(4):562-568. doi:10.1152/jappl.1971.31.4.562

5. Sophia Fox AJ, Bedi A, Rodeo SA. The Basic Science of Articular Cartilage: Structure, Composition, and Function. *Sports Health*. 2009;1(6):461-468. doi:10.1177/1941738109350438

6. Knudson CB, Knudson W. Cartilage proteoglycans. *Seminars in Cell & Developmental Biology*. 2001;12(2):69-78. doi:10.1006/scdb.2000.0243

7. Fuentes-Mera L, Camacho A, Moncada-Saucedo NK, Peña-Martínez V. Current Applications of Mesenchymal Stem Cells for Cartilage Tissue Engineering. In: Pham PV, ed. *Mesenchymal Stem Cells - Isolation, Characterization and Applications*. InTech; 2017. doi:10.5772/intechopen.68172

8. Collagen Type II. U.S National Library of Medicine. Published June 28, 2016. https://meshb.nlm.nih.gov/record/ui?name=Collagen%20type%20II

9. Doulabi A, Mequanint K, Mohammadi H. Blends and Nanocomposite Biomaterials for Articular Cartilage Tissue Engineering. *Materials*. 2014;7(7):5327-5355. doi:10.3390/ma7075327

10. Mohammadi H, Mequanint K, Herzog W. Computational aspects in mechanical modeling of the articular cartilage tissue. *Proc Inst Mech Eng H*. 2013;227(4):402-420. doi:10.1177/0954411912470239

11. Gomoll AH, Minas T. The quality of healing: Articular cartilage: Articular cartilage. *Wound Repair Regen*. 2014;22:30-38. doi:10.1111/wrr.12166

12. What is osteoarthritis ? NIH National Institute of Arthritis and Musculoskeletal and skin disease. https://www.niams.nih.gov/health-topics/osteoarthritis

13. Knee osteoarthritis is the degenrative and ulceration of the joint articular surface. PRP Clinic OSSM. http://www.prpclinic.com.au/what-is-osteoarthritis

14. Safiri S, Kolahi AA, Smith E, Hill C, Bettampadi D, Hoy D, Sepidarkish M, Collins G,

Kaufman J, Qorbani M, Woolf A, Guillemin G, March Lyn, Cross M. Global. Regional and national burden of osteoarthritis 1990-2017: a systematic analysis of the Global Burden of Disease Study 2017. *Ann Rheum Dis*. 2020:annrheumdis-2019-216515. doi:10.1136/annrheumdis-2019-216515

15. Hunter DJ, Bierma-Zeinstra S. Osteoarthritis. *The Lancet*. 2019;393(10182):1745-1759. doi:10.1016/S0140-6736(19)30417-9

16. Kingsbury SR, Gross HJ, Isherwood G, Conaghan PG. Osteoarthritis in Europe: impact on health status, work productivity and use of pharmacotherapies in five European countries. *Rheumatology*. 2014;53(5):937-947. doi:10.1093/rheumatology/ket463

17. Mandl LA. Osteoarthritis year in review 2018: clinical. *Osteoarthritis and Cartilage*. 2019;27(3):359-364. doi:10.1016/j.joca.2018.11.001

18. Hunter DJ, Schofield D, Callander E. The individual and socioeconomic impact of osteoarthritis. *Nat Rev Rheumatol*. 2014;10(7):437-441. doi:10.1038/nrrheum.2014.44

19. Kohn MD, Sassoon AA, Fernando ND. Classifications in Brief: Kellgren-Lawrence Classification of Osteoarthritis. *Clinical Orthopaedics & Related Research*. 2016;474(8):1886-1893. doi:10.1007/s11999-016-4732-4

20. Barhum L, Zashin S. An Overview of Secondary Osteoarthritis. 2020; https://www.verywellhealth.com/secondary-osteoarthritis-4799074

21. Richette P, Poitou C, Garnero P, Vicaut E, Bouillot J-L, Lacorte J-M, Basdevant A, Clément K, Bardin T, Chevalier X.. Benefits of massive weight loss on symptoms, systemic inflammation and cartilage turnover in obese patients with knee osteoarthritis. *Annals of the Rheumatic Diseases*. 2011;70(1):139-144. doi:10.1136/ard.2010.134015

22. Muthuri SG, McWilliams DF, Doherty M, Zhang W. History of knee injuries and knee osteoarthritis: a meta-analysis of observational studies. *Osteoarthritis and Cartilage*. 2011;19(11):1286-1293. doi:10.1016/j.joca.2011.07.015

23. Sandell LJ. Etiology of osteoarthritis: genetics and synovial joint development. *Nat Rev Rheumatol*. 2012;8(2):77-89. doi:10.1038/nrrheum.2011.199

24. Ishikawa J, Takahashi N, Matsumoto T, Yoshioka Y, Yamamoto N, Nishikawa M, Hibi, Naoki Ishigro M, Ueda M, Furukawa K, Yamamoto A. Factors secreted from dental pulp stem cells show multifaceted benefits for treating experimental rheumatoid arthritis. *Bone*. 2016;83:210-219. doi:10.1016/j.bone.2015.11.012

25. Lo Monaco M, Gervois P, Beaumont J, Clegg P, Bronckaers A, Vandeweerd J-M, Lambrichts I. Therapeutic Potential of Dental Pulp Stem Cells and Leukocyte- and Platelet-Rich Fibrin for Osteoarthritis. *Cells*. 2020;9(4):980. doi:10.3390/cells9040980

26. Shahani P, Kaushal A, Waghmare G, Datta I. Biodistribution of Intramuscularly-Transplanted Human Dental Pulp Stem Cells in Immunocompetent Healthy Rats through NIR Imaging. *Cells Tissues Organs*. 2020:1-12. doi:10.1159/000511569

27. Mata M, Milian L, Oliver M, Zurriaga J, Sancho-Tello M, Llano J, Carda C. *In Vivo* Articular Cartilage Regeneration Using Human Dental Pulp Stem Cells Cultured in an Alginate Scaffold: A Preliminary Study. *Stem Cells International*. 2017;2017:1-9. doi:10.1155/2017/8309256

28. Fernandes TL, Shimomura K, Asperti A, Pinheiro C, Caetano H, Oliveira C, Nakamura N, Hernandez A, Bueno D. Development of a Novel Large Animal Model to Evaluate Human Dental Pulp Stem Cells for Articular Cartilage Treatment. *Stem Cell Rev and Rep*. 2018;14(5):734-743. doi:10.1007/s12015-018-9820-2

29. Ahern BJ, Parvizi J, Boston R, Schaer TP. Preclinical animal models in single site cartilage defect testing: a systematic review. *Osteoarthritis and Cartilage*. 2009;17(6):705-713. doi:10.1016/j.joca.2008.11.008

30. McGovern JA, Griffin M, Hutmacher DW. Animal models for bone tissue engineering and modelling disease. *Dis Model Mech*. 2018;11(4):dmm033084. doi:10.1242/dmm.033084

31. Colbath AC, Dow SW, Hopkins LS, Phillips JN, McIlwraith CW, Goodrich LR. Single and repeated intra-articular injections in the tarsocrural joint with allogeneic and autologous equine bone marrow-derived mesenchymal stem cells are safe, but did not reduce acute inflammation in an experimental interleukin-1β model of synovitis. *Equine Vet J*. 2020;52(4):601-612. doi:10.1111/evj.13222

32. Wu KC, Chang YH, Liu HW, Ding DC. Transplanting human umbilical cord mesenchymal stem cells and hyaluronate hydrogel repairs cartilage of osteoarthritis in the minipig model. *Tzu Chi Med J*. 2019;31(1):11. doi:10.4103/tcmj.tcmj_87_18

33. Feitosa MLT, Fadel L, Beltrão-Braga PCB, Wenceslau C, Kerkis I, Kerkis A, Junior E, Martins J, Martins D, Miglino M, Ambrosio C-D. Successful transplant of mesenchymal stem cells in induced osteonecrosis of the ovine femoral head: preliminary results. *Acta Cir Bras*. 2010;25(5):416-422. doi:10.1590/S0102-86502010000500006

34. Gugjoo MB, Amarpal. Mesenchymal stem cell research in sheep: Current status and future prospects. *Small Ruminant Research*. 2018;169:46-56. doi:10.1016/j.smallrumres.2018.08.002

35. Delling U, Brehm W, Ludewig E, Winter K, Jülke H. Longitudinal Evaluation of Effects of Intra-Articular Mesenchymal Stromal Cell Administration for the Treatment of Osteoarthritis in an Ovine Model. *Cell Transplant*. 2015;24(11):2391-2407. doi:10.3727/096368915X686193

36. Music E, Futrega K, Doran MR. Sheep as a model for evaluating mesenchymal stem/stromal cell (MSC)-based chondral defect repair. *Osteoarthritis and Cartilage*. 2018;26(6):730-740. doi:10.1016/j.joca.2018.03.006

37. Al Faqeh H, Nor Hamdan BMY, Chen HC, Aminuddin BS, Ruszymah BHI. The potential of intra-articular injection of chondrogenic-induced bone marrow stem cells to retard the progression of osteoarthritis in a sheep model. *Experimental Gerontology*. 2012;47(6):458-464. doi:10.1016/j.exger.2012.03.018

38. McCoy AM. Animal Models of Osteoarthritis: Comparisons and Key Considerations. *Vet Pathol*. 2015;52(5):803-818. doi:10.1177/0300985815588611

39. Takroni T, Laouar L, Adesida A, Elliott JAW, Jomha NM. Anatomical study: comparing the human, sheep and pig knee meniscus. *J EXP ORTOP*. 2016;3(1):35. doi:10.1186/s40634-016-0071-3

40. Cook JL, Hung CT, Kuroki K, Stoker A. M., Cook C. R., Pfeiffer F.M., Sherman S.L., Stannard J.P. Animal models of cartilage repair. *Bone & Joint Research*. 2014;3(4):89-94. doi:10.1302/2046-3758.34.2000238

41. Kuyinu EL, Narayanan G, Nair LS, Laurencin CT. Animal models of osteoarthritis: classification, update, and measurement of outcomes. *J Orthop Surg Res*. 2016;11(1):19. doi:10.1186/s13018-016-0346-5

42. Proffen BL, McElfresh M, Fleming BC, Murray MM. A comparative anatomical study of the human knee and six animal species. *The Knee*. 2012;19(4):493-499. doi:10.1016/j.knee.2011.07.005

43. Bascuñán AL, Biedrzycki A, Banks SA, Lewis DD, Kim SE. Large Animal Models for Anterior Cruciate Ligament Research. *Front Vet Sci*. 2019;6:292. doi:10.3389/fvets.2019.00292

44. Uthman OA, van der Windt DA, Jordan JL, et al. Exercise for lower limb osteoarthritis: systematic review incorporating trial sequential analysis and network meta-analysis: *Br J Sports Med*. 2014;48(21):1579-1579. doi:10.1136/bjsports-2014-5555rep

45. Bliddal H, Leeds AR, Christensen R. Osteoarthritis, obesity and weight loss: evidence, hypotheses and horizons – a scoping review. *Obes Rev*. 2014;15(7):578-586. doi:10.1111/obr.12173

46. Latourte A, Kloppenburg M, Richette P. Emerging pharmaceutical therapies for osteoarthritis. *Nat Rev Rheumatol*. 2020;16(12):673-688. doi:10.1038/s41584-020-00518-6

47. Glyn-Jones S, Palmer AJR, Agricola R, Price A-J, Vincent T-L, Weinans H, Carr A-J. Osteoarthritis. *The Lancet*. 2015;386(9991):376-387. doi:10.1016/S0140-6736(14)60802-3

48. Yusuf E. Pharmacologic and Non-Pharmacologic Treatment of Osteoarthritis. *Curr Treat Options in Rheum*. 2016;2(2):111-125. doi:10.1007/s40674-016-0042-y

49. Veronese N, Cooper C, Reginster JY, Scheen A. Type 2 diabetes mellitus and osteoarthritis. *Seminars in Arthritis and Rheumatism*. 2019;49(1):9-19. doi:10.1016/j.semarthrit.2019.01.005

50. Jansen MP, Boymans TAEJ, Custers RJH, et al. Knee Joint Distraction as Treatment for Osteoarthritis Results in Clinical and Structural Benefit: A Systematic Review and Meta-Analysis of the Limited Number of Studies and Patients Available. *CARTILAGE*. 2020:194760352094294. doi:10.1177/1947603520942945

51. Hamel MB. Joint Replacement Surgery in Elderly Patients With Severe Osteoarthritis

of the Hip or KneeDecision Making, Postoperative Recovery, and Clinical Outcomes. *Arch Intern Med*. 2008;168(13):1430. doi:10.1001/archinte.168.13.1430

52. Wyles CC, Houdek MT, Behfar A, Sierra RJ. Mesenchymal stem cell therapy for osteoarthritis: current perspectives. *Stem cells and cloning: Advances and Applications, Dovepress*: 2015: http://dx.doi.org/10.2147/SCCAA.S68073.

53. Rothrauff BB, Pirosa A, Lin H, Sohn J, Langhans MT, Tuan RS. Stem Cell Therapy for Musculoskeletal Diseases. In: *Principles of Regenerative Medicine*. Elsevier; 2019:953-970. doi:10.1016/B978-0-12-809880-6.00054-0

54. Carstairs A, Genever P. Stem cell treatment for musculoskeletal disease. *Current Opinion in Pharmacology*. 2014;16:1-6. doi:10.1016/j.coph.2014.01.005

55. Hernigou P, Trousselier M, Roubineau F, et al. Stem Cell Therapy for the Treatment of Hip Osteonecrosis: A 30-Year Review of Progress. *Clin Orthop Surg*. 2016;8(1):1. doi:10.4055/cios.2016.8.1.1

56. Gangji V, Toungouz M, Hauzeur JP. Stem cell therapy for osteonecrosis of the femoral head. *Expert Opinion on Biological Therapy*. 2005;5(4):437-442. doi:10.1517/14712598.5.4.437

57. Jacob G, Shimomura K, Krych AJ, Nakamura N. The Meniscus Tear: A Review of Stem Cell Therapies. *Cells*. 2019;9(1):92. doi:10.3390/cells9010092

58. Wang AT, Feng Y, Jia HH, Zhao M, Yu H. Application of mesenchymal stem cell therapy for the treatment of osteoarthritis of the knee: A concise review. *WJSC*. 2019;11(4):222-235. doi:10.4252/wjsc.v11.i4.222

59. Zhu C, Wu W, Qu X. Mesenchymal stem cells in osteoarthritis therapy: a review. *AJTR*. 2021 ;13(2):448-461.

60. Alison MR, Poulsom R, Forbes S, Wright NA. An introduction to stem cells. *J Pathol*. 2002;197(4):419-423. doi:10.1002/path.1187

61. Rossant J. Stem Cells from the Mammalian Blastocyst. *Stem Cells*. 2001;19(6):477-482. doi:10.1634/stemcells.19-6-477

62. Spencer ND, Gimble JM, Lopez MJ. Mesenchymal Stromal Cells: Past, Present, and Future: Mesenchymal Stromal Cells. *Veterinary Surgery*. 2011;40(2):129-139. doi:10.1111/j.1532-950X.2010.00776.x

63. Dileep C, Suresh P, Khalilullah S, Nama S, Brahmaiah B, Desu PK. STEM CELL: PAST, PRESENT AND FUTURE- A REVIEW ARTICLE. 2013;3(1):11.

64. Karagiannis P, Nakauchi A, Yamanaka S. Bringing Induced Pluripotent Stem Cell Technology to the Bedside. *JMA J*. 2018;1(1):6-14. doi:10.31662/jmaj.2018-0005

65. What are Unipotent Stem Cells. Published March 26, 2020. https://www.betteraging.com/aging-science/what-are-unipotent-stem-cells/

66. Pucéat M, Ballis A. Embryonic Stem Cells: From Bench to Bedside. *Clin Pharmacol Ther*. 2007;82(3):337-339. doi:10.1038/sj.clpt.6100298

67. Worku MG. Pluripotent and Multipotent Stem Cells and Current Therapeutic Applications: Review. *SCCAA*. 2021;Volume 14:3-7. doi:10.2147/SCCAA.S304887

68. Lo B, Parham L. Ethical Issues in Stem Cell Research. *Endocrine Reviews*. 2009;30(3):204-213. doi:10.1210/er.2008-0031

69. Berebichez-Fridman R, Montero-Olvera PR. Sources and Clinical Applications of Mesenchymal Stem Cells: State-of-the-art review. *Sultan Qaboos Univ Med J*. 2018;18(3):264. doi:10.18295/squmj.2018.18.03.002

70. Pittenger MF. Mesenchymal stem cell perspective: cell biology to clinical progress. *npj Regenerative Medicine*. 2019: https://doi.org/10.1038/s41536-019-0083-6.

71. Li Z, Jiang CM, An S, Cheng Q, Huang Y-F, Gou Y-C, Xiao L, Yu W-J, Wang J. Immunomodulatory properties of dental tissue-derived mesenchymal stem cells. *Oral Dis*. 2014;20(1):25-34. doi:10.1111/odi.12086

72. Pierdomenico L, Bonsi L, Calvitti M, Franchina M, Grossi A, Bagnara G-P. Multipotent Mesenchymal Stem Cells with Immunosuppressive Activity Can Be Easily Isolated from Dental Pulp. *Transplantation*. 2005;80(6):836-842. doi:10.1097/01.tp.0000173794.72151.88

73. Anitua E, Troya M, Zalduendo M. Progress in the use of dental pulp stem cells in regenerative medicine. *Cytotherapy*. 2018;20(4):479-498. doi:10.1016/j.jcyt.2017.12.011

74. Kondělková K, Vokurková D, Krejsek J, Borská L, Fiala Z, Andrýs C. Regulatory T cells (Treg) and Their Roles in Immune System with Respect to Immunopathological Disorders. *Acta Med (Hradec Kralove, Czech Repub)*. 2010;53(2):73-77. doi:10.14712/18059694.2016.63

75. Ambrosio C, Zomer H, Vidane A, Gonçalves N. Mesenchymal and induced pluripotent stem cells: general insights and clinical perspectives. *SCCAA*. 2015:125. doi:10.2147/SCCAA.S88036

76. Rodríguez-Fuentes DE, Fernández-Garza LE, Samia-Meza JA, Barrera-Barrera SA, Caplan AI, Barrera-Saldaña HA. Mesenchymal Stem Cells Current Clinical Applications: A Systematic Review. *Archives of Medical Research*. 2021;52(1):93-101. doi:10.1016/j.arcmed.2020.08.006

77. Jones DL, Wagers AJ. No place like home: anatomy and function of the stem cell niche. *Nat Rev Mol Cell Biol*. 2008;9(1):11-21. doi:10.1038/nrm2319

78. Ferraro F, Celso CL, Scadden D. ADULT STEM CELLS AND THEIR NICHES. *The Cell Biology of Stem Cells*: 2010: Chapter 11.

79. Inaba M, Yamashita YM. Asymmetric Stem Cell Division: Precision for Robustness. *Cell Stem Cell*. 2012;11(4):461-469. doi:10.1016/j.stem.2012.09.003

80. Friedenstein AJ, Chailakhjan RK, Lalykina KS. THE DEVELOPMENT OF FIBROBLAST COLONIES IN MONOLAYER CULTURES OF GUINEA-PIG BONE MARROW AND SPLEEN CELLS. *Cell Prolif*. 1970;3(4):393-403. doi:10.1111/j.1365-2184.1970.tb00347.x

81. Zuk PA, Zhu M, Ashjian P, et al. Human Adipose Tissue Is a Source of Multipotent Stem Cells□D. *Molecular Biology of the Cell*. 2002;13:17.

82. Parolini O, Alviano F, Bagnara GP, Wolfbank S, Zeisberger S, Zisch A, Strom S. Concise Review: Isolation and Characterization of Cells from Human Term Placenta: Outcome of the First International Workshop on Placenta Derived Stem Cells. *Stem Cells*. 2008;26(2):300-311. doi:10.1634/stemcells.2007-0594

83. Qiao C, Xu W, Zhu W, Hu J, Qian H, Yin Q, Jiang R, Yan Y, Mao F, Yang H, Wang X, Chen Y. Human mesenchymal stem cells isolated from the umbilical cord. *Cell Biology International*. 2008;32(1):8-15. doi:10.1016/j.cellbi.2007.08.002

84. Gronthos S, Mankani M, Brahim J, Robey PG, Shi S. Postnatal human dental pulp stem cells (DPSCs) in vitro and invivo. *Proceedings of the National Academy of Sciences*. 2000;97(25):13625-13630. doi:10.1073/pnas.240309797

85. Kassis I, Zangi L, Rivkin R, eLevdansky L, Samuel S, Marx G, Gorodetsky R. Isolation of mesenchymal stem cells from G-CSF-mobilized human peripheral blood using fibrin microbeads. *Bone Marrow Transplant*. 2006;37(10):967-976. doi:10.1038/sj.bmt.1705358

86. Bari CD, Dell'Accio F, Tylzanowski P, Luyten FP. Multipotent mesenchymal stem cells from adult human synovial membrane. *Arthritis & Rheumatism:* 2011:doi:10.1002/1529-0131(200108)44:8<1928::AID-ART331>3.0.CO;2-P..

87. Dominici M. Minimal criteria for defining multipotent mesenchymal stromal cells. The International Society for Cellular Therapy position statement. *Cytotherapy*. 2006;8(4):315-7. doi: 10.1080/14653240600855905.

88. Conget PA, Minguell JJ. Phenotypical and functional properties of human bone marrow mesenchymal progenitor cells. *Journal of cellular physiology.* 1999; doi 181(1):67-73. 10.1002/(SICI)1097-4652(199910)181:1<67::AID-JCP7>3.0.CO;2-C.

89. Short B, Brouard N, Occhiodoro-Scott T, Ramakrishnan A, Simmons PJ. Mesenchymal stem cells. *Archives of Medical Research*. 2003;34(6):565-571. doi:10.1016/j.arcmed.2003.09.007

90. Phinney DG, Kopen G, Isaacson RL, Prockop DJ. Plastic adherent stromal cells from the bone marrow of commonly used strains of inbred mice: Variations in yield, growth, and differentiation. *Journal of Cellular Biochemistry*. 1999;15;72(4):570-85. PMID: 10022616

91. Couto de Carvalho LA, Tosta dos Santos SL, Sacramento LV, Almeida junior VD, Xavier FC, Dos Santo JN, Henriques Leitao AC. Mesenchymal stem cell markers in periodontal tissues and periapical lesions. *Acta Histochemica*. 2020;122(8):151636. doi:10.1016/j.acthis.2020.151636

92. Sebastião MJ, Serra M, Gomes-Alves P, Alves PM. Stem cells characterization: OMICS reinforcing analytics. *Current Opinion in Biotechnology*. 2021;71:175-181. doi:10.1016/j.copbio.2021.07.021

93. Tsai MS, Hwang SM, Chen KD, Lee YS, Hsu LW, Chang YJ, Wang CN, Peng HH, Chang TL, Chao AS, Chang SD, Lee KD, Wang TH, Soong YK. Functional Network Analysis of the Transcriptomes of Mesenchymal Stem Cells Derived from Amniotic Fluid, Amniotic Membrane, Cord Blood, and Bone Marrow. *Stem Cells*. 2007;25(10):2511-2523. doi:10.1634/stemcells.2007-0023

94. Wiese DM, Braid LR. Transcriptome profiles acquired during cell expansion and licensing validate mesenchymal stromal cell lineage genes. *Stem Cell Res Ther*. 2020;11(1):357. doi:10.1186/s13287-020-01873-7

95. Cho KA, Park M, Kim YH, Woo SY, Ryu KH. RNA sequencing reveals a transcriptomic portrait of human mesenchymal stem cells from bone marrow, adipose tissue, and palatine tonsils. *Sci Rep*. 2017;7(1):17114. doi:10.1038/s41598-017-16788-2

96. Billing AM, Ben Hamidane H, Dib SS, Comprehensive transcriptomic and proteomic characterization of human mesenchymal stem cells reveals source specific cellular markers. *Sci Rep*. 2016;6(1):21507. doi:10.1038/srep21507

97. Roson-Burgo B, Sanchez-Guijo F, Del Cañizo C, De Las Rivas J. Insights into the human mesenchymal stromal/stem cell identity through integrative transcriptomic profiling. *BMC Genomics*. 2016;17(1):944. doi:10.1186/s12864-016-3230-0

98. De Almeida DC, Ferreira MRP, Franzen J, Waidner CI, Frobel J, Zenke M, Costa IG, Wagner W. Epigenetic Classification of Human Mesenchymal Stromal Cells. *Stem Cell Reports*. 2016;6(2):168-175. doi:10.1016/j.stemcr.2016.01.003

99. Soundararajan M, Kannan S. Fibroblasts and mesenchymal stem cells: Two sides of the same coin? *J Cell Physiol*. 2018;233(12):9099-9109. doi:10.1002/jcp.26860

100. Collart-Dutilleul PY, Chaubron F, Vos JD, Cuisinier FJ. Allogenic banking of dental pulp stem cells for innovative therapeutics. *Wold Journal of Stem Cells.* 2015; 7(7): 1010-1021 DOI: 10.4252/wjsc.v7.i7.1010.

101. Unal GC, Kaya BU, Tac AG, Kececi AD. Survey of attitudes, materials and methods preferred in root canal therapy by general dental practice in Turkey: Part 1. *Eur J Dent*. 2012;06(04):376-384. doi:10.1055/s-0039-1698975

102. WHAT TO EXPECT FROM PULP EXTIRPATION. https://www.emergencydentistsydney.com.au/news/what-to-expect-from-pulp-extirpation

103. Wang H, Zhong Q, Yang T, Qi Y, Fu M, Yang X, Qiao L, Ling Q, Liu S, Zhao Y. Comparative characterization of SHED and DPSCs during extended cultivation invitro. *Mol Med Report*. 2018; 17: 6551-6559. doi:10.3892/mmr.2018.8725

104. Sabbagh J, Ghassibe-Sabbagh M, Fayyad-Kazan M, Differences in osteogenic and odontogenic differentiation potential of DPSCs and SHED. *Journal of Dentistry*.

2020;101:103413. doi:10.1016/j.jdent.2020.103413

105. Sharpe PT. Neural Crest and Tooth Morphogenesis. *Adv Dent Res*. 2001;15(1):4-7. doi:10.1177/08959374010150011001

106. Chang CC, Chang KC, Tsai SJ, Chang HH, Lin CP. Neurogenic differentiation of dental pulp stem cells to neuron-like cells in dopaminergic and motor neuronal inductive media. *Journal of the Formosan Medical Association*. 2014;113(12):956-965. doi:10.1016/j.jfma.2014.09.003

107. Yamada Y, Nakamura-Yamada S, Kusano K, Baba S. Clinical Potential and Current Progress of Dental Pulp Stem Cells for Various Systemic Diseases in Regenerative Medicine: A Concise Review. *IJMS*. 2019;20(5):1132. doi:10.3390/ijms20051132

108. Méndez-Maldonado K, Vega-López GA, Aybar MJ, Velasco I. Neurogenesis From Neural Crest Cells: Molecular Mechanisms in the Formation of Cranial Nerves and Ganglia. *Front Cell Dev Biol*. 2020;8:635. doi:10.3389/fcell.2020.00635

109. Lan X, Sun Z, Chu C, Boltze J, Li S. Dental Pulp Stem Cells: An Attractive Alternative for Cell Therapy in Ischemic Stroke. *Front Neurol*. 2019;10:824. doi:10.3389/fneur.2019.00824

110. Ruminants. Accessed on September 12 2021 http://www.fao.org/3/T0690E/t0690e05.htm

111. Rouge M. Dental Anatomy of Ruminants. http://www.vivo.colostate.edu/hbooks/pathphys/digestion/pregastric/cowpage.html

112. Arshi A, Petrigliano FA, Williams RJ, Jones KJ. Stem Cell Treatment for Knee Articular Cartilage Defects and Osteoarthritis. *Curr Rev Musculoskelet Med*. 2020;13(1):20-27. doi:10.1007/s12178-020-09598-z

113. Barry F. MSC Therapy for Osteoarthritis: An Unfinished Story. *J Orthop Res*. 2019;37(6):1229-1235. doi:10.1002/jor.24343

114. Maldonado DC, Nicoliche T, Faber J, Kerkis I, Saez DM, Sasaki RT. Intra-articular human deciduous dental pulp stem cell administration vs. pharmacological therapy in experimental osteoarthritis rat model. *European Review for medical and Pharmacological Sciences.* 2021; 25: 3546-3556. doi: 10.26355/eurrev_202105_25837.

115. Thermo Fisher. Introduction to Gene Expression Profiling. https://www.thermofisher.com/be/en/home/life-science/pcr/real-time-pcr/real-time-pcr-learning-center/gene-expression-analysis-real-time-pcr-information/introduction-gene-expression-profiling.html

116. Wagner W, Wein F, Seckinger A, frankhauser M, Wirkner U, Krause U, Blake J, Schwager C, Eckstein V, Ansorge W, D. Ho A. Comparative characteristics of mesenchymal stem cells from human bone marrow, adipose tissue, and umbilical cord blood. *Experimental Hematology*. 2005;33(11):1402-1416. doi:10.1016/j.exphem.2005.07.003

117. Kundrotas G. Surface markers distinguishing mesenchymal stem cells from fibroblasts. *AML*. 2012;19(2):75-79. doi:10.6001/actamedica.v19i2.2313

118. Musina RA, Bekchanova ES, Sukhikh GT. Comparison of Mesenchymal Stem Cells Obtained from Different Human Tissues. *Bull Exp Biol Med*. 2005;139(4):504-509. doi:10.1007/s10517-005-0331-1

119. Pagella P, de Vargas Roditi L, Stadlinger B, Moor AE, Mitsiadis TA. A Single Cell Atlas of Human Teeth. *Cell Biology*; 2021. doi:10.1101/2021.02.19.431962

120. Dupont C, Armant D, Brenner C. Epigenetics: Definition, Mechanisms and Clinical Perspective. *Semin Reprod Med*. 2009;27(05):351-357. doi:10.1055/s-0029-1237423

121. Golbabapour S, Abdulla MA, Hajrezaei M. A Concise Review on Epigenetic Regulation: Insight into Molecular Mechanisms. *IJMS*. 2011;12(12):8661-8694. doi:10.3390/ijms12128661

122. Walker CG, Littlejohn MD, Meier S, Roche JR, Mitchell MD. DNA methylation is correlated with gene expression during early pregnancy in *Bos taurus*. *Physiological Genomics*. 2013;45(7):276-286. doi:10.1152/physiolgenomics.00145.2012

123. Mandal C, Halder D, Jung KH, Chai YG. Gestational Alcohol Exposure Altered DNA Methylation Status in the Developing Fetus. *IJMS*. 2017;18(7):1386. doi:10.3390/ijms18071386

124. Queirós AC, Villamor N, Clot G, et al. A B-cell epigenetic signature defines three biologic subgroups of chronic lymphocytic leukemia with clinical impact. *Leukemia*. 2015;29(3):598-605. doi:10.1038/leu.2014.252

125. Lenz M, Goetzke R, Schenk A, Schubert C, Veeck J, Hemeda H, Koschmieder, Zenke M, Schuppert A, Wagner W. Epigenetic Biomarker to Support Classification into Pluripotent and Non-Pluripotent Cells. *Sci Rep*. 2015;5(1):8973. doi:10.1038/srep08973

126. Khan MR, Chandrashekran A, Smith RKW, Dudhia J. Immunophenotypic characterization of ovine mesenchymal stem cells: Immunophenotyping of Sheep MSC. *Cytometry*. 2016;89(5):443-450. doi:10.1002/cyto.a.22849

127. Widbiller M, Rothmaier C, Saliter D, Wolflick M, Rosendahl A, Buchalla W, Schmalz G, Spruss T, Galler KM. Histology of human teeth: standard and specific staining methods revisited. *Archives of Oral Biology*. 2021:105136. doi:10.1016/j.archoralbio.2021.105136

128. Vandiest P. La dentition: caractéristiques et défauts. Published online October 2004. FICOW. 2004;(10):1-2.

129. Cocquyt G, Driessen B, Simoens P. Variability in the eruption of the permanent incisor teeth in sheep. *Veterinary Record*. 2005;157(20):619-623. doi:10.1136/vr.157.20.619

130. Ge Z pu, Ma R han, Li G, Zhang J zong, Ma X chen. Age estimation based on pulp chamber volume of first molars from cone-beam computed tomography images. *Forensic Science International*. 2015;253:133.e1-133.e7. doi:10.1016/j.forsciint.2015.05.004

131. Kazmi S, Mânica S, Revie G, Shepherd S, Hector M. Age estimation using canine pulp volumes in adults: a CBCT image analysis. *Int J Legal Med*. 2019;133(6):1967-1976. doi:10.1007/s00414-019-02147-5

132. Hidayat SR, Oscandar F, Malinda Y, Lita YA. Human age estimation based on pulp volume of canines for chronological age estimation: Preliminary research. *Padjadjaran J Dent*. 2018;30(3):184. doi:10.24198/pjd.vol30no3.19302

133. Cappellesso-Fleury S, Puissant-Lubrano B, Apoil PA, Titeux M, Winterton P, Casteilla L, Bourin P, Blancher A. Human Fibroblasts Share Immunosuppressive Properties with Bone Marrow Mesenchymal Stem Cells. *J Clin Immunol*. 2010;30(4):607-619. doi:10.1007/s10875-010-9415-4

134. Alt E, Yan Y, Gehmert S, Song YH, Altman A, Gehmert S, Vykoukal V, Bai X. Fibroblasts share mesenchymal phenotypes with stem cells, but lack their differentiation and colony-forming potential. *Biology of the Cell*. 2011;103(4):197-208. doi:10.1042/BC20100117

135. Halfon S, Abramov N, Grinblat B, Ginis I. Markers Distinguishing Mesenchymal Stem Cells from Fibroblasts Are Downregulated with Passaging. *Stem Cells and Development*. 2011;20(1):53-66. doi:10.1089/scd.2010.0040

136. Lorenz K, Sicker M, Schmelzer E, Rupf T, Salvetter J, Schulz-Siegmund M, Bader A. Multilineage differentiation potential of human dermal skin-derived fibroblasts. *Experimental Dermatology*. 2008;17(11):925-932. doi:10.1111/j.1600-0625.2008.00724.x

137. Sidney LE, Branch MJ, Dunphy SE, Dua HS, Hopkinson A. Concise Review: Evidence for CD34 as a Common Marker for Diverse Progenitors: CD34 as a Common Marker for Diverse Progenitors. *Stem Cells*. 2014;32(6):1380-1389. doi:10.1002/stem.1661

138. Lin CS, Ning H, Lin G, Lue TF. Is CD34 truly a negative marker for mesenchymal stromal cells? *Cytotherapy*. 2012;14(10):1159-1163. doi:10.3109/14653249.2012.729817

139. Kaiser S, Hackanson B, Follo M, et al. BM cells giving rise to MSC in culture have a heterogeneous CD34 and CD45 phenotype. *Cytotherapy*. 2007;9(5):439-450. doi:10.1080/14653240701358445

140. Zimmerlin L, Donnenberg VS, Rubin JP, Donnenberg AD. Mesenchymal markers on human adipose stem/progenitor cells. *Cytometry*. Published online January 2013. doi:10.1002/cyto.a.22227

141. Zhu H, Mitsuhashi N, Klein A. The Role of the Hyaluronan Receptor CD44 in Mesenchymal Stem Cell Migration in the Extracellular Matrix. *STEM CELLS*. 2006;24(4):928-935. doi:10.1634/stemcells.2005-0186

142. L. Ramos T, Sánchez-Abarca LI, Muntión S. MSC surface markers (CD44, CD73, and CD90) can identify human MSC-derived extracellular vesicles by conventional flow cytometry. *Cell Commun Signal*. 2016;14(1):2. doi:10.1186/s12964-015-0124-8

143. Li W, Lin X, Yang H, Cao Y, Zhang C, Fan Z. Depletion of HOXA5 inhibits the

osteogenic differentiation and proliferation potential of stem cells from the apical papilla: HOXA5 regulates MSC function. *Cell Biol Int*. 2018;42(1):45-52. doi:10.1002/cbin.10860

144. Buechling T, Boutros M. Wnt Signaling. In: *Current Topics in Developmental Biology*. Vol 97. Elsevier; 2011:21-53. doi:10.1016/B978-0-12-385975-4.00008-5

145. Ordóñez-Morán P, Dafflon C, Imajo M, Nishida E, Huelsken J. HOXA5 Counteracts Stem Cell Traits by Inhibiting Wnt Signaling in Colorectal Cancer. *Cancer Cell*. 2015;28(6):815-829. doi:10.1016/j.ccell.2015.11.001

146. Janssens R, Struyf S, Proost P. The unique structural and functional features of CXCL12. *Cell Mol Immunol*. 2018;15(4):299-311. doi:10.1038/cmi.2017.107

147. Pagella P, Nombela-Arrieta C, Mitsiadis TA. Distinct Expression Patterns of Cxcl12 in Mesenchymal Stem Cell Niches of Intact and Injured Rodent Teeth. *IJMS*. 2021;22(6):3024. doi:10.3390/ijms22063024

148. Zhang WM, Käpylä J, Puranen JS. α11β1 Integrin Recognizes the GFOGER Sequence in Interstitial Collagens. *Journal of Biological Chemistry*. 2003;278(9):7270-7277. doi:10.1074/jbc.M210313200

149. NCBI G. MYH11 myosin heavy chain 11 [Homo sapiens (human)]. 2021. https://www.ncbi.nlm.nih.gov/gene?Db=gene&Cmd=ShowDetailView&TermToSearch=4629

150. Muramatsu T. Midkine and Pleiotrophin: Two Related Proteins Involved in Development, Survival, Inflammation and Tumorigenesis. *Journal of Biochemistry*. 2002;132(3):359-371. doi:10.1093/oxfordjournals.jbchem.a003231

151. Ding R, Jiang X, Ha Y, Wang Z, Guo J, Jiang H, Zheng S, Jie W. Activation of Notch1 signalling promotes multi-lineage differentiation of c-KitPOS/NKX2.5POS bone marrow stem cells: implication in stem cell translational medicine. *Stem Cell Res Ther*. 2015;6(1):91. doi:10.1186/s13287-015-0085-2

152. NCBI G. NOTCH1 notch receptor 1 [Homo sapiens (human)]. 2021. https://www.ncbi.nlm.nih.gov/gene?Db=gene&Cmd=ShowDetailView&TermToSearch=4851

153. He Y, Zou L. Notch-1 inhibition reduces proliferation and promotes osteogenic differentiation of bone marrow mesenchymal stem cells. *Exp Ther Med*. Published online July 10, 2019. doi:10.3892/etm.2019.7765

154. Cheng PH, Snyder B, Fillos D, Ibegbu CC, Huang AHC, Chan AW. Postnatal stem/progenitor cells derived from the dental pulp of adult chimpanzee. *BMC Cell Biol*. 2008;9(1):20. doi:10.1186/1471-2121-9-20

155. Bae S, Kang B, Lee H, Luu H, Mullins E, Kingsley K. Characterization of Dental Pulp Stem Cell Responses to Functional Biomaterials Including Mineralized Trioxide Aggregates. *JFB*. 2021;12(1):15. doi:10.3390/jfb12010015

156. Cinelli J, Nguyen E, Kingsley K. Assessment of Dental Pulp Stem Cell (DPSC) Biomarkers Following Induction with Bone Morphogenic Protein 2 (BMP-2). *JABB*. 2018;19(2):1-12. doi:10.9734/JABB/2018/44215

157. Hu L, Zhao B, Gao Z, et al. Regeneration characteristics of different dental derived stem cell sheets. *J Oral Rehabil*. 2020;47(S1):66-72. doi:10.1111/joor.12839

158. Mitchell JB, McIntosh K, Zvonic S. Immunophenotype of Human Adipose-Derived Cells: Temporal Changes in Stromal-Associated and Stem Cell–Associated Markers. *STEM CELLS*. 2006;24(2):376-385. doi:10.1634/stemcells.2005-0234

159. Karagianni M, Brinkmann I, Kinzebach S.. A comparative analysis of the adipogenic potential in human mesenchymal stromal cells from cord blood and other sources. *Cytotherapy*. 2013;15(1):76-88.e2. doi:10.1016/j.jcyt.2012.11.001

160. Mushahary D, Spittler A, Kasper C, Weber V, Charwat V. Isolation, cultivation, and characterization of human mesenchymal stem cells: hMSC. *Cytometry*. 2018;93(1):19-31. doi:10.1002/cyto.a.23242

161. Hanna H, Mir LM, Andre FM. In vitro osteoblastic differentiation of mesenchymal stem cells generates cell layers with distinct properties. *Stem Cell Res Ther*. 2018;9(1):203. doi:10.1186/s13287-018-0942-x

162. Shayegan A, Zucchi A, De Swert K, Balau B, Truyens C, Nicaise C. Lipoteichoic acid stimulates the proliferation, migration and cytokine production of adult dental pulp stem cells without affecting osteogenic differentiation. *Int Endod J*. 2021;54(4):585-600. doi:10.1111/iej.13448

163. Elkhenany H, Amelse L, Caldwell M, Abdelwahed R, Dhar M. Impact of the source and serial passaging of goat mesenchymal stem cells on osteogenic differentiation potential: implications for bone tissue engineering. *J Animal Sci Biotechnol*. 2016;7(1):16. doi:10.1186/s40104-016-0074-z

164. Kretlow JD, Jin YQ, Liu W. Donor age and cell passage affects differentiation potential of murine bone marrow-derived stem cells. *BMC Cell Biol*. 2008;9(1):60. doi:10.1186/1471-2121-9-60

165. Jiang T, Xu G, Wang Q. In vitro expansion impaired the stemness of early passage mesenchymal stem cells for treatment of cartilage defects. *Cell Death Dis*. 2017;8(6):e2851-e2851. doi:10.1038/cddis.2017.215

166. Shall G, Menosky M, Decker S. Effects of Passage Number and Differentiation Protocol on the Generation of Dopaminergic Neurons from Rat Bone Marrow-Derived Mesenchymal Stem Cells. *IJMS*. 2018;19(3):720. doi:10.3390/ijms19030720

167. Yang YHK, Ogando CR, Wang See C, Chang TY, Barabino GA. Changes in phenotype and differentiation potential of human mesenchymal stem cells aging in vitro. *Stem Cell Res Ther*. 2018;9(1):131. doi:10.1186/s13287-018-0876-3

168. Bahsoun S, Coopman K, Akam EC. Quantitative assessment of the impact of

cryopreservation on human bone marrow-derived mesenchymal stem cells: up to 24 h post-thaw and beyond. *Stem Cell Res Ther*. 2020;11(1):540. doi:10.1186/s13287-020-02054-2

169. Denu RA, Nemcek S, Bloom DD, Goodrich A, Kim J, Mosher DF, Hematti P. Fibroblasts and Mesenchymal Stromal/Stem Cells Are Phenotypically Indistinguishable. *Acta Haematol*. 2016;136(2):85-97. doi:10.1159/000445096

170. Ugurlu B, Karaoz E. Comparison of similar cells: Mesenchymal stromal cells and fibroblasts. *Acta Histochemica*. 2020;122(8):151634. doi:10.1016/j.acthis.2020.151634

171. Pasanisi E, Ciavarella C, Valente S, Ricci F, Pasquinelli G. Differentiation and plasticity of human vascular wall mesenchymal stem cells, dermal fibroblasts and myofibroblasts: a critical comparison including ultrastructural evaluation of osteogenic potential. *Ultrastructural Pathology*. 2019;43(6):261-272. doi:10.1080/01913123.2019.1673863

172. Chang Y, Li H, Guo Z. Mesenchymal Stem Cell-Like Properties in Fibroblasts. *Cell Physiol Biochem*. 2014;34(3):703-714. doi:10.1159/000363035

173. Sindberg GM, Lindborg BA, Wang Q, Clarkson C, Graham M, Donahue R, Verfaillie CM, Pakala P, O'Brien T. Comparisons of phenotype and immunomodulatory capacity among rhesus bone-marrow-derived mesenchymal stem/stromal cells, multipotent adult progenitor cells, and dermal fibroblasts. *J Med Primatol*. 2014;43(4):231-241. doi:10.1111/jmp.12122

174. Cakiroglu F, Osbahr JW, Kramer J, Rohwedel J. Differences of cell surface marker expression between bone marrow- and kidney-derived. *Cellular and molecular Biology.* 2016, 62 (12): 11-17. doi: 10.14715/cmb/2016.62.12.3

175. Lupatov AYu, Vdovin AS, Vakhrushev IV, Poltavtseva RA, Yarygin KN. Comparative Analysis of the Expression of Surface Markers on Fibroblasts and Fibroblast-Like Cells Isolated from Different Human Tissues. *Bull Exp Biol Med*. 2015;158(4):537-543. doi:10.1007/s10517-015-2803-2